Mara Lília Soares da Silva

Licenciatura em Engenharia Química

Development of molecularly imprinted polymers using supercritical fluid technology

Dissertação para obtenção do Grau de Doutor em
Química Sustentável

FACULDADE DE
CIÊNCIAS E TECNOLOGIA
UNIVERSIDADE NOVA DE LISBOA

Outubro de 2011

Development of molecularly imprinted polymers using supercritical fluid technology

Copyright

Mara Lília Soares da Silva

Universidade Nova de Lisboa, Faculdade de Ciências e Tecnologia

A Faculdade de Ciências e Tecnologia e Universidade Nova de Lisboa têm o direito, perpétuo e sem limites geográficos, de arquivar e publicar esta dissertação através de exemplares impressos reproduzidos em papel ou de forma digital, ou por qualquer outro meio conhecido ou que venha a ser inventado, e de a divulgar através de repositórios científicos e de admitir a sua cópia e distribuição com objectivos educacionais ou de investigação, não comerciais, desde que seja dado crédito ao autor e editor.

As secções desta dissertação já publicadas por editores para os quais foram transferidos direitos de cópia pelos autores, encontram-se devidamente identificadas ao longo da dissertação e são reproduzidas sob permissão dos editores originais e sujeitas às restrições de cópia impostos pelos mesmos.

To my son Martim

Acknowledgements

I have learned much during my PhD and the first person to whom I really want to express my gratitude is Dr. Teresa Casimiro. I am very thankful for the guidance, the helpful brainstormings and the friendship. Things would have been much more complicated if I did not have the luck of having a supervisor who pushed me up in the hard days and shared my happiness with the achievements. I will always keep in mind the useful teachings concerning polymers and supercritical fluid technology and the good moments in New Orleans (MIP… NIP…MIP…NIP). Teresa is a great scientist and a wonderful person.

I also acknowledge Prof. Ana Aguiar Ricardo for receiving me in her laboratory, allowing me to take the research of my thesis under her supervision and always get time when I needed her.

My sincere thanks to "the big boss" Prof. Manuel Nunes da Ponte, for the financial support in Socrates course that greatly contributed to my knowledge about supercritical fluid technology and also for the polka dance.

I also would like to thank Prof. Eurico Cabrita (HP NMR) and Dr. Luis Mafra (Solid-state NMR) for helping me in the characterization of the imprinting systems.

Further I want thank Dr. Jorge Caldeira for the guidance in my first contact with chromatography and Dr. José Catita for the knowledge transfer in HPLC and for letting me know the importance and difficulty of my work ("…You know what you're doing? If that works you'll be rich."). As for now, I am not… but maybe one day I will!

To Prof. Ílidio Correia thanks for the cytotoxicity studies that had greatly enriched my work and to Dr. Maria Manuela Marques for providing me the cyclodextrin derivatives. To Dr. Vasco Bonifácio I want to thank the help in organic chemistry.

To Fundação Ciência e Tecnologia thanks for financially supporting this thesis through grant SFRH/BD/31085/2006 and projects PTDC/QUI/66086/2006 and PTDC/QUI-QUI/102460/2008.

To all my supercritical colleagues of Lab. 510, for turning days at work in nice moments. A special thanks to Rachel (Raquel) for sharing with me the enthusiasm of molecular imprinting, to Telma, Vanessa, Margarida, Rita, Eunice and Franklin and to the former member, Marcio. Also to Ricardo and Pedro for providing the laboratory the nice fragrance of roasted coffee beans.

To Dª Idalina and Dª Conceição, to Dª Maria José and Sr. Ramalho I thank for the technical help.

I would also like to thank my friends for standing by me through tough times and for understanding the lack of time.

I finally thank to my family. I am very grateful to my parents for always believe me and support my decisions, no matter in what direction they were. You are my mentors in life. I also thank my

grandparents for their love and teaching that helped me to grow as person. To my husband and soul mate, Pedro, I want to thank for always being there for me and finally to by beloved son, Martim, I thank for fulfilling my days with love and tender and for being the source of my strength. I would not have made it this far if it was not you. I love you all!

Resumo

Ao longo da última década, o interesse em polímeros com impressão molecular tem vindo a intensificar-se devido à sua utilização promissora em processos de separação, libertação controlada de fármacos, sensores biomiméticos e catálise. O trabalho descrito nesta tese apresenta o uso da tecnologia supercrítica como uma alternativa sustentável na síntese e processamento de polímeros com impressão molecular. A afinidade das matrizes para determinadas moléculas foi introduzida através das técnicas de impressão molecular não-covalente e semi-covalente. O reconhecimento molecular dos polímeros foi avaliado em aplicações específicas de libertação controlada de fármacos, separação enantiomérica e adsorção de poluentes ambientais. A influência de determinados parâmetros experimentais no reconhecimento molecular das matrizes foi estudada através da variação do grau de reticulação, da natureza do monómero funcional e da razão molar entre a molécula a introduzir afinidade e o monómero. Os resultados obtidos mostram que é possível ajustar a afinidade dos polímeros através da optimização da mistura reaccional. Os polímeros com impressão molecular apresentam maiores constantes de afinidade para a molécula em questão e conseguem incorporar na sua matriz uma quantidade mais elevada dessa mesma molécula, quer seja em meio supercrítico ou em meio aquoso. Uma parte do trabalho desenvolvido envolveu a produção de membranas híbridas preparadas pelo método de inversão de fases, utilizando o dióxido de carbono supercrítico como não solvente. Os resultados obtidos evidenciam a possibilidade de preparar estruturas porosas com afinidade através da imobilização de partículas poliméricas com impressão molecular. A utilização dos polímeros como enchimento quiral em colunas de HPLC revelou que as matrizes poliméricas sintetizadas possuem uma elevada afinidade para a molécula que reconhecem, sendo capazes de diferenciar os dois enantiómeros quando a mistura racémica é injectada na coluna.

O trabalho desenvolvido no decorrer desta tese contribui para a consolidação da utilização do dióxido de carbono como um solvente alternativo na síntese e processamento de polímeros e demonstra a exequibilidade de sintetizar fácil e rapidamente polímeros com afinidade molecular utilizando tecnologias sustentáveis.

Termos chave

Tecnologia de fluidos supercríticos, processos sustentáveis, impressão molecular, libertação de fármacos, cromatografia, membrana híbrida com impressão molecular.

Abstract

Within the last decade, the interest in molecularly imprinted polymers (MIPs) has strongly increased because of their promising applications in separation processes, drug delivery, biomimetic sensing and catalysis. This thesis reports the development of MIPs using supercritical fluid technology as a viable and greener alternative to the synthesis and processing of these molecular recognition polymers. The affinity to the target molecule was introduced by means of non-covalent and semi-covalent molecular imprinting and the performance of the materials was evaluated in specific applications of drug delivery, chiral chromatography and adsorption of environmental pollutants. The influence of experimental parameters, such as crosslinking degree, functional monomer nature and template: monomer ratio, on molecular recognition was investigated. The results show that it is possible to tune the affinity of the polymers by optimizing the imprinting reactional mixture. MIPs show higher loading capacities and affinity constants to the template molecule, both in supercritical and aqueous environments. Hybrid membranes were prepared by a $scCO_2$-assisted phase inversion method, showing that imprinted particles can be immobilized into porous structures introducing affinity to the materials. Further, HPLC experiments attested that the synthesized MIPs have high selectivity towards the template, as an enantiomeric differentiation was achieved when the racemic mixture was loaded into the imprinted polymeric stationary phase.

The work developed in this thesis contributes to the consolidation of $scCO_2$ as alternative solvent and demonstrates the feasibility of synthesizing clean, easy-to-make and ready-to-use molecular recognition polymers using sustainable technologies.

Keywords

Supercritical fluid technology, sustainable processes, molecular imprinting, drug delivery, chromatography, hybrid imprinted membrane.

List of Contents

List of Figures

List of Tables

List of Abbreviations

AA	Acrylic Acid
AM	Acrylamide
AIBN	Azobis(isobutyronitrile)
BET	Brunauer–Emmet–Teller
Boc-Trp	Boc-Tryptophan
BPA	Bisphenol A
BPADM	Bisphenol A dimethacrylate
CD	Cyclodextrin
$CDCl_3$	Deuterated Chloroform
CE	Capillary Electrophoresis
CSP	Chiral Stationary Phase
DDS	Drug Delivery System
DEAEM	2-(diethylamino) ethyl methacrylate
DEGDMA	Diethylene Glycol Dimethacrylate
DMA	Dynamic Mechanical Analysis
DMAEMA	2-(Dimethylamino)ethyl methacrylate
DMF	Dimethylformamide
DVB	Divinylbenzene
EE	α-Ethinylestradiol
EGDMA	Ethylene Glycol Dimethacrylate
EMEM, EBSS	Eagles Minimum Essential Medium with Earle's Balanced Salt Solution
EtOH	Ethanol
FA	Flufenamic Acid
FBS	Fetal Bovine Serum
FTIR	Fourier Transform Spectroscopy
GAS	Gas Antisolvent
GC	Gas Chromatography
Gly	Glycine
HCl	Hydrochloric Acid
HEMA	2-hydroxyethylmethacrylate
HOESY	Heteronuclear Overhauser Effect Spectroscopy
HPLC	High Performance Liquid Chromatography
HP NMR	High-pressure NMR
IA	Itaconic Acid
KBr	Potassium Bromide

LCST	Lower critical solution temperature
MAA	Methacrylic Acid
MALDI-TOF	Matrix-assisted laser desorption/ionization – time of flight
MeCN	Acetonitrile
MeOH	Methanol
MIM	Molecularly Imprinted Membrane
MIP	Molecularly Imprinted Polymer
MIP CD	Molecularly imprinted polymer with Cyclodextrin moiety
MTS	3-(4,5-dimethylthiazol-2-yl)-5-(3-carboxymethoxyphenyl)-2-(4-sulfophenyl)-2H-tetrazolium
n-Bu_4NOH	Tetrabutylammonium hydroxide
NEAA	Non-essential amino acids
NIP	Non-Imprinted Polymer
NIPAAm	N-isopropylacrylamide
NIP CD	Non-imprinted polymer with cyclodextrin moiety
NOE	Nuclear Overhauser Effect
NOESY	Nuclear Overhauser Effect Spectroscopy
NVP	N-vinyl pyrrolidone
PBS	Phosphate Buffer Solution
PEG200DMA	Polyethylene glycol (200) dimethacrylate
PGSS	Particles from Gas-Saturated Solutions
PMMA	Poly(methyl methacrylate)
PRO	Progesterone
PVA	Poly(vinyl alcohol)
PVP	Poly(vinylpyrrolidone)
REACH	Registration, Evaluation, Authorization and Restriction of Chemical Substances
RESS	Rapid Expansion of Supercritical Solutions
SAA	Supercritical Assisted Atomization
$scCO_2$	Supercritical carbon dioxide
SEM	Scanning electron microscopy
SPE	Solid Phase Extraction
TFMAA	2-(trifluoromethyl)acrylic acid
Vpy	Vinylpyridine

CHAPTER 1

Introduction

1. Introduction

Over the last years, chemistry and related industries have transformed our daily life in such a way that it is impossible to imagine how our life would be without pharmaceutical drugs, plastics, diesel, food packages, detergents and many others. Even with such high impact on the society, the majority of the population still misinterprets the benefits of chemistry and associates it with pollution and environmental harm. However, great efforts have been done by chemists and engineers to develop greener and more sustainable processes. Moreover, with the increased restrictions imposed by REACH (Registration, Evaluation, Authorization and Restriction of Chemical Substances – EC 1907/2006), much attention has been given to the protection of human health and environment, enhancing the development of new greener alternatives to already well-established processes. The substitution of hazardous organics by green solvents, such as ionic liquids and supercritical fluids has the potential to yield more sustainable processes and improved final products. Within this purpose, the use of supercritical fluid technology to synthesize and process molecular recognition polymers was investigated and will be presented in this thesis.

1.1 Supercritical fluids

A supercritical fluid is a substance above its critical temperature and pressure but bellow the pressure required to condense it from the fluid to the solid state [1]. Figure 1.1 illustrates the phase diagram for carbon dioxide.

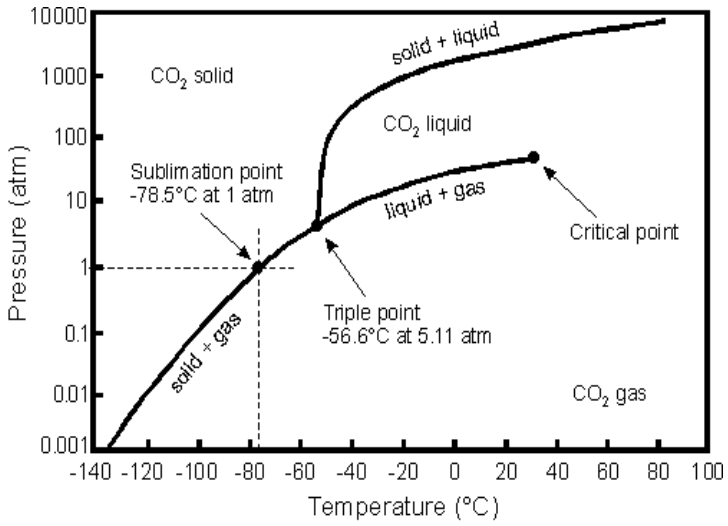

Figure 1.1- Phase diagram of carbon dioxide.

The properties of supercritical fluids are somewhat intermediate between those of liquids and gases (Table 1.1), with the exception of compressibility and heat capacity that are significantly higher in the vicinity of the critical point. Properties such as gas-like diffusivities and liquid-like densities, in addition to the easily tuneable solvent power are some advantageous properties of supercritical fluids [2].

Table 1.1. - Physical properties of gases, liquids and supercritical fluids.

	Diffusivity (cm^2/s)	**Density (g/mL)**	**Viscosity (Pa.s)**
Gases	0.1	10^{-3}	10^{-5}
Supercritical fluids	10^{-3}	0.3	10^{-4}
Liquids	5×10^{-6}	1	10^{-3}

The most commonly used supercritical fluids and their corresponding critical parameters are shown in Table 1.2.

Table 1.2 - Critical data for some fluids.

Fluid	**Critical temperature (ºC)**	**Critical pressure (MPa)**
Carbon dioxide	31.1	7.38
Water	374.0	22.06
Methane	-82.6	4.60
Ethane	32.2	4.87
Propane	96.7	4.25
Methanol	239.5	8.08
Ammonia	132.4	11.32

Supercritical carbon dioxide ($scCO_2$), in particular, possesses numerous properties that made it emerge as the most extensively studied supercritical fluid. It has a low critical point, is inexpensive, readily available in high purity and is a gas under ambient conditions, meaning that by simple depressurization of the system no solvent residues will be found in the final product. In the last years, $scCO_2$ has already proved to be an excellent medium for the synthesis and processing of polymers [3, 4, 5], impregnation of active substances [6], formation of porous structures [7, 8], dry cleaning [9], chemical reactions [10], extraction [11], etc.

Within this thesis special focus will be given to $scCO_2$-assisted polymerization, impregnation and membranes' preparation.

1.2 Molecular recognition

Molecular recognition comprises the specific interactions that enable one chemical entity to selectively recognize its physical and chemically complementary target molecule. The recognition mechanism is mainly mediated by weak non-covalent interactions, such as hydrogen bonding, ion-pairing, hydrophobic interactions and dipolar associations that as a whole govern the structural conformation of macromolecules and influence their interaction with other molecules. In nature there are several examples of successful recognition mechanisms in biological systems, such as DNA-protein, RNA-ribosome and antigen-antibody. Biomolecules however tend to lose their recognition properties in abiotic environments. Furthermore they are considerably expensive, which limits their applicability. For those reasons scientists have shown a great interest in the design of artificial supramolecular systems that exhibit molecular recognition. Examples of these materials are crown ethers and calixarenes, that selectively bind specific cations [12], derivatives of natural cyclodextrins [13], dendrimers [14] and molecularly imprinted polymers.

1.2.1 Molecularly imprinted polymers

The first time that selectivity effects was observed and explained in terms of a template influence was in 1931 in the group of Professor Polyakov [15], that reported some unusual adsorption properties in silica particles. The work reported a higher capacity for uptake the additive that had been in contact with the silica than for its structurally related ligands. At the time of Polyakov's first papers, the origin of the selectivity of antibody-antigen was under discussion [16]. Linus Pauling, in 1940, suggested that antibody formation took place in the presence of an antigen that was captured by the cell and served as a template for antibody formation. Although this hypothesis was not correct, it somehow describes the principle of the synthesis of molecularly imprinted polymers.

Molecularly imprinted polymers (MIPs) are architectured using a synthetic approach to design affinity matrices towards a target molecule, the template, via molecular imprinting process. During imprinting, the complexes between template and functional monomer(s) are frozen within a rigid porous polymeric matrix by copolymerization with a crosslinker in the presence of a porogen [17]. Template removal from the imprinted polymer at the end of the reaction leaves accessible chemical and sterically complementary binding sites. The generally accepted mechanism for the formation of MIPs is schematically presented in Figure 1.2.

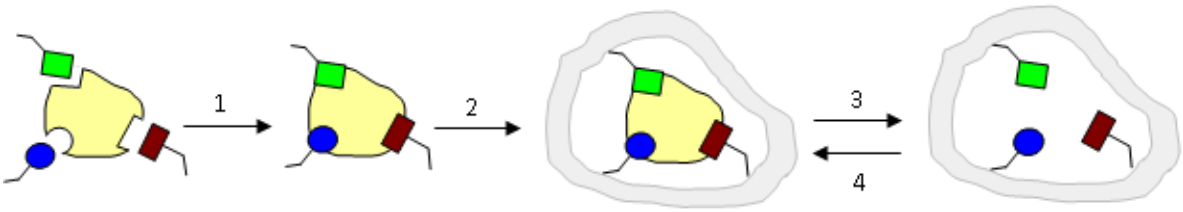

Figure 1.2- Molecular imprinting schematic mechanism: (1) Monomer and template pre-assembly; (2) Polymerization with crosslinking agent; (3) Polymer-template bonds disruption and subsequent template removal; (4) Template rebinding.

Imprinted polymers are synthetic receptors with binding constants comparable to natural receptors [18,19], but capable of withstanding harsh conditions of temperature [20], pressure [21], extreme pH [20] and organic solvents [22]. MIPs are also less expensive to synthesize and can be manufactured in large quantities with good reproducibility. These properties have led to a significant increase in reported applications in the last decade such as in synthesis and catalysis [23,24], solid-phase extraction [25, 26], chromatography [27,28], sensing [29,30] and in drug delivery [31,32]. There are, even, some pioneer companies (MIP Technologies, now part of Biotage and Polyintell) that commercially developed imprinted polymers to act as sorbents for analytical applications such as solid-phase extraction.

Although molecular imprinting process seems conceptually simple, the molecular level events that take place in the polymerization mixture are very complex. The basis for successful imprinting relies in the formation of stable monomer-template adducts, whose interaction strength varies from van der Waals to reversible covalent bonds. The energetic contributions to the thermodynamic balance, first developed by Williams [33] that are the basis for the recognition event that rules both binding site formation and template-MIP rebinding [34, 35] are described in Equation 1.1.

$$\Delta G_{bind} = \Delta G_{t+r} + \Delta G_r + \Delta G_h + \Delta G_{vib} + \sum \Delta G_p + \Delta G_{conf} + \Delta G_{vdW} \qquad \text{(Equation 1.1)}$$

Where the Gibbs free energy changes are: ΔG_{bind}, complex formation; ΔG_{t+r}, translational and rotational Gibbs free energy, associated with the combination of two or more entities in a complex, carries implications with the order of complexes that may form; ΔG_r, restriction of rotors upon complexation, is related with the higher selectivity observed in systems with more rigid structures because the lower number of possible conformations leads to narrower site distribution; ΔG_h, hydrophobic interactions, are especially important when using water as the solvent; ΔG_{vib}, Gibbs free energy associated with the residual soft vibrational modes, is dependent on the polymerization

temperature; $\sum \Delta G_p$, the sum of interacting polar contributions, rules the degree of template binding selectivity as a result of different template-functional monomer interaction strengths; ΔG_{conf} and ΔG_{vdW}, Gibbs free energies, are related with adverse conformational changes and unfavourable van der Waals interactions, respectively, reflecting the need of matrix conformation compromise and degree of effective solvation. The resultant ΔG_{bind}, determines the number of interaction sites formed and their heterogeneity. The more stable and numerous the template-monomer complexes, the higher the number and homogeneity of the affinity sites in imprinted polymer.

1.2.2 Strategies in molecular imprinting

Molecularly imprinted polymers can be prepared according to a number of approaches that essentially differ in the way the template interact with the functional monomer and later with the polymeric binding sites. Although the divisions among them are becoming somewhat blurred due to the emergence of more complex hybrid strategies, the main molecular imprinting approaches considered are covalent, non-covalent, semi-covalent and metal ion-mediated imprinting. Table 1.3 highlights some works found in literature, developed on the basis of these strategies.

Table 1.3 - MIPs prepared using different imprinting approaches.

Imprinting Strategy	Reactional System	References
Covalent	β-D-Fru-Val-*O*-bis(4-vinylphenylboronate) and ethylene glycol dimethacrylate (EGDMA)	[36]
Non-Covalent	(-)-nicotine, methacrylic acid (MAA) and EGDMA	[37]
Semi-Covalent	propazine methacrylate and EGDMA	[38]
Metal ion	Tetracycline, Fe^{2+}, Mg^{2+} or Cu^{2+}, MAA and EGDMA	[39]

Covalent imprinting, pioneered by Wulff [40], was the first strategy to introduce molecular affinity in organic polymeric networks. This imprint methodology makes use of covalent bonds both on binding site formation, by using templates with covalently bound polymerizable groups, and in the rebinding process. At the end of the polymerization the template is cleaved from the matrix and the functionality left in the binding site is available for future covalent rebind. The great advantage when using this approach is that the functional groups are only associated with template sites. However, limitations found in the type of compounds that can be imprinted by this way (alcohols(diols), aldehydes, ketones,

amines and carboxylic acids) and difficulties in the cleavage of the template, led to the development of other imprinting methodologies.

Non-covalent imprinting, first developed by the group of Mosbach [41], is currently the most widely applied approach to produce molecular recognition matrices. By means of this technique, template and functional monomer(s) self-assembly through non-covalent interactions such as hydrogen bonding, ion-paring and dipole-dipole interactions, and template rebinding is achieved also via non-covalent interactions. The simplicity of this method, allied with the easy and cheap preparation, as well as the high selectivity that the polymers prepared by this approach can have, seem to overcome potential template-monomer complex stabilization issues, in which the success of this route relies.

Semi-covalent imprinting route combines both covalent interactions, by using a template with polymerizable groups and non-covalent bonds during the rebinding process. The advantages of this route are a narrower distribution of the binding sites and the inexistence of other kinetic restrictions than those encountered by diffusion. Two different approaches have been developed in which the template and the monomer are directly connected or, hence, have a sacrificial spacer group between them. This latter has been intensively developed by the group of Whitcombe [42].

Metal ion-mediated imprinting uses the ability of metal ions to target a wide range of functional groups through the donation of electrons from heteroatoms of ligands to the unfilled orbitals of the outer coordination sphere of the metal. The general procedure for active site formation usually consists in using a polymerizable ligand to complex the metal ion that coordinates to the template [43].

1.2.3 Rational design of MIPs

The development of MIPs involves the optimization of a number of experimental variables that determine the thermodynamic balance of the system and consequently the formation of high specific active sites towards the template molecule. The more important considerations are related with a careful choice of monomer, template and ratios between them, crosslinking degree and porogen.

The template molecule has a central role in imprinting process, as it directs the organization of the functional groups of the monomers. For that reason, when choosing the template, an appropriate monomer with complementary functionality should be chosen so that the complex formation can be maximized. [44] The crosslinker agent fulfils three main purposes in imprinting technique, it controls the polymer morphology (whether the matrix formed is of gel type, macroporous or microgel powder), it freezes the functional monomer-template complex within the matrix and imparts mechanical stability to the polymeric network. From the polymerization and molecular recognition process point of view it is generally advantageous to work with high crosslinking degrees. Nevertheless, depending on the applications, low crosslinked polymers can be a valuable option. In this thesis the study of these parameters will be presented in Chapter 2.

Sellergren [45] studied the influence of the polymerization pressure in the imprinting process by using three different solvents (dichlorometane, methanol and 2-propanol) and two different triazines as templates. The idea was to understand if template monomer assemblies could be stabilized in high pressure and if this would result in higher affinities. The results showed that, depending on the template, high-pressure could enhance the selectivity of the polymer or else have no effect. In both cases the affinity and selectivity in the rebinding process increased with decreasing hydrogen-bonding capacity of the porogen. Although the study was performed by using hydrostatic pressure and no supercritical conditions, their results support the idea that high-pressure could stabilize template-monomer complexes.

1.2.4 Molecular imprinting in $scCO_2$

The porogen used in the imprinting process has a significant effect in surface morphology and molecular recognition properties of the polymers. [46,47] The effect is particularly important when developing imprinted matrices by non-covalent imprinting route. Non-covalent imprinting, although technically straightforward, demands an efficient stabilization of the individually weak non-covalent interactions between template and functional monomers. As the process occurs in the presence of the porogen, imprinting success depends on the relative amount of cross interaction between the solvent and the intended non-covalent interactions (hydrogen bonding, hydrophobic interactions, π–π orbital interactions, ionic interactions, and van der Waals forces) employed during template–monomer complex formation. If the solvent interferes or competes with any of these interactions, less effective recognition will occur.

The most common method to produce MIPs, bulk polymerization, yields a monolithic polymer which has to be crushed, ground and sieved, leading to product loss of about 50% and resulting in irregular particles in both shape and size with binding sites partly destroyed [48,49]. Alternative methods have been proposed, such as *in situ*, multi-step swelling and suspension polymerizations [50]. However they still show limitations such as heterogeneity, complicated procedures, large use of template, phase partitioning and excessive use of organic solvents.

The increasing restrictions in the use of organic solvents prompted the development of new greener preparation methods. Some efforts have been made in the synthesis of imprinted polymers in aqueous environment, by using functional monomers that may stabilize the complexes through hydrophobic interactions, such as cyclodextrins [51] or by multi-step polymerization procedure. Nevertheless the use of water weakens other non-covalent interactions, such as hydrogen bond and electrostatic interactions and the two step procedures are time-consuming. Furthermore at the end of polymerization, energy intensive drying steps are required.

$ScCO_2$ – assisted molecular imprinting has recently demonstrated to be a clean and one-step synthetic route for the preparation of affinity polymeric materials, with attested performance in chromatography [52], drug delivery [53] and extraction [54,55] The advantages of using $scCO_2$ as porogenic solvent in imprinting process go beyond environmental concerns. By performing the synthesis in an apolar aprotic porogen, such as $scCO_2$, the template-functional monomer complexes can be highly stabilized giving rise to well-defined active sites and leading to materials with high affinity. Furthermore the matrices can have a controlled morphology and are obtained as dry powders, with no solvent residues, avoiding purification and drying steps. These are major advantages over conventional methods.

1.3 Molecularly imprinted polymers in drug delivery

Traditional drug delivery of pharmaceutical compounds requires pulsatile delivery, being frequently associated with high concentration doses and therefore increasing the risk of toxic side effects. Figure 1.3 illustrates these drug concentration fluctuations found in traditional delivery. If the active compound possesses a narrow therapeutic window, concentrations in plasma can easily be found above the toxic levels or otherwise below the minimum effective concentration level. Drug delivery systems (DDS) are often required to overcome this issue and others such as the need to protect the drug against metabolic attack, effectively delivering it at the right site and at the right time. Drug delivery systems can comprise polymers, liposomes, cyclodextrins and several combinations among them.

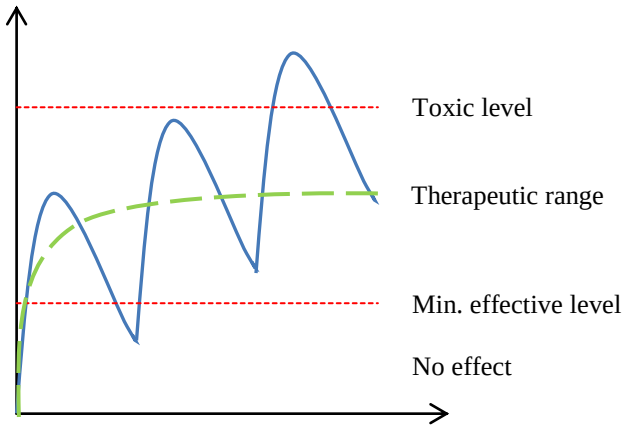

Figure 1.3- Drug concentration as function of time. Adapted from [56].

Over the last years polymeric materials have found a wide range of applications in medicine, not only as pharmaceutical excipients in drug delivery systems [57], but also in prostheses, contact lenses and other medical devices [58]. Polymer-based drug release devices carry the active molecule dispersed

within the matrix and, depending on the formulation, they can release the therapeutic agent over a prolonged period of time and under determined physiological conditions of temperature and/or pH. The sustained release increases the drug residence time in the body and therefore can enhance the therapeutic activity of the molecule. Moreover, tuning the drug delivery at specific body targets reduces the toxicity of the molecule and increases the therapeutic index.

The development of new drugs with enhanced complexity has increased the need in designing improved drug delivery systems. Moreover, the existing polymeric-based still shows some limitations such as the ability to release the drug only when the equilibrium concentrations in the plasma reach the minimum critical values. This feedback-controlled release would benefit from a drug delivery system with molecular recognition properties, able to store and release the drug while monitoring its concentration levels. The use of MIPs in this area could contribute to the development of better delivery devices.

Imprinted polymers have gained much importance over the last years due to their unique properties. Although no commercial MIPs for drug delivery are available in the market, the application of molecular imprinting technique in the development of drug delivery systems could be advantageous. The use of these recognition elements could improve the control over the therapeutic release by sustaining the delivery of the agent and, adjusting the crosslinking ratio, intelligently releasing the drug in response to the environment. Moreover molecular imprinting technique also enhances the loading capacity of the polymers towards the template drug.

Molecularly imprinted polymers can be used as unique delivery systems or incorporated into other drug release systems. Furthermore, the majority of the drugs act by a molecular recognition mechanism, which explains the growing interest in designing new and improved performance MIPs.

The first report on sustained drug delivery from a molecularly imprinted polymer was conducted by the group of Norell [59] that investigated the drug dissociation kinetic from theophylline-imprinted polymers, at different pH and loaded with different amounts of drug. Theophylline, a methylxanthine drug structurally similar to caffeine, used in the treatment of respiratory diseases such as asthma, has a narrow therapeutic window with pronounced side-effects at concentrations slightly above the therapeutic. The imprinted polymers synthesized demonstrated higher affinity towards theophylline than caffeine and displayed more sustained delivery than the corresponding non-imprinted polymer. Since the first work for specific application in drug delivery was described, many others have been reported which attempt to develop imprinted polymers with potential to be used as DDS. Some recent developments include the use of molecular imprinting to prepare materials for ocular, transdermal and oral drug delivery. Table 1.4 highlights some of those studies.

Table 1.4 – MIPs develeloped as DDS.

Type of drug delivery	Polymer/Drug system	References
Ocular	Poly(AA-co-Am-co-HEMA-co-PEGDMA), Poly(AA-co-HEMA-co-PEG200DMA), Poly(AM-co-HEMA-co-PEG200DMA) loaded with ketotifen	[60]
	P(HEMA-co-Vpy-co-EGDMA), P(HEMA-co-AA-co-EGDMA) loaded with norfloxacin	[61]
	Poly(PVA(macromer)-co-AM-co-NVP-co-DEAEM) loaded with hyaluronic acid	[62]
Transdermal	Cellulose membrane with MIP layer (MAA and EGDMA) loaded with S-propranolol	[63]
	Poly(MAA-co-EGDMA) loaded with 5-Fluorouracil	[64]
Oral	Poly(MAA-EGDMA) loaded with sulfasalazine	[65]
	Poly(NIPAAm-MAA-EGDMA) loaded with 4-aminopyridine	[66]

Over the last years a great effort has been made to develop imprinted matrices for drug delivery applications with some chain flexibility. Although the majority of imprinted polymers reported possess high crosslinking degree and therefore limited chain mobility, a certain degree of flexibility can be found in biological systems, with recognition occurring in aqueous environment as the result of numerous non-covalent interactions. Much of the theory concerning conformational memory in biological macromolecules, such as proteins, is valid for molecularly imprinted polymers. Thus, the design of imprinted matrices with a certain mobility of the polymeric chains has been studied to improve the properties of common hydrogels. Low crosslinked polymeric networks can experience reversible volume phase transitions in response to external stimuli, such as pH, temperature, electric field, light or even when in the presence of certain molecules, if stimuli-responsive monomers are used. The stimuli-sensitive properties, in combination with imprinting effect, engage considerable advantages. The imprinting process can impart the polymer high drug loading capacity whilst the flexible chains can provide a stimuli-sensitive character. Different conformation of the chains leads to different affinity of the matrix to the target molecule, which provides different drug release profiles, with "on-off" delivery being already documented [67].

The study of molecularly imprinted polymers as potential drug delivery systems although in an early stage has shown a significant growth within the last years and seems a promising way to introduce additional degrees of control in drug release. The development of MIPs to be used in drug delivery applications will be highlighted in Chapter 2 of this thesis.

1.4 Molecular recognition materials in chromatography

The worldwide research concerning drug development, food industry, enzyme engineering and catalyst technology, among many others, requires novel and improved methods to separate enantiomeric molecules. In pharmaceutical industry, in particular, much attention has been given to this issue as the research for new drugs with more targeted specificity and reduced side effects leads to the development of complex chemical structures that often exhibit chirality. With regulations demanding the use of the single enantiomeric form, market-share of pure enantiomer is in expansion. Figure 1.4 illustrates the distribution of approved drugs according to their chirality character. Pharmaceutical applicants have to determine the amount of each form and separate the enantiomers present in specific product samples [68]. The most common techniques for assessing the optical purity of pharmaceutical samples are high performance liquid chromatography (HPLC), gas chromatography (GC) and capillary electrophoresis (CE).

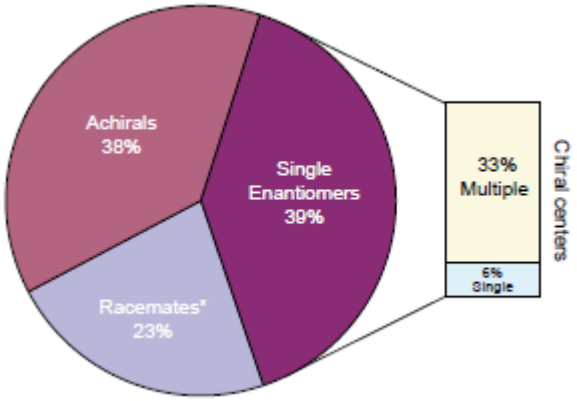

Figure 1.4 - Worldwide distribution of the approved drugs in the period of 1983-2002 according to their chirality character. *Including diastereomeric mixtures. Adapted from [68].

Chiral separations are the most challenging separations of chemical molecules, because the compounds possess the same molecular weight and properties and very similar molecular structures, as they are mirror images of each other. The need to differentiate so closely related molecules, led to the upsurge of methods able to resolve the racemates, either by using a chiral stationary phase (CSP), a pre-column chiral derivatisation or a chiral additive in the mobile phase [69]. Pre-column derivatisation with a chiral derivatisation reagent converts enantiomers into diastereomers that can be further separated using an achiral stationary phase. Although this method usually provides good separations, the presence of a functional group that can be derivatised and a high enantiomeric purity of the chiral derivatisation agent are necessary [70]. Chiral additives, mainly cyclodextrin derivatives, when added to the mobile phase form adducts with the enantiomeric species and allow the separation to be achieved in achiral columns. Chiral additives are readily available or can be easily synthesized

and can provide the separation of several important drugs. Their use is however restricted, as additives with high UV absorbance may decrease the detection limit of the separated enantiomeric molecules, when using a UV detector, being disadvantageous for the separation [71]. Chiral stationary phases are generally achieved by means of immobilizing small chiral molecules or polymers into supports such as silica gel. CSP based on optically active polysaccharide biopolymers, such as cellulose and amylose, that possess perfectly defined structures with high site density are readily available, although they usually lack from predictability of elution order and separation [72]. Some cyclodextrin-derivative CSPs proved to be efficient on the separation of amino acid enantiomers [73] although their high cost turn the chromatographic process economically disadvantageous. The use of imprinted polymers with chiral recognition ability could be considered a viable alternative as MIPs can replace expensive chiral columns and avoid chiral mobile phase additives and derivatisation with chiral reagents.

Chapter 3 of this thesis reports the development of an imprinted polymeric stationary phase with chiral recognition ability and the first studies concerning the design of a dual molecular recognition host of MIP and cyclodextrins.

1.4.1 Molecularly imprinted polymers as chiral stationary phases

A successful imprinting process is able to deliver polymeric networks with effective enantiomeric recognition properties when templating a chiral molecule. Higher affinity to the template enantiomer is translated in a predictable order of elution when using MIPs as chiral stationary phases, as the template establishes a higher number of interactions with the polymeric matrix and therefore is more retained. The use of imprinted polymers as stationary phases has been object of much research, with several papers published in the area. Table 1.5 summarizes some relevant works in this field.

The commercial application of MIPs as chiral stationary phases is thus far hampered essentially by the common peak broadening associated with these column packings. The broadening can be explained by mass transfer limitations and binding sites heterogeneity, with binding sites distribution ranging from high to low affinity, and by the irregularity of the particles obtained upon crushing the polymers prepared by bulk polymerization [74,75]. To overcome this latter drawback, much attention has been given to engineering suitable chromatographic imprinted formats and polymerization methods for enantiomeric separations. Porous monolithic devices, polymeric beads and composite MIP beads are some novel MIP formats [76,77].

Table 1.5 – Some MIPs tested as CSP reported in the literature.

Analyte	Polymeric system and Polymerization method	References
(S)-Nilvadipine	MAA, TFMAA, 2-Vpy, 4-Vpy as functional monomers, EGDMA as crosslinker and polystyrene seed particles. *Multistep swelling*	[78]
(-)-Norepinephrine	MAA or IA as functional monomers and EGDMA as crosslinker. *In situ*	[79]
(D)-Phenylalanine	MAA as functional monomer, EGDMA as crosslinker and PVA as stabilizer. *Suspension*	[80]
Boc-L-tryptophan	NIPAAm as functional monomer and EGDMA as crosslinker. *Precipitation polymerization*	[52]
(-)-Isoproterenol	TFMAA as functional monomer and DVB as crosslinker. *Polymerization inside silica pores*	[81]

Monolithic imprinted chiral stationary phases are prepared by *in situ* polymerization within the chromatographic columns, using solvents with good porogenic properties in order to assure high porosity. Yin and co-workers had performed a comparative study of the chromatographic performance of nateglinide imprinted monolith and bulk polymer [82]. In their work, monolithic MIPs showed superior chromatographic properties than MIPs prepared in bulk, namely higher mass transfer kinetics and hence more rapid separation, as well as lower backpressures. A key parameter when developing this type of CSPs is the choice of the porogenic solvent, as the relative polarity necessary to prepare a porous rod with good flow-through properties may be disadvantageous for imprinting, because the solvent may compete with the template-monomer interactions.

Imprinted polymeric beads can be easily prepared by precipitation polymerization, leading to particles with a more homogeneous binding site distribution than bulk polymers [83]. Precipitation polymerization is a surfactant-free synthetic strategy that, depending on the operational variables can provide agglomerates or spherical particles, from an initial high diluted mixture in a poor solvent. Studies concerning the application of imprinted particles prepared by precipitation polymerization as CSPs revealed this is a straightforward and viable method to prepared HPLC column packings [84, 52].

Spherical imprinted particles, with controllable size, are usually prepared by suspension polymerization. In a typical procedure, water is used as the dispersing phase for the suspension of the stabilized droplets of hydrophobic monomers. This aqueous environment, however, may be prejudicial to the stabilization of the crucial template-monomer complexes, as water can disrupt the non-covalent interactions between those species and only relatively strong interactions, such as charge-supported

hydrogen bonds are compatible with this medium. To overcome this issue, Mosbach developed an alternative method for preparing spherical imprinted particles, by substituting water by perfluoroalkanes [85]. Although these particles led to a chromatographic packing with low pressure drops, allowing the increase of the flow rate, the high number of non-specific binding sites, attributed to a possible interaction of the surfactant with the template and the high cost of perfluoroalkanes compromised an extensive development of this method.

The group of Haginaka developed a sophisticated and efficient method for preparing uniformly sized spherical imprinted particles by multistep-swelling polymerization [86,87]. In a first step, polystyrene seed particles were mixed with a microemulsion prepared with activating solvent, surfactant and water. Once the particles were swollen, a second swelling was carried also in aqueous environment, in the presence of the imprinting reactional mixture. The resulting particles were tested as selective chromatographic packing and their chiral recognition ability attested in the separation of racemic naproxen, chlorpheniramine and others.

The synthesis of molecular recognition polymeric beads by imprinting inside the pores of preformed silica particles or by grafting a MIP film on porous silica supports are other reported methods to prepare CSPs [81,88]. Silica particles are most used mainly because they are commercially available in a wide variety of sizes and porosities [89]. Although the imprinted particles prepared by these methods present low back-pressures and high mass transfers, a significant peak broadening was observed.

Although MIP-based chiral stationary phases can be considered powerful tools to overcome some analytical challenges, much has to be done so that imprinted materials can be marketed. Efforts concerning the development of new materials with improved chromatographic performance properties could benefit from the use of alternative technologies and from the combination of already well-established molecular recognition materials, such as MIPs and cyclodextrins.

1.4.2 Cyclodextrins as molecular recognition materials

Cyclodextrins (CDs) are cyclic oligosaccharides composed of D-glucose units connected through α-(1,4) glucosidic linkages that are produced from starch by means of its enzymatic degradation. The most commonly used native cyclodextrins are α, β and γ-CD, which consist respectively of 6, 7 and 8 glucose units. Figure 1.5 illustrates the chemical structures of these cycloamyloses. The spatial distribution of the glucose units in the toroid structure allocate the polar hydroxyl groups at the outer surface of the cyclodextrin molecules, with primary hydroxyls at the narrow side and secondary hydroxyls at the wider side. For this reason the external surface is considerably hydrophilic, imparting water solubility, while the inner cavity, with less hydrophilic character, is capable of acting as a host for suitably sized low molecular weight molecules [73,90] or even polymers [91,92].

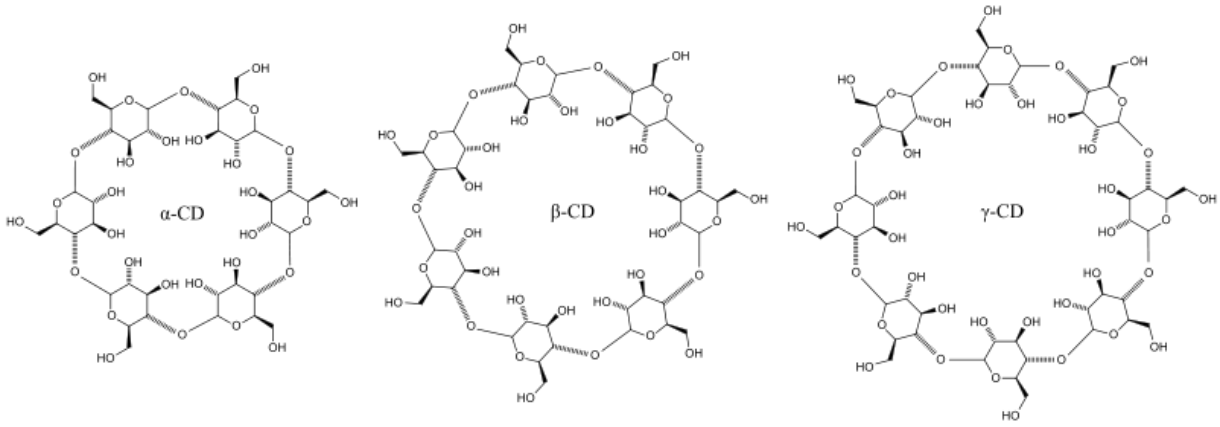

Figure 1.5 – Molecular structure of α, βand γ-CD

Ever since they were discovered in 1891 [93], cyclodextrins have been widely used because of their availability, low cost and ability to form complexes. Applications include pharmaceutical applications [94], cosmetics [95], textiles [96] and food industry [97], as well as analytical sciences and separation processes. Among their characteristic properties is the capability of forming complexes with different free energies for a given pair of enantiomers [98], allowing their chiral separation. Moreover, the increasing number of derivative molecules has opened up the applications of cyclodextrins, with a special focus on the possibility of synthesizing highly selective cyclodextrin-silica composites to be used as chiral stationary phases. Cyclodextrin-based chiral stationary phases with attested performance in the separation of a wide range of molecules such as amino acids, anti-inflammatory molecules, antibiotics and pesticides are reported in the literature [13, 99, 100].

Cyclodextrins can be polymerized and their recognition properties enhanced by means of molecular imprinting [101]. Molecularly imprinted cyclodextrin polymers can be polymerized in aqueous environments without disturbing the host-guest complexes, exhibiting therefore improved recognition properties in aqueous solutions. CD-based imprinted networks are usually prepared by crosslinking cyclodextrin molecules using diisocyanates [102,103] or epichlorohydrin [104]. However, novel procedures are emerging and the derivatization of the native cyclodextrins to prepare functional vinyl monomers that can be incorporated in typical polymeric networks conveys some advantages, such as the possibility of creating dual recognition hosts and stimuli-sensitive matrices.

1.5 Imprinted porous structures

Molecular recognition properties of MIPs in addition to their thermal, chemical and physical properties make them suitable alternatives to natural receptors in many applications. Nevertheless, the use in some diffusion-dependent processes such as sensing and membrane affinity separations demand an efficient immobilization onto solid surfaces, which is the most challenging issue. Nevertheless, successful immobilization of MIPs in a wide variety of material devices, such as in sensors, carbon nanotubes, electrospun fibers and flat sheet membranes are reported [105, 106, 107, 108, 109, 110, 111, 112].

The integration of MIPs in porous structures, such as membranes, can have a synergistic effect because the molecular recognition process benefits from the high surface area of the membrane and in turn the structure is able to selectively recognize a target molecule or a group of analogous molecules.

An ideal membrane should possess good mechanical properties, such as strength and flexibility, high permeability and ability to selectively transport the components that diffuse through it. Membranes are widely used in many industrial sectors in chemical, petrochemical, pharmaceutical and biotechnology processes. New trends in membrane technology encounter the development of highly selective membranes with molecular affinity character, inspired in natural recognition mechanisms. Molecularly imprinted membranes (MIMs) emerge as suitable candidates due to their low cost, ease of preparation and good molecular recognition performance.

The first report concerning molecularly imprinted membranes was presented by Piletsky [113], in 1990 and studied the recognition ability of an imprinted film prepared by bulk polymerization using adenosine monophosphate (AMP) as template. Ever since that work was published, many others have been reported aiming to improve the properties of imprinted membranes and increase their affinity to the target molecules. Table 1.6 shows some relevant publications in the field.

The preparation of imprinted membranes has been achieved by means of different strategies: synthesis of the imprinted polymer and sequential preparation of the membrane, simultaneous formation of imprinted sites and membrane morphology and synthesis of MIPs on a preformed membrane matrix. *In situ* crosslinking polymerization and synchronous film solidification had been reported in the early years of molecularly imprinted membranes preparation. Although the pioneer idea of creating imprinted membranes should be highlighted, the products obtained using this approach were far from an ideal affinity membrane as the high levels of crosslinker agent required to achieve the desirable selectivity, resulted in fragile membranes with poor mechanical stability [114,115].

Table 1.6 – Literature concerning the design and development of MIMs.

Analyte	Membrane composition	Preparation technique	References
Atrazine	Poly(methacrylic acid-co-tri(ethylene glycol) dimethacrylate-co-oligourethane acrylate)	In situ polymerization	[116]
Bisphenol A	Poly(bisphenol A dimethacrylate-co-divinyl benzene) with polystyrene, cellulose acetate, nylon 66 and polysulfone as scaffold polymers	Polymer solution casting	[117]
Folic acid	Poly(acrylonitrile-co-acrylamide)	Phase inversion	[118]
Lysozyme, Albumin, Immunoglobulin G	Fluoropolymer, disaccharide, epoxy resin and glass coverslip on mica support	Plasma deposition	[119]
Theophylline	Poly(methacrylic acid-co-ethylene glycol dimethacrylate) in cellulose support	Grafting	[120]

Simultaneous formation of the porous structure and recognition sites by phase inversion technique has been widely studied by many groups. Kobayashi has several papers concerning the preparation of imprinted membranes using this approach. The first work using this technique lacked a viable water flux, as the membranes had usually very low permeability [121]. However, recent research has led to the development of membranes with an acceptable water flux [122]. The major challenge engaged with this method centres on the different optimal conditions required to obtain an adequate porous structure formation without disturbing the complexes necessary to the molecular recognition mechanism.

Composite imprinted membranes prepared by casting the reactive imprinting mixture in the base scaffold membrane and polymerizing it using photo initiators [123] are well reported in the literature. The main advantage concerning this method is the possibility of choosing the base membrane which best corresponds to the need of the process and graft the structure with the recognition polymer, yielding either symmetric or asymmetric membranes.

The incorporation of pre-synthesized MIPs in a casting solution for membrane preparation has been reported only a few times up to now, maybe because blending a crosslinked polymer with an appropriate polymeric material for membrane production requires certain compatibility between the matrices that, not always, is easy to achieve. Furthermore the amount of MIP introduced is always limited to a fraction of the polymers. However, if a compatible blend of a polymeric material that acts

as a suitable scaffold and a functional polymer with recognition properties are able to form sufficiently strong intermolecular interactions, a stable porous hybrid imprinted structure can be prepared. In Chapter 4 of this thesis, the development of hybrid molecularly imprinted membranes prepared by $scCO_2$-assisted phase inversion will be presented.

1.6 Aims and structure of the thesis

The aim of this thesis was to develop molecularly imprinted polymers using supercritical fluid technology and investigate their performance in concrete applications.

The thesis is structured into four chapters. Chapter 1 highlights the use of supercritical fluids and reviews the state-of-the-art of molecular recognition materials, namely MIPs and cyclodextrins. The latter chapters describe the experimental work developed in the scope of the thesis.

Chapter 2 reports the rational design of MIPs as potential drug delivery systems (DDS). This chapter is subdivided in two parts. The first part states the influence of some experimental variables in the performance of MIPs as drug delivery carriers. Copolymers of methacrylic acid (MAA) with ethylene glycol dimethacrylate (EGDMA) and N-isopropylacrylamide (NIPAAm) with EGDMA were designed to have molecular recognition to flufenamic acid (FA), the template drug. The synthesized polymeric matrices with different ratios between template and functional monomer and different crosslinking degrees were further impregnated with FA in $scCO_2$ and the drug release profiles evaluated *in vitro*. The second part of the chapter describes the development of a low crosslinked imprinted polymer with molecular recognition to ibuprofen. Both MIP and NIP composed of 2-(dimethylamino)ethyl methacrylate (DMAEMA) and EGDMA were loaded with ibuprofen in $scCO_2$-assisted impregnation and evaluated as potential DDS in two different *in vitro* situations. In the first one the polymers were allowed to release the drug over several days and in the second one an oral administration situation was simulated and the polymers were subjected to different pHs and the drug release profiles studied for a period of 8 hours.

Chapter 3 reports the development of MIP-based chiral stationary phases for enantiomeric separations in HPLC using aqueous-organic mobile-phases. The chapter is subdivided in two parts. The first describes the synthesis and enantiomeric recognition ability of PEGDMA and P(NIPAAm-EGDMA) MIPs towards Boc-L-Tryptophan (Boc-L-Trp), the template molecule and its enantiomer, Boc-D-Trp. The analytical method was optimized to ensure that the best chromatographic conditions were used. The influence of some experimental variables, such as sample load and temperature on the retention factors of both enantiomeric species was studied. The second part of the chapter reports the design of a dual molecular recognition host of MIP and cyclodextrin with chiral recognition properties. The cyclodextrin derivative, 2-monoacryloyl-β-cyclodextrin monomer was copolymerized with NIPAAm and EGDMA in the presence of Boc-L-Trp and the performance of the resultant polymer evaluated by HPLC analysis.

Chapter 4 reports the development of imprinted polymeric materials for extraction of environmental pollutants, namely bisphenol A (BPA). The chapter is organized in two parts. The first describes the synthesis of the non-covalent MIP with further immobilization into a hybrid PMMA membrane structure, prepared using a $scCO_2$-assisted phase inversion method. The affinity of both polymeric

beads (MIP and NIP) and membranes (PMMA MIP and PMMA NIP) to bind BPA was tested in aqueous solutions, in batch equilibrium conditions. Moreover, the molecular recognition performance of the membranes was evaluated through filtration experiments. The second part of the chapter reports the synthesis of an imprinted polymer with molecular recognition to BPA, using the semi-covalent approach. By means of this route a polymerizable template molecule, bisphenol A dimethacrylate, was crosslinked with EGDMA. The hydrolysis of BPA from the matrix was performed in $scCO_2$, using tetratbutylammonium hydroxide (*n*-Bu_4NOH) as cleavage agent. Both MIP and NIP were evaluated with respect to their ability to adsorb BPA from aqueous solutions. Moreover, binding tests with progesterone (PRO) and α-ethinylestradiol (EE) were carried out to study the selectivity of MIP towards the template molecule.

1.7 References

[1] Jessop, P., Leitner, W., Chemical Synthesis using supercritical fluids, Wiley-VCH, New York, USA, 1999.

[2] Leitner, W., Jessop, P.G., Handbook of green chemistry, Volume 4: Supercritical Solvents, Wiley-VCH, Weinheim, 2010.

[3] Kendall, J.L., Canelas, D.A., Young, J.L., DeSimone, J.M., Polymerizations in supercritical carbon dioxide, Chem. Rev. 1999, 99, 543-563.

[4] Giles, M.R., Griffiths, R.M.T., Aguiar-Ricardo, A., Silva, M.M.C.G., Howdle, S.M., Fluorinated graft stabilizers for polymerization in supercritical carbon dioxide: the effect of stabilizer architecture, Macromolecules 2001, 34, 20-35.

[5] Jung, J., Perrut, M., Particle design using supercritical fluids: Literature and patent survey, J. Supercrit. Fluids 2001, 20, 179-219.

[6] Kikic, I., Vecchione, F., Supercritical impregnation of polymers, Curr. Opin. Solid State Mater. Sci. 2003, 7, 399-405.

[7] Reverchon, E., Cardea, S., Production of controlled polymeric foams by supercritical CO2, J. Supercrit. Fluids 2007, 40, 144-152.

[8] Temtem, M., Casimiro, T., Aguiar-Ricardo, A., Solvent power and depressurization rate effects in the formation of polysulfone membranes with CO_2-assisted phase inversion method, J. Membr. Sci. 2006, 283, 244-252.

[9] Sousa, M., João Melo, M., Casimiro, T., Aguiar-Ricardo, A., The art of CO_2 for art conservation: a green approach to antique textile cleaning, Green Chem. 2007, 9, 943- 947.

[10] Bogel-ukasik, E., Fonseca, I., Bogel-ukasik, R., Tarasenko, Y.A., Nunes da Ponte,M., Paiva, A., Brunner, G., Phase, equilibrium-driven selective hydrogenation of limonene in high-pressure carbon dioxide. Green Chem. 2007, 9, 427 – 430.

[11] Simões, P.C., Carmelo, P.J., Pereira, P.J., Lopes, J.A., Nunes da Ponte, M., Brunner, G., Quality assessment of refined olive oils by gas extraction. J. Supercrit. Fluids 1998, 13, 337-341.

[12] Ludwig, R., Dzung, N.T.K., Calixarene-based molecules for cation recognition, Sensors 2002, 2, 397-416.

[13] Malta, L.F.B., Cordeiro, Y., Tinoco, L.W., Campos, C.C., Medeiros, M.E., Antunes, O.A.C., Recognition mechanism of D- and L-tryptophan enantiomers using 2-hydroxypropyl-α- or β-cyclodextrins as chiral selectors, Tetrahedron: Asymmetry 2008, 19, 10, 1182-1188.

[14] Pittelkow, M., Nielsen, C.B., Kadziola, A., Christensen, J.B., Molecular recognition: minimizing the acid-base interaction of a tunable host–guest system changes the selectivity of binding, J. Incl. Phenom. Macrocycl. Chem 2009, 63, 257-266.

[15] Polyakov MV., Adsorption properties and structure of silica gel., Zhur. Fiz. Khim. 1931, 2, 799–805.

[16] Whitcombe, M.J., Vulfson, E.N., Imprinted polymers, Adv. Mater. 2001, 13, 7, 467-478.

[17] Alexander, C., Andersson, H.S., Andersson, L.I., Ansell, R.J., Kirsch, N., Nicholls, I.A., O'Mahony, J., Whitcombe, M.J., Molecular imprinting science and technology: a survey of the literature for the years up to and including 2003, J. Mol. Recognit. 2006, 19, 106-180.

[18] Chianella, I., Lotierzo, M., Piletsky, S.A., Tothill, I.E., Chen, B., Karim, K., Turner, A.P.F., Rational Design of a polymer specific for microcystin-LR using a computational approach, Anal. Chem. 2002, 74, 1288-1293.

[19] Hoshino, Y., Shea, K.J., The evolution of plastic antibodies, J. Mater. Chem. 2011, 21, 3517-3521.

[20] Svenson, J., Nicholls, I.A., On the thermal and chemical stability of molecularly imprinted polymers, Anal. Chim. Acta 2001, 435, 19-24.

[21] Baggiani, C., Giraudi, G., Trotta, F., Giovannoli, C., Vanni, A., Chromatographic characterization of a molecular imprinted polymer binding cortisol, Talanta 2000, 51, 71-75.

[22] Bossi, A., Bonini, F., Turner, A.P.F., Piletsky, S.A., Molecularly imprinted polymers for the recognition of proteins: The state of the art, Biosens. Bioelectron. 2007, 22, 1131-1137.

[23] Wulff, G., Enzyme-like catalysis by molecularly imprinted polymers, Chem. Rev. 2002, 102, 1-28.

[24] Ramström, O., Mosbach, K., Synthesis and catalysis by molecularly imprinted materials, Curr. Opin. Chem. Biol. 1999, 3, 759-764.

[25] Baggiani, C., Anfossi, L., Giovannoli, C., Solid phase extraction of food contaminants using molecular imprinted polymers, Anal. Chim. Acta 2007, 59, 29-39.

[26] Andersson, L.I., Paprica, A., Arvidsson, T., A highly selective solid phase extraction sorbent for pre-concentration of sameridine made by molecular imprinting, Chromatographia 1997, 46, 57-62.

[27] Wei, S., Mizaikoff, B., Recent advances on noncovalent molecular imprints for affinity separations. J. Sep. Sci. 2007, 30, 1794-1805.

[28] Kempe, M., Antibody-mimicking polymers as chiral stationary phases, Anal. Chem. 1996, 68, 1948-1953.

[29] Guan, G., Liu, B., Wang, Z., Imprinting of molecular recognition sites on nanostructures and its applications in chemosensors, Sensors 2008, 8, 8291-8320.

[30] Haupt, K, Mosbach, K., Molecularly imprinted polymers and their use in biomimetic sensors, Chem. Rev. 2000, 100, 2495-2504.

[31] C. Hung, Y.Huang, H. Huang, C. Hwang, Preparation of (S)-Ibuprofen-Imprinted Polymer and Its Molecular Recognition Study, J. Appl. Polym. Sci. 2006, 102, 2972–2979.

[32] Alvarez-Lorenzo, C., Concheiro, A., Molecularly imprinted polymers for drug delivery, J. Chromatogr. B 2004, 804, 231-245.

[33] Wiiliams, D.H., Cox, J.P.L., Doig. A.J., Gardner, M., Gerhard, U., Kaye, P.T., Lal, A.R., Nicholls, I.A., Salter, C.J., Mitchell, R.C., Towards the semiquantitative estimation of binding constants. Guides for peptide-peptide binding in aqueous solution, J. Am. Chem. Soc. 1991, 113, 7020-7030.

[34] Nicholls, I.A., Adbo, K., Andersson, H.S., Andersson, P.O., Ankarloo, J., Hedin-Dahlstrom, J., Jokela, P., Karlsson, J.G., Olofsson, L, Rosegren, J., Shoravi, S., Svenson, J., Wikman, S., Can we reationally design molecularly imprinted polymers?, Anal. Chim. Acta 2001, 435, 9-18.

[35] Nicholls, I.A.,Towards the rational design of molecularly imprinted polymers, J. Mol. Recognit. 1998, 11, 79-82.

[36] Rajkumar, R., Warsinke, A., Möhwald, H., Scheller, F.W., Katterle, M., Development of fructosyl valine binding polymers by covalent imprinting, Biosens. Bioelectron. 2007, 22, 3318-3325.

[37] Andersson, H.S., Karlsson, J.G., Piletsky, S.A., Koch-Schidt, A.-C., Mosbach, K., Nicholls, I.A., Study of the nature of recognition in molecularly imprinted polymers, II [1] Influence of monomer-template ratio and sample load on retention and selectivity, J. Chromatogr. A 1999, 848, 39-49.

[38] Cacho, C., Turiel, E., Martín-Esteban, A., Ayala, D., Pérez-Conde, C., Semi-covalent imprinted polymer using propazine methacrylate as template molecule for the clean-up of triazines in soil and vegetable samples, J. Chromatogr. A 2006, 1114, 255-262.

[39] Qu, G., Zheng, S., Liu, Y., Xie, W., Wu, A., Zhang, D., Metal ion mediated synthesis of molecularly imprinted polymers targeting tetracyclines in aqueous samples, J. Chromatogr. B 2009, 877, 3187-3193.

[40] Wulff, G., Schauhoff, S., Enzyme-analog-built polymers. 27. Racemic resolution of free sugars with macroporous polymers prepared by molecular imprinting. Selectivity dependence on the arrangement of functional groups versus spatial requirements, J. Org. Chem. 1991, 56, 395-400.

[41] Siemann, M., Andersson, L.I., Mosbach, K., Selective Recognition of the Herbicide Atrazine by Noncovalent Molecularly Imprinted Polymers, J. Agric. Food Chem. 1996, 44, 141-145.

[42] Kirsch, N., Alexander, C., Davies, S., Whitcombe, M.J., Sacrificial spacer and non-covalent routes toward the molecular imprinting of "poorly-functionalized" *N*-heterocycles, Anal. Chim. Acta 2004, 504, 63–71.

[43] Qu, S., Wang, X., Tong, C., Wu, J., Metal ion mediated molecularly imprinted polymer for selective capturing antibiotics containing beta-diketone structure, J. Chromatogr. A 2010, 1217, 8205–8211.

[44] Cormack, P.A.G., Elorza, A.Z., Molecularly imprinted polymers: synthesis and characterization, J. Chromatogr. B 2004, 804, 173-182.

[45] Sellergren, B., Dauwe, C., Schneider, T., Pressure-Induced Binding Sites in Molecularly Imprinted Network Polymers, Macromolecules 1997, 30, 2454-2459.

[46] Esfandyari-Manesh, M., Javanbakht, M., Atyabi, F., Badiei, A., Rassoul D., Effect of porogenic solvent on the morphology, recognition and release properties of carbamazepine-molecularly imprinted polymer nanospheres, J. Appl. Polym. Sci. 2011, 121, 118-1126.

[47] Yu, C., Mosbach, K., Influence of mobile phase composition and cross-linking density on the enantiomeric recognition properties of molecularly imprinted polymers, J. Chromatogr. A 2000, 888, 63-72.

[48] Baggiani, C., Baravalle, P., Anfossi, L., Tozzi, C., Comparision of pyrimethanil-imprinted beads and bulk polymer as stationary phase by non-linear chromatography, Anal. Chim. Acta 2005, 542, 125–134.

[49] Qiao, F., Sun, H., Yan, H., Row, K.H., Molecularly imprinted polymers for solid phase extraction, Chromatographia 2006., 64, 625–634

[50] Wei, S., Mizaikoff, B., Recent advances on noncovalent molecular imprints for affinity separations, J. Sep. Sci. 2007, 30, 1794–1805.

[51] Asanuma, H., Akiyama, T., Kajiya, K., Hishiya, T., Komiyama, M., Molecular imprinting of cyclodextrin in water for the recognition of nanometer-scaled guests, Anal. Chim. Acta 2001, 435, 25-33.

[52] Soares da Silva, M., Vão, E.R., Temtem, M., Mafra, L., Caldeira, J., Aguiar-Ricardo, A., Casimiro, T., Clean synthesis of molecular recognition polymeric materials with chiral sensing capability using supercritical fluid technology. Application as HPLC stationary phases, Biosens. Bioelectron. 2010, 25, 1742-1747.

[53] Duarte, A.R.C., Casimiro, T., Aguiar-Ricardo, A., Simplício, A.L., Duarte, C.M.M., Supercritical fluid polymerisation and impregnation of molecularly imprinted polymers for drug delivery, J. Supercrit. Fluids 2006, 39, 102-106.

[54] Ye, L., Yoshimatsu, K., Kolodziej, D., Francisco, J.D.C., Preparation of molecularly imprinted polymers in supercritical carbon dioxide, J. Appl. Polym. Sci. 2006, 102, 2863-2867.

[55] Kobayashi, T., Leong, S.S., Zhang, Q., Using polystyrene-co-maleic acid for molecularly imprinted membranes in supercritical carbon dioxide, J.Appl. Polym. Sci 2008, 108, 757-768.

[56] Kryscio, D.R., Peppas, N.A., Mimicking biological delivery through feedback-controlled drug release systems based on molecular imprinting, AIChE Journal 2009, 55, 1311-1324.

[57] Gaspar, R., Duncan, R., Polymeric carriers: Preclinical safety and the regulatory implications for design and development of polymer therapeutics, Adv. Drug Deliver. Rev. 2009, 61, 1220–1231.

[58] Xinming, L., Yingde, C., Lloyd, A.W., Mikhalovsky, S.V., Sandeman, S.R., Howel, C.A., Liewen, L., Polymeric hydrogels for novel contact lens-based ophthalmic drug delivery systems: A review, Contact Lens & Anterior Eye 2008, 31, 57–64.

[59] Norell, M.C., Andersson, H.S., Nicholls, I.A., Theophylline molecularly imprinted polymer dissociation kinetics: a novel sustained release drug dosage mechanism, J. Mol. Recognit. 1998, 11, 98-102.

[60] Venkatesh, S., Sizemore, S.P., Byrne, M.E., Biomimetic hydrogels for enhanced loading and extended release of ocular therapeutics. Biomaterials 2007, 28, 717-724.

[61] Alvarez-Lorenzo, C., Yañez, F., Barreiro-Iglesias, R., Concheiro, A., Imprinted soft contact lenses as norfloxacin delivery systems. J. Control. Release, 2006, 113, 236-244.

[62] Ali, M., Byrne, M.E., Controlled Release of High Molecular Weight Hyaluronic Acid from Molecularly Imprinted Hydrogel Contact Lenses, Pharmaceut. Res. 2009, 26, 714-726.

[63] Bodhibukkana, C., Srichana, T., Kaewnopparat S., Tangthong, N., Bouking, P., Martin, G.P., Suedee, R., Composite membrane of bacterially-derived cellulose and molecularly imprinted polymer for use as transdermal enantioselective controlled-release system of racemic propanolol, J. Control Release 2006, 113, 43-56.

[64] Puoci, F., Iemma, F., Cirillo, G., Picci, N., Matricardi, P., Alhaique, F., Molecularly Imprinted Polymers for 5-Fluorouracil Release in Biological Fluids, Molecules 2007, 12, 805-814.

[65] Puoci, F., Iemma, F., Muzzalupo, R., Spizzirri, U.G., Trombino, S., Cassano, R., Picci, N., Spherical molecularly impronte polymers (SMIPs) via a novel precipitation polymerization in the controller delivery of sulfasalazine, Macromol. Biosci. 2004, 4, 22-26.

[66] Liu, X.-Y., Ding, X.-B., Guan, Y., Peng, Y.-X., Long, X.-P., Wang, X.-C., Chang, K., Zhang, Y., Fabrication of Temperature-Sensitive Imprinted Polymer Hydrogel, Macromol. Biosci. 2004, 4, 412-415.

[67] Moritani, T., Alvarez-Lorenzo, C., Conformational imprinting effect on stimuli-sensitive gels made with an "Imprinter" monomer, Macromolecules 2001, 34, 7796.

[68] Caner, H., Groner, E., Levy, L., Agranat, I., Trends in the development of chiral drugs, Drug Discov. Today 2004, 9, 105-110.

[69] Davies, N.M., Methods of analysis of chiral non-steroidal anti-inflammatory drugs, J. Chromatogr. B 1997, 691, 229-261.

[70] Gübitz, G., Schmid, M.G., Chiral separation by capillary electromigration techniques, J. Chromatogr. A 2008, 1204, 140-156.

[71] Kazakevich, Y., Lobrutto, R., HPLC for pharmaceutical scientists, John Wiley & Sons, New Jersey, USA, 2007.

[72] Sellergren, B., Imprinted chiral stationary phases in high-performance liquid chromatography, J. Chromatogr. A 2001, 906, 227-252.

[73] Fujimura, K., Suzuki, S., Hayashi, K., Masuda, S., Retention behavior and chiral recognition mechanism of several cyclodextrin-bonded stationary phases for dansyl amino acids, Anal. Chem. 1990, 62, 2198-2205.

[74] Sajonz, P., Kele, M., Zhong, G., Sellergren, B., Guiochon, G., Study of the thermodynamics and mass transfer kinetics of two enantiomers on a polymeric imprinted stationary phase, J. Chromatogr. A 1998, 810, 1-17.

[75] Andersson, L.I., Molecular imprinting:developments and applications in the analytical chemistry field, J. Chromatogr. B 2000, 745, 3-13.

[76] Maier, N.M., Lindner, W., Chiral recognition applications of molecularly imprinted polymers: a critical review. Anal. Bioanal. Chem., 2007, 389, 377-397.

[77] Pérez-Moral, N., Mayes, A.G., Novel MIP formats, Bioseparation 2002, 10, 287-299.

[78] Fu, Q., Sanbe, H., Kagawa, C., Kunimoto, K.-K., Haginaka, J., Uniformly sized molecularly imprinted polymer for (S)-Nilvapidine. Comparison of chiral recognition ability with HPLC chiral stationary phases based on a protein. Anal. Chem. 2003, 75, 191-198.

[79] Huang, B.-Y., Chen, Y.-C., Wang, G.-R., Liu, C.-Y., Preparation and evaluation of a monolithic molecularly imprinted polymer for the chiral separation of neurotransmitters and their analogues by capillary electrochromatography, J. Chromatogr. A 2011, 1218, 849-855.

[80] Khan, H., Khan, T., Park, J.K., Separation of phenylalanine racemates using d-phenylalanine imprinted microbeads as HPLC stationary phases, Separation and Purification Technology 2008, 62, 363-369.

[81] Yilmaz, E., Ramström, Möller, P., Sanchez, D., Mosbach, K., A facile method for preparing molecularly imprinted spheres using spherical silica templates, J. Mater. Chem. 2002, 12, 1577-1581.

[82] Yin, J., Yang, G., Chen, Y., Rapid and efficient chiral separation of nateglinide and its L-enantiomer on monolithic molecularly imprinted polymers, J. Chromatogr. A 2005, 1090, 68-75.

[83] Cacho, C., Turiel, E., Martin-Esteban, A., Perez-Conde, C., Camara, C., Characterization and quality assessment of binding sites on a propazine-imprinted polymer prepared by precipitation polymerization, J. Chromatogr. B 2004, 802, 347-353.

[84] Wang, J., Cormack, P.A.G., Sherrington, D.C., Khoshdel, E., Monodisperse, molecularly imprinted polymer microspheres prepared by precipitation polymerization for affinity separation applications. Angew. Chem. Int. Ed. 2003, 42, 5336-5338.

[85] Mayes, A.G., Mosbach, K., Molecularly Imprinted Polymer Beads: Suspension Polymerization Using a Liquid Perfluorocarbon as the Dispersing Phase, Anal. Chem. 1996, 68, 3769-3774.

[86] Haginaka, J., Takehira, H., Hosoya, K., Tanaka, N., Molecularly imprinted uniform-sized polymer-based stationary phase for naproxen. Comparison of molecular recognition ability of the molecularly imprinted polymers prepared by thermal and redox polymerization techniques, J. Chromatogr. A, 1998, 816, 113-121.

[87] Haginaka, J., Kagawa, C., Uniformly sized molecularly imprinted polymer for d-chlorpheniramine. Evaluation of retention and molecular recognition properties in an aqueous mobile phase, J. Chromatogr. A 2002, 948, 77-84.

[88] Quaglia, M., De Lorenzi, E., Sulitzky, C., Massolini, G., Sellergren, B., Surface initiated molecularly imprinted polymer films: a new approach in chiral capillary electrochromatography, Analyst 2001, 126, 1495-1498.

[89] Turiel, E., Martin-Esteban, A., Molecularly imprinted polymers: towards highly selective stationary phases in liquid chromatography and capillary electrophoresis, Anal. Bioanal. Chem. 2004, 378, 1876-1886.

[90] Rüdiger, V., Eliseev, A., Simova, S., Schneider, H.-J., Blandamer, M.J., Cullis, P.M., Meyer, A.J., Conformational, calorimetric and NMR spectroscopic studies on inclusion complexes of cyclodextrins with substituted phenyl and adamantine derivatives, J. Chem. Soc., Perkin Trans. 2 1996, 2, 2119-2123.

[91] Rusa, C. C., Luca, C., Tonelli, A. E., Polymer-cyclodextrin inclusion compounds: toward new aspects of their inclusion mechanism, Macromolecules 2001, 34, 1318-1322.

[92] Harada, A., Okada, M., Li, J., Kamachi, M., Preparation and characterization of inclusion complexes of poly(propylene glycol) with cyclodextrins, Macromolecules 1995, 28, 8406-8411.

[93] Villiers, A., Sur la transformation de la fécule en dextrine par le ferment butyrique, Compt. Rend. Fr. Acad. Sci. 1891, 435-438.

[94] Loftsson, T., Duchêne, D., Cyclodextrins and their pharmaceutical applications, Int. J. Pharm. 2007, 329, 1-11.

[95] Centini, M., Maggiore, M., Casolaro, M., Andreassi, M., Facino, R.M., Anselmi, C., Cyclodextrins as cosmetic delivery systems, J. Incl. Phenom. Macrocycl. Chem. 2007,57, 109-112.

[96] Wang, J.-H., Cai, Z., Incorporation of the antibacterial agent, miconazole nitrate into a cellulosic fabric grafted with β-cyclodextrin, Carbohyd. Polym. 2008, 72, 695-700.

[97] Szente, L., Szejtli, J., Cyclodextrins as food ingredients, Trends Food Sci. Tech. 2004, 15, 137-142.

[98] Han, S., Direct enantiomeric separations by high performance liquid chromatography using cyclodextrins, Biomed. Chromatogr. 1997, 11, 259-271.

[99] Zhao, J., Tan, D., Chelvi, S.K.T., Yong, E.L., Lee, H.K., Gong, Y., Preparation and application of rifamycin-capped (3-(2-O-β-cyclodextrin)-2-hydroxypropoxy)-propylsilyl-appended silica particles as chiral stationary for high-performance liquid chromatography, Talanta 2010, 83, 286-290.

[100] Shishovska, M., Trajkovska, V., HPLC-method for determination of permethrin enantiomers using chiral β-cyclodextrin-based stationary phase, Chirality, 2010, 22, 527-533.

[101] Song, S.-H., Shirasaka, K., Katayama, M., Nagaoka, S., Yoshihara, S., Osawa, T., Sumaoka, J., Asanuma, H., Komiyama, M., Recognition of solution structures of peptides by molecularly imprinted cyclodextrin polymers, Macromolecules 2007, 40, 3530-3532.

[102] Egawa, Y., Shimura, Y., Nowatari, Y., Aiba, D., Juni, K., Preparation of molecularly imprinted cyclodextrins microspheres, Int. J. Pharm. 2005, 293, 165-170.

[103] Asanuma, H., Hishiya, T., Komiyama, M., Efficient separation of hydrophobic molecules by molecularly imprinted cyclodextrin polymers, J. Incl. Phenom. Macrocycl. Chem. 2004, 50, 51-55.

[104] Tsai, H.-A., Syu, M.-J., Synthesis of creatinine-imprinted poly(β-cyclodextrin) for the specific binding of creatinine, Biomaterials 2005, 26, 2759-2766.

[105] Reimhult, K., Yoshimatsu, K., Risveden, K., Chen, S., Ye, L., Krozer, A., Characterization of QCM sensor surfaces coated with molecularly imprinted nanoparticles, Biosens. Bioelectron. 2008, 23, 1908-1914.

[106] Lakshmi, D., Bossi, A., Whitcombe, M.J., Chianella, I., Fowler, S.A., Subrahmanyam, S., Piletska, E.V., Piletsky, S.A., Electrochemical sensor for catechol and dopamine based on a catalytic molecularly imprinted polymer-conducting polymer hybrid recognition element, Anal. Chem. 2009, 81, 3576-3584.

[107] Whitcombe, M.J., Chianella, I., Larcombe, L., Piletsky, S.A., Noble, J., Porter,R., Horgan, A., The rational development of molecularly imprinted polymer-based sensors for protein detection, Chem. Soc. Rev. 2011, 40, 1547-1571.

[108] Lee, E., Park, D.-W., Lee, J.-O., Kim, D.S., Lee, B.H., Kim, B.S., Molecularly imprinted polymers immobilized on carbon nanotube, Colloid Surfaces A 2008, 313-314, 202-206.

[109] Chronakis, I.S., Jakob, A., Hagström, B., Ye, L., Encapsulation and selective recognition of molecularly imprinted theophylline and 17β-estradiol nanoparticles within electrospun polymer nanofibers, Langmuir 2006, 8960-8965.

[110] Piperno, S., Bui, B.T.S., Haupt, K., Gheber, L.A., Immobilization of molecularly imprinted polymer nanoparticles in electrospun poly(vinyl alcohol) nanofibers, Langmuir, 27, 1547-1550.

[111] Pegoraro, C., Silvestri, D., Ciardelli, G., Cristallini, C., Barbani, N., Molecularly imprinted poly(ethylene-co-vinyl alcohol) membranes for the specific recognition of phospholipids, Biosens. Bioelectron. 2008, 24, 748-755.

[112] Hillberg, A.L., Brain, K., Allender, C.J., Dsign and evaluation of thin and flexible theophylline imprinted polymer membrane materials, J. Molec. Recognit. 2009, 22, 223-231.

[113] Piletsky, S.A., Dubey, I.Y., Fedoryak, D.M., Kukhar, V.P., Substrate-selective polymeric membranes. Selective transfer of nucleic acids components, Biopolym. Cell 1990, 6, 55-58.

[114] Ulbricht, M., Membrane separations using molecularly imprinted polymers, J. Chromatogr. B 2004, 804, 113-125.

[115] Mathew-Krotz, J., Shea, K.J., Imprinted polymer membranes for the selective transport of targeted neutral molecules, J. Am. Chem. Soc. 1996, 118, 8154-8155.

[116] Sergeyeva, T.A., Piletsky, S.A., Piletska, E., Brovko, O.O., Karabanova, L.V., Sergeeva, L.M., El'skaya, A.V., Turner, A.P.F., In situ formation of porous molecularly imprinted polymer membranes, Macromolecules 2003, 36, 7352-7357.

[117] Takeda, K., Kobayashi, T., Hybrid molecularly imprinted membranes for targeted bisphenol derivatives, J. Membrane Sci. 2006, 275, 61-69.

[118] Donato, L., Tasselli, F., Drioli, E., Molecularly imprinted membranes with affinity properties for folic acid, Separ. Sci. Tech. 2010, 45, 2273-2279.

[119] Shi, H., Tsai, W.-B., Garrison, M.D., Ferrari, S., Ratner, B., D., Template-imprinted nanostructured surfaces for protein recognition, Nature 1999, 398, 593-597.

[120] Hattori, K., Hiwatari, M., Iiyama, C., Yoshimi, Y., Kohori, F., Sakai, K., Piletsky, S.A., Gate effect of theophylline-imprinted polymers grafted to the cellulose by living radical polymerization, J. Membrane Sci. 2004, 233, 169-173.

[121] Wang, H.Y., Kabayashi, T., Fujii, N., Molecular imprint membranes prepared by the phase inversion precipitation technique, Langmuir 1996, 12, 4850-4856.

[122] Ramamoorthy, M., Ulbricht, M., Molecular imprinting of cellulose acetate-sulfonated polysulfone blend membranes for Rhodamine B by phase inversion technique, J. Membrane Sci. 2003, 217, 207-214.

[123] Pieracci, J., Wood, D.W., Crivello, J.V., Belfort, G., UV-assisted graft polymerization of N-vinyl-2-pyrrolidinone onto poly(ether sulfone) ultrafiltration membranes: comparison of dip versus immersion modification techniques, Chem. Mater. 2000, 12, 2123-2133.

CHAPTER 2

Design of MIPs for drug delivery applications

2. Design of MIPs for drug delivery applications

The use of supercritical carbon dioxide in the pharmaceutical area is already well established. Currently there are a number of pharmaceutical applications in which supercritical fluids are used as solvents (RESS), anti-solvents (GAS) or processing aid (PGSS, SAA).

Molecular recognition properties of imprinted polymers could also be advantageous in the pharmaceutical area. One of the goals of this thesis was to use supercritical fluid technology to prepare imprinted polymers with recognition to some drugs and investigate the influence of imprinting parameters on the ability of the matrix to be reloaded with the drug in supercritical environment. In addition, the influence of molecular recognition on the drug release profiles was studied and presented in this chapter.

2.1 MIPs with recognition to Flufenamic Acid

Process design for obtaining high affinity MIPs encounters a number of operational variables that need to be optimized. The most important, perhaps, is polymer composition wherein the choice of a functional monomer able to interact with the target molecule has a central role, as the basis of a successful molecular recognition mechanism. In the development of imprinted polymers with recognition to flufenamic acid, two functional monomers were studied, methacrylic acid (MAA) and N-isopropylacrylamide (NIPAAm). Methacrylic acid is the most common monomer in non-covalent imprinting due to its ability to establish ionic and hydrogen bonds through its carboxylic acid group [1]. On the other hand, NIPAAm has been only few times reported in imprinting works [2,3], but is well known because of the thermoresponsive character that its polymers may have [4]. Figure 2.1 illustrates the molecular structures of MAA and NIPAAm, as well as the structures of the crosslinker, ethylene glycol dimethacrylate (EGDMA) and the template, Flufenamic Acid (FA).

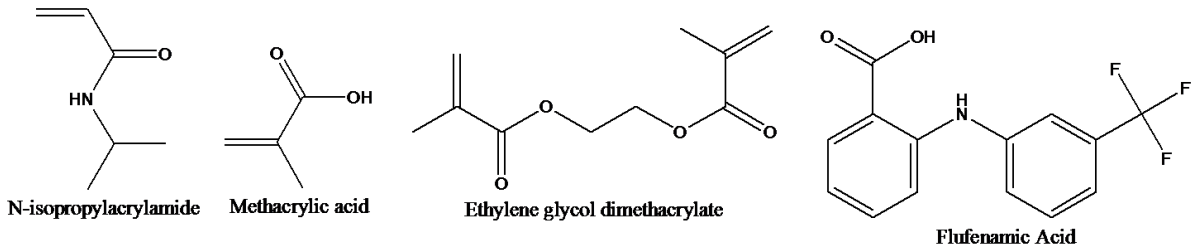

Figure 2.1 - Molecular structures of NIPAAm, MAA, EGDMA and FA

Further optimization of these specific systems also involved the study of different monomer:template ratios and crosslinking degrees. Functional monomer-template ratio has a major influence on the formation of complexes in non-covalent imprinting. Low concentration of template leads to lower number of binding sites on the polymer, with the non-imprinted polymer being the extreme. On the other hand, high concentrations of template lead to an increased number of random affinity binding sites, increasing non-specific interactions [5,6]. The integrity of the binding sites responsible for the recognition mechanism usually requires a rigid structure, with high crosslinking density, that minimizes the possible conformations of the matrix. However, when lower ratios of crosslinker are used, the matrix is more flexible, which can turn the equilibrium between drug release and uptake in the recognition site faster. Therefore, a compromise between the rigidity and flexibility of the network is necessary.

In this work, the influence of those parameters were studied by synthesizing MIPs of P(MAA-EGDMA) and P(NIPAAm-EGDMA) at two different template concentrations and crosslinking degrees. As control, NIPs were synthesized using the same experimental conditions, except that no template was added.

This part of the thesis was published in the Journal of Supercritical Fluids [7].[1]

2.1.1 Experimental

2.1.1.1 Materials

Crosslinker ethylene glycol dimethacrylate (EGDMA, 98% purity), functional monomers *N*-isopropylacrylamide (NIPAAm, 97% purity) and methacrylic acid (MAA, 99% purity), template drug flufenamic acid (FA, 99% purity) and polymerization initiator azobis(isobutyronitrile) (AIBN, 98% purity) were purchased from Sigma-Aldrich and used as received. Carbon dioxide was obtained from Air Liquide with purity better than 99.998%.

2.1.1.2 Preparation of MIP and NIP copolymers in $scCO_2$

Controlled delivery MIP devices were synthesized in $scCO_2$ using NIPAAm or MAA as functional monomers and EGDMA as crosslinker. All the copolymers were synthesized maintaining constant the total number of moles of functional monomer plus crosslinker introduced (16.4 mmol). P(NIPAAm-EGDMA) and P(MAA-EGDMA) were prepared using two different functional monomer:crosslinker ratios, 32:20 (typically 10.1 mmol of functional monomer and 6.3 mmol EGDMA) and 12:40 (3.8 mmol of functional monomer, 12.6 mmol EGDMA) which, respectively, corresponds to 58 and 89 wt% of crosslinker with respect to the total weight of monomers introduced; and two

[1] Reproduced with the authorization of the editor and subjected to the copyrights imposed.

template:monomer:crosslinker ratios: 1:32:20 and 5:32:20 (0.3 and 1.5 mmol of FA respectively). The corresponding non-imprinted copolymers (NIP), 0:32:20 and 0:12:40, were prepared without using template. In all reactions the weight percentage of the initiator (2 wt %) was kept constant with respect to the total weight of monomers (functional monomer plus crosslinker). Table 2.1 illustrates the amounts of reactants used in each synthesis.

Table 2.1 – Amounts of template and monomers used in each polymerization.

	Polymer (T:M:C)*	**Template (mmol)**	**Monomer (mmol)**	**Crosslinker (mmol)**
P(MAA-EGDMA)	0:32:20	0	10.1	6.3
	0:12:40	0	3.8	12.6
	1:32:20	0.3	10.1	6.3
	1:12:40	0.3	3.8	12.6
	5:32:20	1.5	10.1	6.3
	5:12:40	1.5	3.8	12.6
P(NIPAAm-EGDMA)	0:32:20	0	10.1	6.3
	0:12:40	0	3.8	12.6
	1:32:20	0.3	10.1	6.3
	1:12:40	0.3	3.8	12.6
	5:32:20	1.5	10.1	6.3
	5:12:40	1.5	3.8	12.6

Polymerizations were carried out in a high-pressure apparatus illustrated in Figure 2.2. Briefly, the reaction mixture was loaded into a 33 ml stainless steel high-pressure cell equipped with two aligned sapphire windows and a teflon coated magnetic stir bar inside [8].The cell was immersed in a thermostatted water bath set to 65 ºC. Temperature control was made through an open bath circulator Julabo Ed with stability ±0.1 ºC. Stirring was achieved by means of a Teflon coated magnetic bar. Carbon dioxide was added up to 21 MPa. These pressure and temperature conditions assure an initial homogeneous system, as it can be seen through the sapphire windows. All reactions proceeded for 24 hours. At the end, the polymer was slowly washed for 1 hour with continuous fresh high-pressure CO_2 in order to extract the template molecule and the residues of unreacted material.

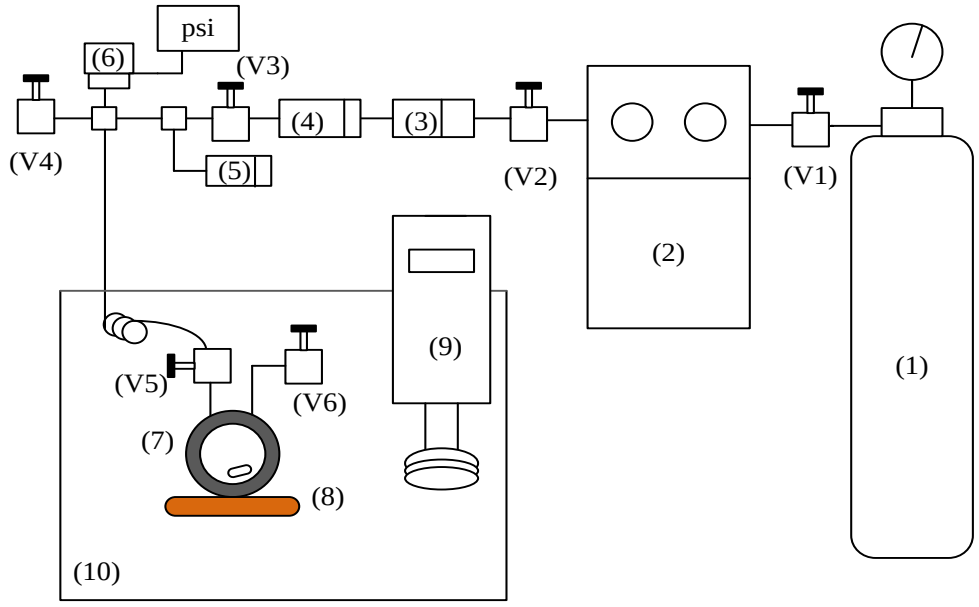

Figure 2.2 – Schematic representation of the experimental apparatus used in the polymerizations. 1- CO_2 cylinder, 2 - CO_2 liquid pump, 3- line filter, 4 - check-valve, 5 - rupture disk, 6 - high-pressure transducer, 7- high-pressure cell, 8 – magnetic stirrer, 9 – heating bath circulator, 10 – open water bath; V1 to V6 – high-pressure valves

2.1.1.3 $ScCO_2$-assisted template desorption

In order to ensure that all the template used in the imprinting step was removed from the synthesized MIPs, the material was packed in a stainless steel extractor (ID 7mm, 15 cm length) and washed continuously with $scCO_2$ and ethanol as co-solvent (2.5 wt %). Typically when using supercritical fluids to remove the template molecules, the diffusion coefficient can be increased at least 10-fold being most suitable for extraction of relatively non-polar compounds from solid matrices [9]. The apparatus used is described elsewhere [10]. Briefly, the reactor is immersed in a visual thermostatted water bath at 65 ºC with ±0.01 °C of stability. CO_2 was loaded up until the desired pressure was reached (20 MPa), using a Gilson piston pump (model 305). After reaching the operational pressure, the system is controlled through a back pressure regulator (Jasco, BP-2080 plus). The pressure inside the system is monitored with a pressure transducer (Setra Systems Inc., Model 204) with a precision of ±100 Pa. Each copolymer was washed at a flow rate of 5 ml/min for 5 h, followed by 1 h of fresh $scCO_2$ stream at 10 ml/min, in order to remove any ethanol residues. After template desorption, 20 mg of the polymers were finely crushed and put in 2 ml of buffer solution pH 7.4 at 37ºC for 24 hours. Quantification by UV spectroscopy at 285 nm showed no detectable traces of flufenamic acid.

2.1.1.4 $ScCO_2$-assisted impregnation of FA into the matrices

MIP and NIP copolymers were impregnated with FA in batch conditions at 65 ºC and 21 MPa for 20 hours. FA was used in excess to guarantee saturation conditions, assuring that this was not a limiting

step in the impregnation procedure [11]. The polymers were put inside cellulose membranes (cutoff 3.5 kDa) and then placed inside a 33 ml stainless steel high-pressure cell. The matrices were never in contact with the drug to prevent physical mixtures. A macroporous net separates the cell in two parts. The polymers are placed at the top part. The drug is introduced at the bottom and kept under stirring. At the end of the impregnation the system was quickly depressurized.

2.1.1.5 MIPs and NIPs characterization

The morphology of the synthesized copolymers was characterized using scanning electron microscopy (SEM) in a Hitachi S-2400 instrument, with an accelerating voltage set to 15 kV. Samples were mounted on aluminium stubs using carbon tape and were gold coated. Specific surface area and pore diameter of the polymeric particles were determined by N_2 adsorption according to the BET method. An accelerated surface area and porosimetry system (ASAP 2010 Micromeritics) was used under nitrogen flow.

Fourier transform infrared spectroscopy (FTIR) analyses were performed using a Bruker Tensor 27 (16 scans and 1 cm^{-1} resolution). Pellets containing finely grounded powder of a small amount of each copolymer mixed with dried KBr (1:5 mass ratio) were made before recording.

2.1.1.6 In vitro controlled drug release experiments

After impregnation, the polymers were put into 200 ml of phosphate buffer saline solution (pH 7.4) and 37 ºC, at sink conditions. 1 ml aliquots were withdrawn at time intervals and the same volume of fresh medium was added to the suspension. Quantification was performed by UV, making the calibration at 285 nm and the total mass released was determined considering the aliquots and the dilution produced due to the addition of fresh buffer solution.

2.1.1.7 High-pressure NMR study of the complex formation

In the aim of an on-going collaboration with Professor Eurico Cabrita (Requimte, FTC/UNL), high-pressure NMR experiments were carried out to study the interactions among monomers and template in the pre-polymerization mixture.

High-pressure NMR (HP-NMR) was recently used as a powerful method for the investigation of interactions that occur in polymerization and cyclodextrin inclusion complex formation in $scCO_2$ [12,13]. In this work we have performed experiments at the conditions of the polymerization in order to elucidate the nature of the interactions established during the template/monomer pre-assembly in the imprinting process. More specifically nuclear overhauser effect (NOE) experiments were used to probe the interactions between the monomers of both copolymers and flufenamic acid. HP-NMR

experiments were recorded using a previously described apparatus [13]. The polymerization mixtures (FA plus the monomer, NIPAAm or MAA, and EGDMA in a 1:12:40 molar ratio) were loaded directly into the NMR tube. No initiator was added to prevent polymerization inside the tube. The tube is evacuated and placed in a thermostatted water bath at 65 ºC, pressurized to 18 MPa and left to stabilize for 24h. NMR spectra were recorded at 65 ºC on a Bruker Avance III 400 spectrometer operating at 400.15 MHz for hydrogen and 376.90 MHz for fluorine, equipped with a temperature control unit, and a pulse gradient unit capable of producing magnetic field pulsed gradients in the z-direction of 56.0 G/cm.

2.1.2 Results and discussion

All synthesized polymers were obtained as dry and fluffy powders in high yields (~90%, determined gravimetrically), ready to be impregnated without further drying and purification steps (Figure 2.3). These are huge advantages over traditional MIPs formation processes where materials have traces of solvents and must be ground and sieved prior to use, leading to the partial destruction of the recognition sites. Figure 2.4 shows the SEM images of non-imprinted and imprinted P(MAA-EGDMA) a) and b) and P(NIPAAm-EGDMA) c) and d). SEM images revealed no significant differences between imprinted and non-imprinted polymers, all presenting a similar morphology, comprised of micron-sized agglomerates of nano-primary smooth surfaced particles. This morphology is consistent with other reported precipitation polymerizations in $scCO_2$ [8].

Figure 2.3 - High-pressure reactor used in the polymerizations and typical P(MAA-EGDMA) with molar ratios of 1:32:20.

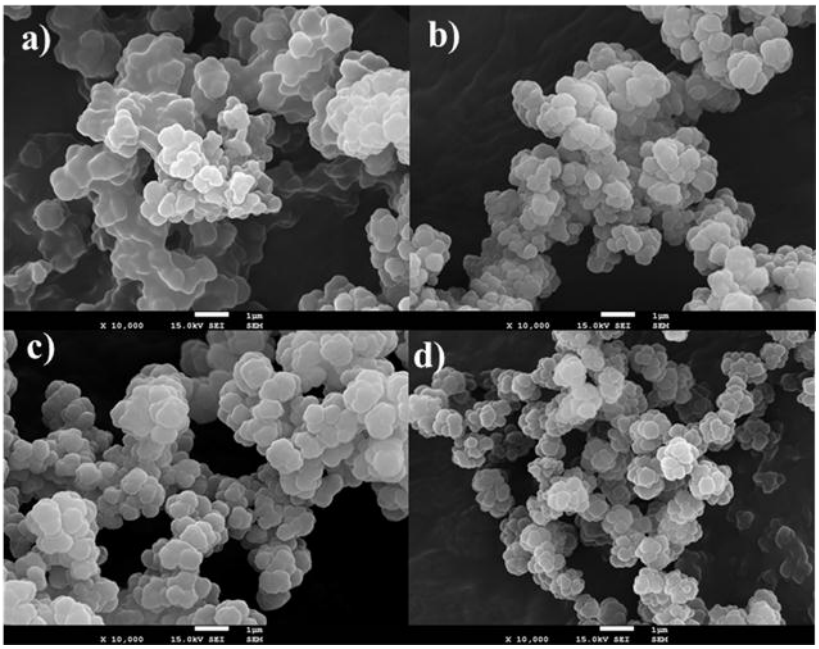

Figure 2.4. - SEM images of the synthesized P(MAA-EGDMA): (a) 0:12:40 and (b) 1:12:40; and P(NIPAAm-EGDMA) copolymers: (c) 0:12:40 and (d) 1:12:40 template:monomer: crosslinker ratios.

Both NIPs and MIPs were analysed by nitrogen porosimetry. Multipoint BET method results (type II), shown in Table 2.2, evidences some differences between MAA and NIPAAm-containing polymers concerning surface area, total pore volume and pore diameter. P(MAA-EGDMA) particles have higher surface area and present a higher porosity. This was observed in all molar ratios studied in this work. In addition, the crosslinking degree influenced the physical characteristics of the particles, with the less crosslinked structures presenting higher surface area and porosity due to a less rigid structure.

The amount of template drug introduced in the synthesis of imprinted polymers has also an effect on the surface area of the particles. At the same crosslinker ratios, by increasing the template:monomer ratio (from 1:12 to 5:12 and from 1:32 to 5:32) , the surface area decreases. These can be related with the influence of the nature of the monomers and the interference of different template-monomer systems that influence the conformation of the growing polymer and the reaction rate of polymerizations.

Table 2.2 - Physical characteristics (surface area, average pore diameter and specific pore volume) of both MIPs and NIPs, obtained by multipoint BET method (type II).

	Polymer (T:M:C)*	BET surface Area (m^2/g)	Total Pore Volume (cm^3/g)	Pore Diameter (nm)
P(MAA-EGDMA)	0:32:20	33.4	0.045	5.3
	0:12:40	15.5	0.023	6.0
	1:32:20	37.2	0.043	4.6
	1:12:40	25.8	0.038	5.9
	5:32:20	20.9	0.032	6.2
	5:12:40	16.7	0.021	5.1
P(NIPAAm-EGDMA)	0:32:20	13.2	0.015	4.5
	0:12:40	11.2	0.015	5.3
	1:32:20	15.9	0.023	5.8
	1:12:40	14.1	0.017	4.8
	5:32:20	13.1	0.019	5.7
	5:12:40	11.1	0.010	3.8

* Template:Monomer:Crosslinker molar ratios

FTIR analysis was performed on clean and impregnated copolymeric structures. Figure 2.5 shows the detail of the FTIR spectra of P(MAA-EGDMA) with different template compositions, washed and impregnated with FA, in the only region where differences could be observed. Both NIPs and MIPs, after supercritical template desorption, present similar spectra given the fact that polymers have the same composition. However after impregnation, changes could be observed in the region of OH vibrational frequencies, from 3446 cm^{-1} in the 0:12:40 to 3432 cm^{-1} in the 5:12:40. This can evidence a higher affinity of the imprinted polymers towards the drug since these frequencies tend to shift to lower frequencies upon hydrogen bonding [14]. Also, the broad band at 3560 cm^{-1} due to free OH that can be observed in the NIP (0:12:40, Figure 2.5), disappears in the MIPs supporting the formation of more interactions between imprinted polymers and FA. FTIR spectra of P(NIPAAm-EGDMA) were also performed but no significant shifts were observed in the bands suggesting that the hydrogen bonds between drug and polymeric matrices are weaker than for P(MAA-EGDMA).

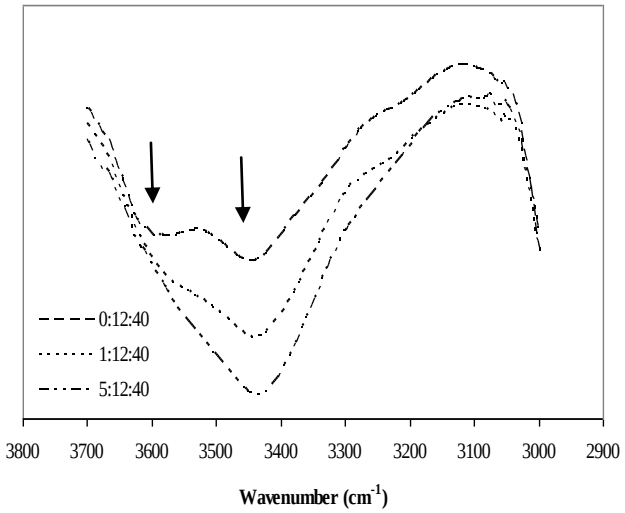

Figure 2.5 - FTIR spectra detail for the impregnated P(MAA-EGDMA) copolymers.

Figure 2.6 and Figure 2.7 show the *in vitro* release kinetic profiles of FA from the NIPs and MIPs of both copolymers as a function of time, for 7 days at 37 ºC. The release amount is expressed as the ratio of drug released (R) towards the total drug impregnated in the matrices (R_0). These total amounts, showed in Table 2.3, were calculated upon the crush of the polymeric devices in a mortar at the end of release experiments and quantification of the release solutions.

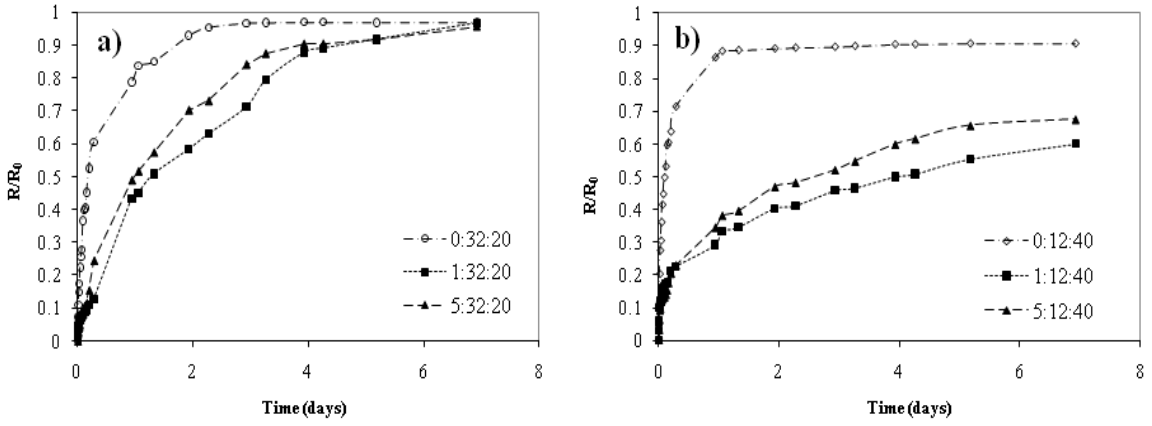

Figure 2.6 - Release profiles of FA from P(MAA-co-EGDMA): (a) less crosslinked and (b) more crosslinked structures where (-○-) represents the NIP, (-■-) the MIP with lower T:M and (-▲-) the MIP with higher T:M ratio.

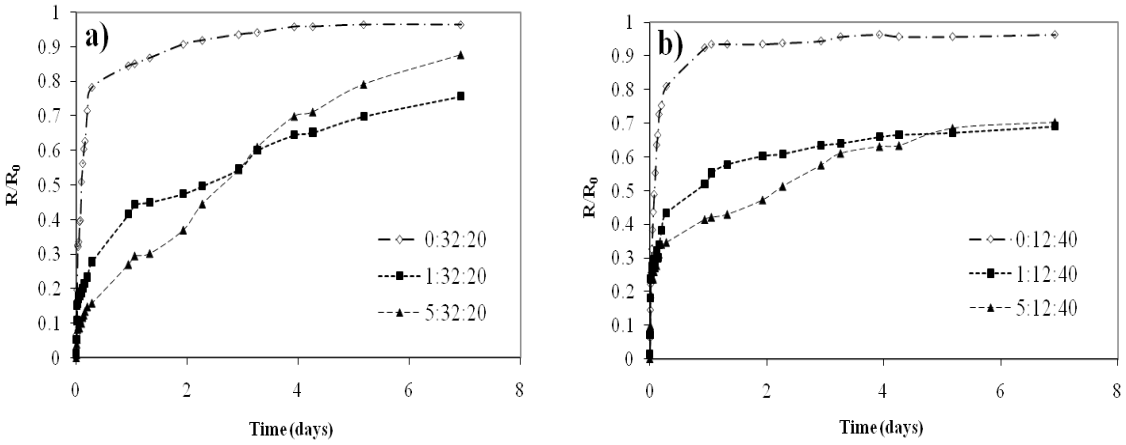

Figure 2.7 - Release profiles of FA from P(NIPAAm-EGDMA): (a) less crosslinked and (b) more crosslinked structures where (-○-) represents the NIP, (-■-) the MIP with lower T:M and (-▲-) the MIP with higher T:M.

As it can be seen in Table 2.3, FA uptake during impregnation was highly dependent on the rigidity of the polymeric structures. The copolymers with more flexible chains, i.e., less crosslinked, were able to incorporate more drug. This higher uploading can be explained by the higher plasticization and mobility of the chains in the impregnation step. Moreover in the release experiments those matrices show higher release rates than the more crosslinked structures. This is in agreement with other studies of drug delivery systems synthesized and processed in $scCO_2$ [10]. Low crosslinking degree decreases the imprinting factor and differences in drug uptake and release between imprinted and non-imprinted polymers become smaller which means that the imprinting process is more efficient in more crosslinked structures. This is clearly seen in the higher affinity of MIP polymers for the drug, translated in their higher drug loading and slower overall release rate. In fact, imprinted polymers show a much more sustained delivery than NIP matrices, taking about one week to reach the release plateau, while NIPs reach the maximum release after only one day.

The template: monomer ratio (T:M) revealed to be a parameter with a high impact on the amount of drug uptaken in the impregnation step. For the P(MAA-EGDMA) system the increase of the initial template concentration led to an increase in the drug loading during impregnation, which accounts for a higher affinity of the matrices to the drug as a reflex of an efficient imprinting mechanism. Furthermore there is no significant trend in the porosity or in the surface area that could contribute to this impregnation data, meaning that the formation of more specific binding sites is the responsible cause for this loading increase.

Table 2.3 - Polymer loading during impregnation and corresponding maximum *in vitro* drug release after 7 days at 37 ºC.

	Polymer (T:M:C)*	Drug loaded (mg/g)**	Drug released (%)
P(MAA-EGDMA)	0:32:20	102.3	97.0
	1:32:20	105.2	96.7
	5:32:20	118.8	95.7
	0:12:40	50.5	90.7
	1:12:40	63.8	60.0
	5:12:40	101.5	67.6
P(NIPAAm-EGDMA)	0:32:20	57.6	96.5
	1:32:20	70.8	75.7
	5:32:20	49.8	87.7
	0:12:40	30.6	96.3
	1:12:40	42.9	69.1
	5:12:40	38.9	70.2

* Template:Monomer:Crosslinker molar ratios

** *w*t FA (mg) with respect to the copolymer (g).

The influence of changing the molar ratios among the components of the imprinting mixture (T:M:C) on the drug release kinetics by the copolymers synthesized is shown in Figure 2.6 and Figure 2.7. R/R_0 is the ratio between the amount of drug released and the amount of drug impregnated. By looking at the figures it is obvious that for both crosslinking degrees, MIPs have always a much more sustained release than NIPs, which is consistent with the recognition for the template due to a stronger interaction with the matrix. By comparing the NIP profiles for both less and more crosslinked MAA-containing copolymers (Figure 2.6.a and b), one can observe that the less crosslinked is able to release the drug in a sustained way, for two days until it reaches a plateau, which corresponds to the release of almost all the impregnated drug. By comparing with P(NIPAAm-EGDMA) the less crosslinked polymer (Figure 2.7.a) does not show the same behaviour as the MAA containing NIP since it releases around 80 % of the drug in the first hours. This can be explained by a higher affinity of the drug to the MAA matrix due to the establishment of stronger hydrogen bonding. The more crosslinked NIPs for both copolymers show a similar behaviour of the less crosslinked P(NIPAAm-EGDMA). In addition the less crosslinked P(MAA-EGDMA) non-imprinted matrix, shows a higher porosity, which can influence a deeper impregnation within the particles thus leading to more sustained release.

In the case of the more crosslinked MIPs (Figure 2.6b and Figure 2.7b) only about 60-70 % of the impregnated drug is released. This is explained by the structure of the polymer, more rigid, where part of the drug impregnated has difficulty in being released from the highly crosslinked net. Similar

results can be found in literature where the high crosslinking degree can cause over-enhancement of the drug affinity to the system causing the release of insufficient drug and hence limiting its therapeutic utility [15]. By increasing the crosslinking degree in both copolymers MIPs there is a slight increase in the initial drug release that can be explained by the lower porosity of the more crosslinked structures as it can be seen by comparison of the different polymers in Table 2.2.

Also, there is a different effect on the drug release by increasing the template concentration. While for P(MAA-EGDMA) the less imprinted polymers (1:32:20 and 1:12:40, on Figure 2.6) show a slower drug release than the polymers synthesized with the highest amount of template, the P(NIPAAm-EGDMA) shows the opposite behaviour. In the less crosslinked NIPAAm-containing polymer there is even a cross-over. These observations are related with the porosity, the affinity of the drug to the functional monomers and the specificity and the number of the imprinted sites.

The profiles for the more crosslinked P(NIPAAm-EGDMA) are similar to those of the P(MAA-EGDMA). However for the less crosslinked matrices the release from the MIPs is slower, more sustained, compared to P(MAA-EGDMA). In this case we think that this may have two different contributions: i) the temperature-responsiveness of NIPAAm. The release experiments are performed at 37 ºC which is above its LCST meaning that the chains are collapsed and can retard the drug release, especially in the less crosslinked polymeric matrix where the chains have more freedom; ii) the ability of acrylamides such as NIPAAm to establish hydrogen bonds through its amide group both on polar and apolar media also contributed to a slower release of the drug [16].

The less crosslinked P(MAA-EGDMA) MIPs present the highest rate of release because PMAA is pH-sensitive and at pH 7.4 there is dissociation of the carboxylic acids, the polymeric chains repel leading to a higher water uptake, increasing the hydrophilicity of the matrices and thus leading to a better diffusion of the drug to the medium. In the more crosslinked matrices this behaviour is less obvious due to the rigidity of the polymeric nets. Nevertheless by comparing the less crosslinked MIPs from both copolymers there is a more pronounced initial burst release for the NIPAAm-containing polymers, about 35 % of the drug in the first minutes, compared to 15 % for the MAA polymers. This difference could be explained by the lower pore volume and surface area of the particles that are less advantageous to impregnation within the pores and with the drug being retained more at the surface, which is responsible for that rapid initial release.

HP-NMR experiments were undertaken in order to understand the interactions between FA and the monomers of the MIP copolymers, NIPAAm and EGDMA or MAA and EGDMA, during the imprinting process in $scCO_2$, at supercritical conditions 18 MPa and 65 ºC. Prior to these experiments proton spectra of the individual components were acquired in a conventional NMR solvent ($CDCl_3$) at room temperature and compared with the spectra of the mixtures (FA:MAA:EGDMA and

FA:NIPAAm:EGDMA). No evidence for specific interactions could be seen from the comparison of individual chemical shifts at these conditions.

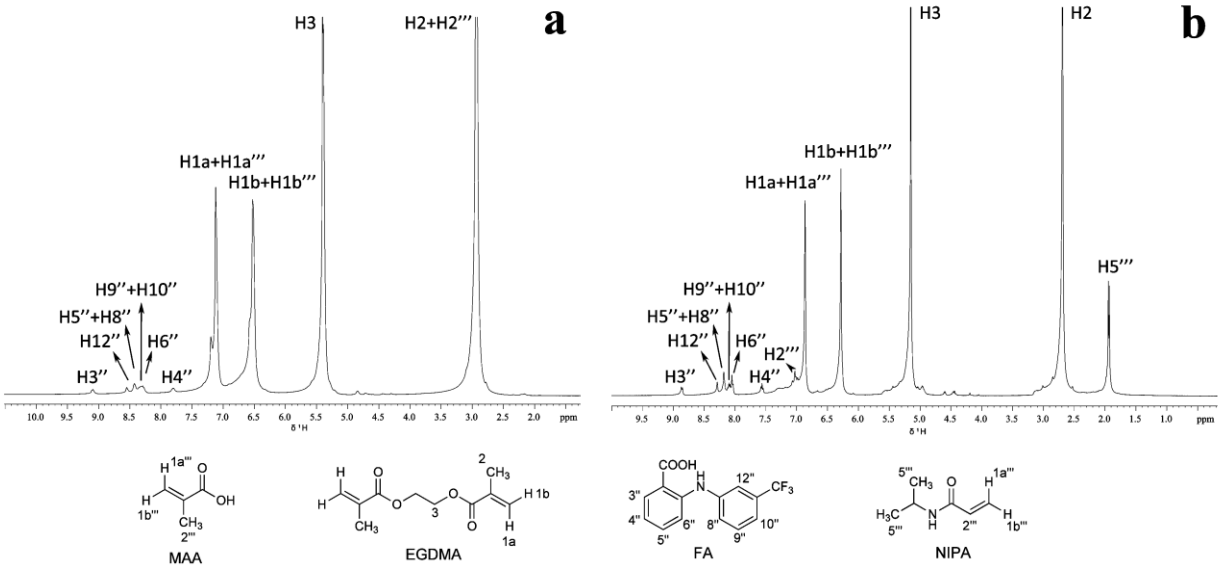

Figure 2.8 - 1H NMR spectra (400MHz) in $scCO_2$ of: a) EGDMA + FA + MAA with resonances assignment; b) EGDMA + FA + NIPA with H1 resonances assignment.

Figure 2.8a and Figure 2.8b, show the ^{1}H HP-NMR spectra recorded for both systems, FA:MAA:EGDMA and FA:NIPAAm:EGDMA, respectively. Proton assignments were based on the spectra acquired under conventional conditions. The FA assignment is in accordance with previous results [12]. Due to the structural similarity of MAA and EGDMA there is resonance overlapping for the vinylic and methyl protons of the two monomers. The full assignment is indicated in Figure 2.8a. In the NIPAAm containing system, the FA is better resolved, the methyl protons of NIPAAm and the methylene protons of EGDMA are also well resolved but there is signal overlapping from both olefinic protons (Figure 2.8b). The interaction of the monomers with the template was studied by performing a series of nuclear overhauser enhancement spectroscopy (NOESY) experiments, both homonuclear (^{1}H-NOESY) and heteronuclear (^{1}H-, ^{19}F-HOESY), to take advantage from the fluorine atoms of the drug. The NOESY recorded for the MAA system revealed, besides the expected intramolecular contacts, the presence of cross peaks between the methyl proton moiety of the monomer and the protons of FA. These contacts are best seen in the expansion of the FA region of the NOESY spectra presented in Figure 2.9, which are clear evidence of intermolecular interaction between the drug and the monomers under the studied conditions.

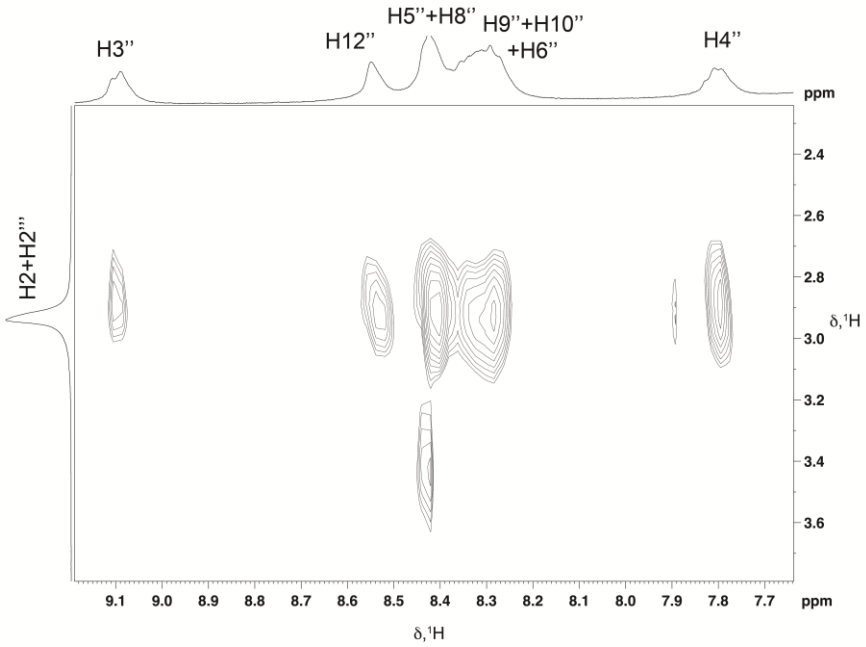

Figure 2.9 - Expansion of the 400 MHz $^{1}H/^{1}H$ 2D NOESY of FA+MAA+EDGMA system in $scCO_2$.

However due to the resonance overlap between the methyl protons of both MAA and EGDMA this experiment is insufficient to determine the origin of the cross peaks, they could be either due to intermolecular interactions with MAA or EGDMA alone, or with both. Therefore the same experiment was performed with the NIPAAm system where the EGDMA methyl protons are well resolved. In the NOESY spectrum recorded for the NIPAAm system only the expected cross peaks due to intramolecular interactions were detected, no cross peak between the well resolved methyl signal of EGDMA and the protons of FA are observed. This is a strong indication that the cross peaks observed in the MAA NOESY spectra are due to an intermolecular interaction between this drug and the MAA monomer and are not related with the EGDMA moiety. Our previous works however proved that polymeric materials with molecular recognition could be developed using only the crosslinker monomer EGDMA and DEGDMA [17,18]. It is likely that the interactions with EGDMA become stronger when the polymerization occurs, unfortunately the NMR tube has that limitation since the polymer formation could block the NMR tube.

^{1}H-,^{19}F- HOESY experiments were performed taking advantage of the fluorine atoms of FA. As the fluorine spectra has only one resonance, a cross peak between this signal and any of the protons of the monomers is a clear evidence of intermolecular interaction. For the NIPAAm system, only the expected ^{1}H, ^{19}F intramolecular interactions within the FA moiety were observed. However, the HOESY spectrum obtained for the MAA system is in accordance with the NOESY results. Besides the expected ^{1}H, ^{19}F intramolecular contacts for the drug, intermolecular interactions could also be detected with the MAA moiety. These contacts can be perfectly observed in the expansion of the

HOESY spectra at the fluorine chemical shift, Figure 2.10a, as well as in the 1D trace, extracted from the 2D matrix at the ^{19}F chemical shift, Figure 2.10b. It is also possible to see that there is also some interaction with the methylene protons of EGDMA.This interaction seems however to be weaker than the interaction with MAA, since it is not detected in the NOESY and since the EGDMA/FA interaction was also not detected in the HOESY study performed with the NIPAAm system.

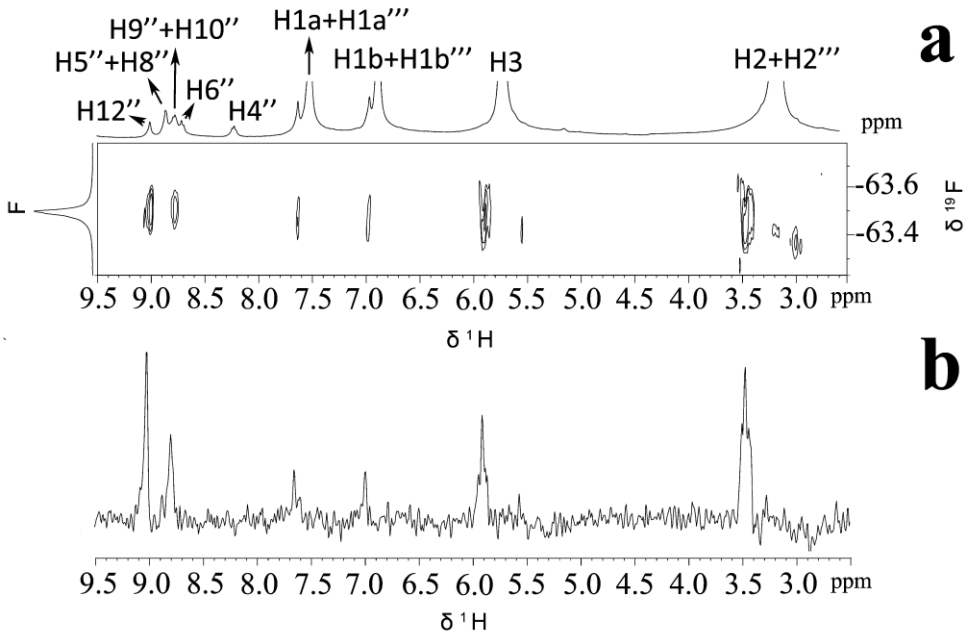

Figure 2.10 - a) 400 MHz 1H/19F 2D HOESY of FA+MAA+EDGMA in $scCO_2$, b) 1D trace of the 2D spectrum in a) at the FA 19F chemical shift.

From a purely chemical point of view the intermolecular interaction detected between the MAA monomer and the FA makes sense. In fact both molecules possess a carboxylic acid moiety and there is the possibility to form two hydrogen bonds, having both molecules acting as hydrogen bond donors and acceptors and forming a type of dimeric complex. The interaction between FA and EGDMA through the formation of a hydrogen bond is also possible but it should be weaker than with MAA because the carbonyl group of EGDMA would only act as a hydrogen bond acceptor. From these HP-NMR studies it was possible to prove the existence of intermolecular interactions through hydrogen bonding between MAA, EGDMA and FA. However there are no evidences of these interactions in the NIPAAm system. This could be due to weak interactions between NIPAAm and FA at the initial conditions of the reaction as discussed above. The interactions established become probably stronger over the reaction during the crosslinked structure formation and could not be completely accessed using this technique. These results prove that a determinate level of pre-organization in the reaction mixture, due to favourable intermolecular interactions prior to the polymerization, is important to the

imprinting and may influence positively the number of imprinted sites. It also shows that some important interactions are established during the polymerization reaction, and are not so strong in the initial mixture or in the early stage of the polymerization.

2.1.3 Conclusion

This work proves that supercritical fluid technology is a viable alternative to the synthesis and impregnation of molecularly imprinted copolymers with tuneable molecular recognition properties towards a specific target compound. By comparing imprinted and non-imprinted materials we can conclude that imprinted matrices can be loaded with higher amounts of drug than their corresponding NIPs and that the release is more sustained due to their stronger affinity to the template drug. The template/monomer ratio, the functional monomer used and the degree of crosslinking are processing parameters that enable to control the drug uptake and release from the imprinted matrices. By lowering the crosslinking degree it is possible to obtain more flexible structures while still preserving the molecular recognition effect. High-pressure NMR studies confirm that there are hydrogen bond interactions between the carboxylic acid group of FA and the carboxylic acid groups from the monomers, which are responsible for the specificity of the binding sites.

Supercritical carbon dioxide is a promising medium for the development of molecular recognition polymers, yielding ready-to-use materials synthesized without hazardous organic solvents, which could be used in many applications such as in controlled drug delivery systems.

2.2 Low crosslinked MIPs

The study concerning the optimization of molecular recognition of flufenamic acid revealed that, with the right balance between the components of the reaction mixture, it is possible to prepare imprinted polymers in $scCO_2$ with a crosslinker degree lower than the one usually employed in molecular imprinting (around 90 wt%). This gave rise to the idea of synthesizing MIPs with such a low crosslinking degree, as 20 wt%.

The design of MIPs with flexible chains is gaining more attention in the last years, with the exponential number of papers in the field embracing the potential of creating a flexible macromolecular structure with molecular memory. Byrne et al has two instructive reviews [19,20] (2002 and 2008) in the area of imprinting within hydrogels and has dedicated a part of his work to the development of sustained ocular delivery through the design of imprinted contact lenses [21,22]. Other authors have focused on the possibility of creating intelligent gels with stimuli-responsive character. One example is the work reported by Suedee and co-workers [23] regarding the design of precisely engineered binding sites for enantioselective recognition of (S)-omeprazole within a pH-responsive polymeric network. Their pioneer work is a proof of concept for the stereoselective drug delivery from an imprinted matrix able to respond to changes in pH.

Poly(DMAEMA) is a cationic polymer widely used in biomedical applications such as in gene delivery [24] and in pharmaceutical formulations such as in EUDRAGIT® E 100, E 12,5 and E PO. In molecular imprinting, the study of DMAEMA as a functional monomer is still at an early stage, although some work positively attested the performance of DMAEMA-containing MIPs in protein adsorption [25], chromatography [26] and drug delivery [27].

In this work, a weakly crosslinked MIP composed of DMAEMA and EGDMA was synthesized to have molecular recognition to ibuprofen, a nonsteroidal anti-inflammatory drug. Figure 2.11 illustrates the molecular structures of both functional monomer and template used in this study. Drug loading capacity in $scCO_2$-assisted impregnation and release profiles at different pHs were compared with the ones of the corresponding non-imprinted polymer. In addition, cytotoxicity assays were performed with human colorectal carcinoma-derived Caco-2 cells.

This work was published in International Journal of Pharmaceutics [28].[2]

[2] Reproduced with the authorization of the editor and subjected to the copyrights imposed.

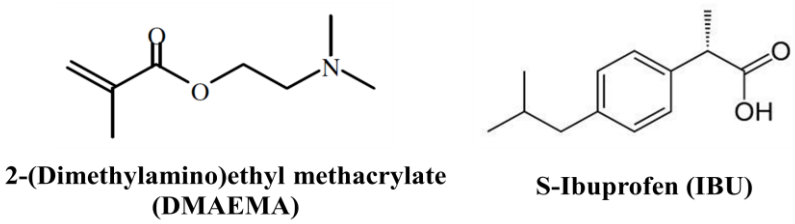

2-(Dimethylamino)ethyl methacrylate (DMAEMA)

S-Ibuprofen (IBU)

Figure 2.11 - Molecular structures of DMAEMA and Ibuprofen.

2.2.1 Experimental

2.2.1.1 Materials

Ethylene glycol dimethacrylate (EGDMA, 98% purity) as cross-linker, 2-(dimethylamino)ethyl methacrylate (DMAEMA, 98% purity) as functional monomer, (S)-(+)-Ibuprofen (99% purity) as template molecule and initiator azobis(isobutyronitrile) (AIBN, 98% purity) were purchased from Sigma-Aldrich and used without further purification. Carbon dioxide was obtained from Air Liquide with purity better than 99.998%. Amphotericin B, Eagles minimum essential medium with Earle's balanced salt solution (EMEM, EBSS), Human colorectal carcinoma-derived Caco-2 cells, L - glutamine, 3-(4,5-dimethylthiazol-2-yl)-5-(3-carboxymethoxyphenyl)-2-(4-sulphofenyl)-2H-tetrazolium (MTS), non-essential amino acids (NEAA), penicillin G, streptomycin, and trypsin were purchased from Sigma-Aldrich. Fetal bovine serum (FBS) was purchased from Biochrom AG (Berlin, Germany).

2.2.1.2 MIP and NIP synthesis

In a typical process to produce the MIP, EGDMA (16.7 mol % with respect to the total amount of monomers), DMAEMA, AIBN (2 wt %) and ibuprofen (16.7 mol %) were loaded into the high-pressure cell. The procedure to synthesize NIP was the same except that no template was added in the reaction mixture. Experimental conditions concerning temperature and pressure as well as the apparatus used for the polymerizations are the ones described in section 2.1.

2.2.1.3 scCO_2-assisted template desorption

Template desorption was performed using the experimental procedure described in section 2.1. Quantification of ibuprofen in PBS solution was performed in a UV/Vis spectrophotometer Lambda 25 at 265 nm. No significant traces of ibuprofen were detected in the solution, assuring that all the ibuprofen quantified in the release assays was proceeding from the supercritical impregnation step and not from the synthesis.

2.2.1.4 MIP and NIP characterization

SEM and Nitrogen Porosimetry

Polymers were morphologically characterized using scanning electron microscopy (SEM) in a Hitachi S-2400 instrument, with an accelerating voltage set to 15 kV. Samples were mounted on aluminium stubs using carbon tape and gold coated.

Specific surface area and pore diameter of the polymeric particles were determined by adsorption of N_2 according to the BET method. An accelerated surface area and porosimetry system (ASAP 2010 Micromeritics) was used under nitrogen flow.

Swelling degree

The water uptake of the polymeric matrices was determined in similar conditions to those tested in the drug release experiments. Samples with 50 milligrams of polymer were put inside a sleeve filter of 1 µm mesh and immersed in PBS solution (pH 2.2) for 3 hours, followed by immersion in a pH 7.4 solution, for 5 hours. Briefly, the water content was estimated by the difference between the weight of the swollen polymer samples (W), after careful wiping with a soft tissue, and the weight of the dry polymer samples (W_0).

$$Swelling = \frac{W - W_0}{W_0} \qquad \text{(Equation 2.1)}$$

Zeta potential

Potentiometric measurements were performed to both NIP and MIP matrices in a Zetasizer Nano ZS from Malvern. The particles were resuspended in PBS (pH 7.4), with a concentration of 5 mg/mL, sonicated for 3 minutes and then transferred to a disposable folded capillary cell. The zeta potential was measured using the supplied software.

Cytotoxicity assays

In the aim of an on-going collaboration with Professor Ilídio Correia (UBI), cytotoxicity assays with human colorectal Caco 2-cells were performed in order to evaluate the potential of the imprinted polymer to be used as drug delivery system. Although Caco 2-cells are derived from colon carcinoma, when they are cultured under specific conditions, they resemble the intestinal absorptive cells of the small intestine. This cell line is commonly used by the pharmaceutical industry as an *in vitro* model of

the human intestinal mucosa to evaluate the absorption of orally administrated drugs and was herein used to predict the cytotoxicity of the synthesized polymers.

Caco-2 cell culture

Human colorectal carcinoma-derived Caco-2 cells were seeded in T-flasks of 25 cm^3 with 6 ml of EMEM (EBSS), supplemented with 2mM L-Glutamine, heat-inactivated FBS (10% v/v), NEAA (1% v/v) and 1% antibiotic/antimycotic solution. After the cells reached confluence, they were subcultivated by a 3-5 minute incubation in 0.18% trypsin (1:250) and 5mM EDTA. Then cells were centrifuged, resuspended in culture medium and then seeded in T-flasks of 75 cm^3. Hereafter, cells were kept in culture at 37°C in a 5% CO_2 humidified atmosphere inside an incubator.

Proliferation of Caco-2 cells in the presence of polymers

Dry samples, at a concentration of 20 mg/mL, were placed in 48-well plates (Nunc) and sterilized by UV exposure for at least 30 minutes. Then, EMEM (EBSS) was added to each well and was left in contact with the materials for 24 hours.

Meanwhile, Caco-2 cells were cultured in 96-well plates (Nunc) at a density of $3x10^4$ cells per well, with EBSS. After 24 hours, the cell culture medium was removed and replaced by that in contact with polymers. This procedure was repeated during 3 days. Cell growth was monitored using an Olympus CX41 inverted light microscope (Tokyo, Japan) equipped with an Olympus SP-500 UZ digital camera.

The adhesion and proliferation of Caco-2 cells in the presence of polymers were also characterized by SEM. Cells ($4x10^4$ cells per well) were seeded with the sterilized polymers in 48-well plates, over a coverslip, for 48 hours. Samples were fixed in 2.5% glutaraldehyde during 10 minutes. Then, they were rinsed three times with PBS for 2 minutes and dehydrated in graded ethanol of 70, 80, 90, and 100% during 10 minutes each. Finally, the coverslips were mounted on an aluminium board using a double-side adhesive tape and sputter coated with gold using an Emitech K550 (London, England) sputter coater. The samples were then analyzed using a Hitachi S-2700 (Tokyo, Japan) scanning electron microscope operated at an accelerating voltage of 20 kV and at various amplifications.

Cytotoxic profile of the polymers

To evaluate the cytotoxicity of the polymers, cells ($3x10^4$ cells per well) were seeded in a 96-well plate and cultured with EMEM (EBSS). At the same time, in another 96-well plate culture EMEM (EBSS) was added to the sterilized polymers, and left there for 24 h, 48 h and 72 h. After 24, 48 and 72 h of incubation, the cell culture medium was removed and replaced with 100 µL of medium that

was in contact with the polymers. Then, cells were incubated at 37°C in a 5% CO_2 humidified atmosphere for more 24h for each case. Subsequently, cell viability was assessed through the reduction of MTS into a water-soluble brown formazan product (n=5), by an adaptation of a method previously described in the literature [29]. To do so, the culture medium of each well was removed and replaced with a mixture of 100 µL of fresh culture medium and 20 µL of MTS/PMS reagent solution. The cells were incubated for 4 hours, at 37 °C, in a 5% CO_2 humidified atmosphere. Absorbance at 490 nm was measured using a microplate reader (Sanofi, Diagnostics Pauster). Wells containing cells in the culture medium without polymers were used as negative control. EtOH 96% was added to wells containing cells as a positive control [30, 31, 32].

2.2.1.5 Impregnation in $scCO_2$ environment

$ScCO_2$-assisted impregnation was performed using the experimental procedure and conditions described in section 2.1.

2.2.1.6 In vitro drug release experiments

Drug release profiles were studied at sink conditions in two different experiments. In case I, the polymers were put in 200 ml of PBS at pH 7.4, for 3 days. In case II, the loaded polymers were allowed to release ibuprofen in a simulated oral administration situation. In this experiment the matrices were put in 200 ml of Glycine-Hydrochloric acid buffer solution (pH 2.2) for 3 hours and then for 5 hours in 200 ml of PBS (pH 7.4). In both cases the temperature was set at 37 ºC and 1 ml aliquots were withdrawn at time intervals and the same volume of fresh medium was added to the solution. Quantification was performed by making calibration curves in a spectrophotometer at 223 nm for the solution with pH 2.2 and 265 nm for PBS (pH 7.4). The total mass released was determined considering the aliquots and the dilution produced by addition of fresh buffer solution. Impregnated amounts of ibuprofen that were not released during the delivery experiments were calculated upon the crush of the polymeric networks with a mortar at the end of the experiments and quantified also by UV.

Ibuprofen transport through the synthesized polymeric networks in solution with different pH was modelled using a semi-empirical Korsmeyer–Peppas equation:

$$\frac{\mathbf{M_t}}{\mathbf{M_\infty}} = \mathbf{kt^n} \qquad \text{(Equation 2.2)}$$

where M_t is the absolute cumulative amount of drug released at time t, M_∞ is the total amount of drug impregnated in the polymer samples; k is the diffusion coefficient that reflects the structural and

geometric characteristics of the device, and *n* is the release exponent, which gives an insight on the specific transport mechanism.

2.2.2 Results and Discussion

2.2.2.1 Synthesis and Characterization of the polymers

The synthesized polymeric matrices were obtained in high yields (~85 %, determined gravimetrically) as dry powders, as it can be seen in Figure 2.12. This represents a major advantage over traditional MIPs that have to be ground and sieved leading to the destruction of some interaction sites [33]. The initial pressure-temperature conditions reactions were adjusted to assure a homogeneous system, as it could be seen through the sapphire windows.

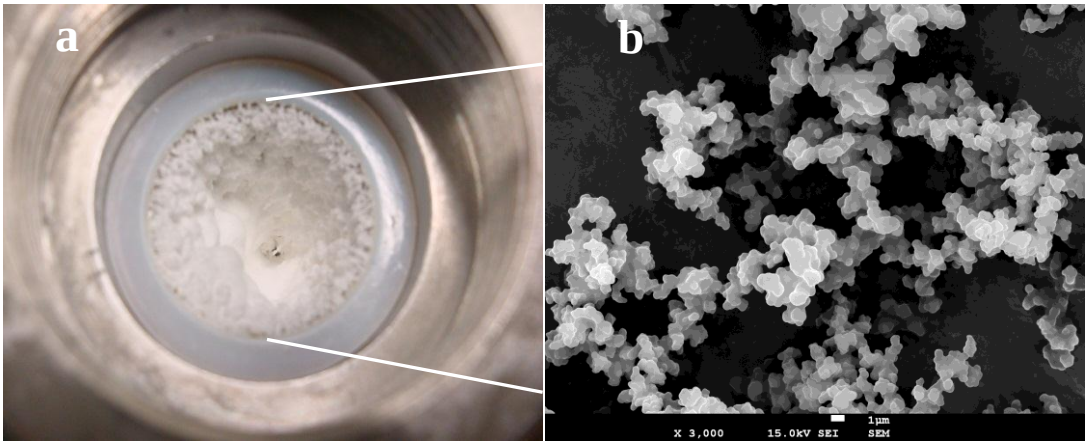

Figure 2.12 - Synthesized imprinted P(DMAEMA-EGDMA). a) Inside the polymerization cell and b) SEM image.

Figure 2.12b shows a SEM image of a synthesized imprinted polymer. From the SEM images obtained it was not possible to see any morphological differences between the imprinted and non-imprinted polymers. Polymers are formed by agglomerates of well-defined particles (~1 µm).

The physical characteristics concerning surface area and porosity of the synthesized polymers are shown in Table 2.4. The addition of the template molecule in the synthesis process does not seem to affect the nucleation of this polymerization system, with MIP and NIP presenting similar porosities and surface areas. These physical characteristics are consistent with other precipitation polymerizations in $scCO_2$ [4].

Table 2.4 - Physical characteristics of NIP and MIP particles and ibuprofen load in $scCO_2$-assisted impregnation. Each result is the mean ± standard error of at least three independent experiments.

Polymer	BET Surface Area (m^2/g)	Pore Volume (cm^3/g)	Pore Diameter (nm)	Zeta potential (mV)	Total amount of drug impregnated (mg/g polymer)
MIP	10.4	0.0106	4.1	6.7 ± 0.4	331 ± 44
NIP	9.2	0.0105	4.4	17.5 ± 0.6	102 ± 25

Potentiometric measurements disclosed different zeta potential values of NIP and MIP particles. This suggests that the introduction of ibuprofen in the polymerization influences the charge distribution through the polymeric particles with the potentially ionizable amino group of DMAEMA having a different spatial orientation on the particles.

Figure 2.13 shows the variation of water uptake by the synthesized NIP and MIP at acidic and neutral pH. In the first three hours the polymers were immersed in a solution of pH 2.2 and afterwards they were immersed in a solution of pH 7.4. As it can be seen, both imprinted and blank polymers exhibit a degree of swelling that is in the same order of magnitude, although NIP presents a slightly higher swelling ratio. At acidic pH the polymers swell more because the tertiary amine group of DMAEMA is highly protonated, which increases the charge density on the networks and leads to an income of mobile counterions to balance the charge. At that point the internal osmotic pressure of the network increases and the matrices become swollen [34].

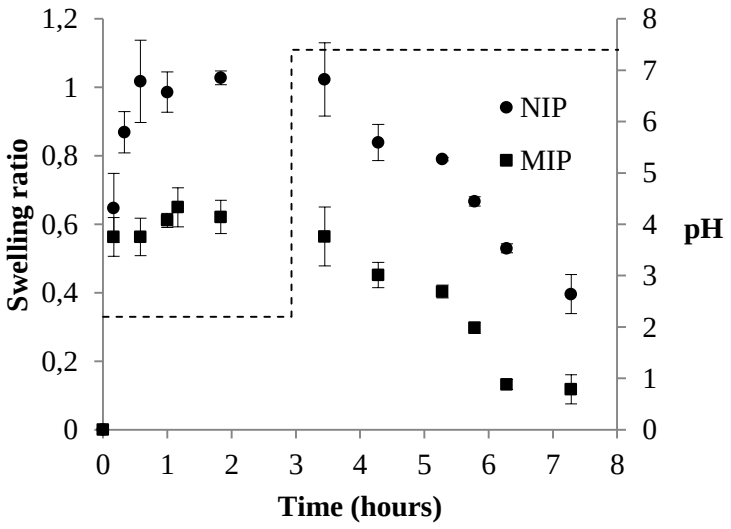

Figure 2.13 - Swelling ratio of both NIP and MIP matrices at 37ºC and pH 2.2 in the first 3 hours, and pH 7.4 in the subsequent time. Filled dots represent the water uptake from NIP and filled squares the water uptake from MIP (mean±SD, n=3).

2.2.2.2 Cytotoxicity of the synthesized polymers

Over the last years DMAEMA has been used in the development of therapeutic drug delivery formulations. In order to study the applicability of the materials for biomedical applications, the cytocompatibility of NIP and MIP matrices was characterized through *in vitro* studies. As already mentioned, Caco-2 cells were seeded at the same initial density in the 96-well plates, with or without polymers to assess the cytoxicity. Cell adhesion and proliferation was noticed in wells where cells were in contact with the medium, which was previously incubated with the polymer, in a concentration of 20 mg/mL, (Figure 2.14A and B) and in the negative control (Figure 2.14C). In the positive control, no cell adhesion or proliferation was observed. Dead cells with their typical spherical shape can be observed in Figure 2.14D. The observation of cell growth in the presence of materials showed that MIP and NIP are biocompatible. However, a higher number of cells were observed in the vicinity of MIP. The observed difference in the cytotoxicities of NIP and MIP can be explained by their zeta potential values. A polymeric material with positively charged particles can interact more extensively through electrostatic interactions with the negatively charged cell surface [35]. It seems that the introduction of ibuprofen in the polymerization step and its subsequent removal induces a modification on the particle surface with the imprinted polymer showing less surface positive charge, 6.7 mV, against 17.5 mV for NIP. The polymeric network of NIP with higher positive zeta potential will interact more with the anionic components of the proteins of the extracellular matrix.

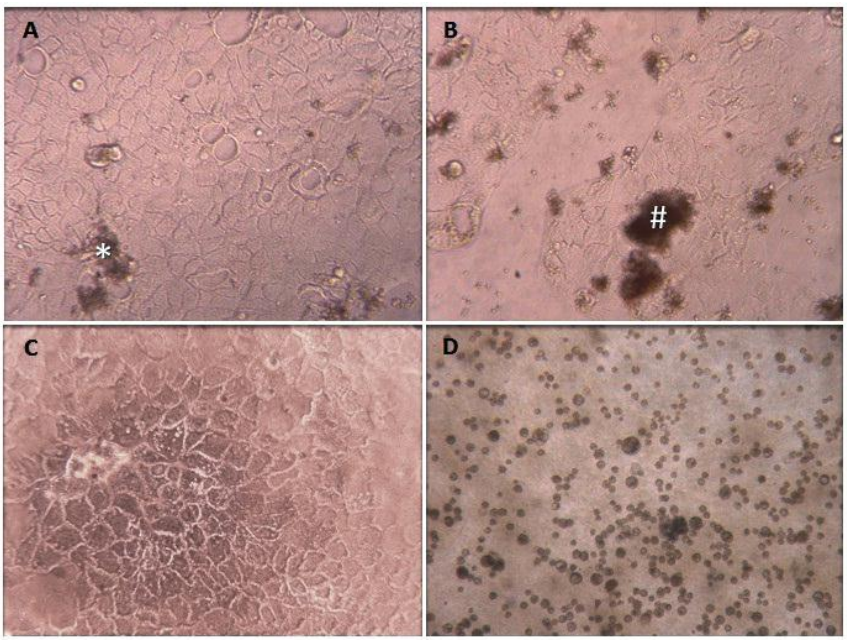

Figure 2.14 - Microscopic Photographs of Caco-2 cells after being seeded in the presence of the culture medium that was previously put in contact with MIP* (A) and NIP$^{\#}$ (B). The negative and positive controls are presented in (C) and (D). Original magnification x100.

To further evaluate the biocompatibility of the polymers, MTS assay was also performed. To perform this assay, culture medium that was in contact with MIP and NIP samples for 24, 48 and 72 hours, was added to the Caco-2 cells. The MTS assay results (Figure 2.15) showed that cell viability was higher for the negative control, in which cells were seeded just with EMEM (EBSS), followed by those that were seeded in the presence of the test samples, MIP and NIP. As should be expected the positive control showed almost no viable cells.

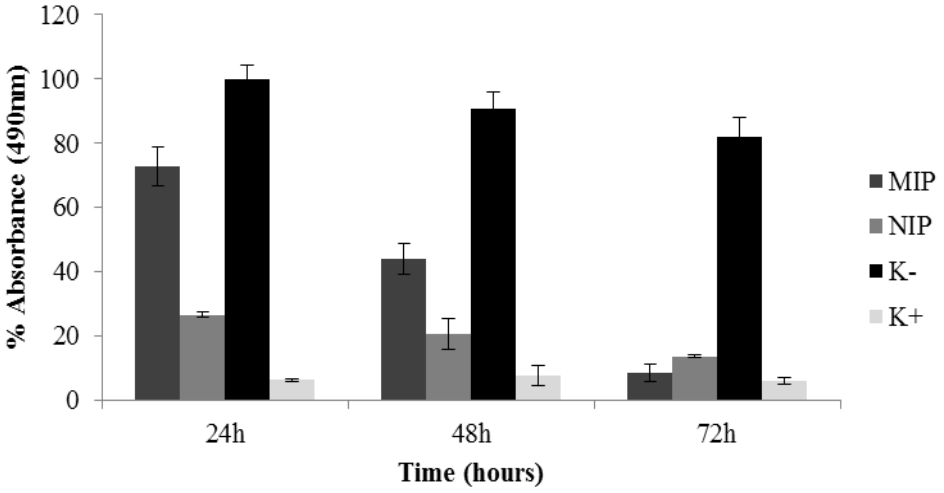

Figure 2.15 - Cellular activities measured by the MTS assay after 24, 48 and 96 hours in contact with the polymers. MIP, NIP, K+, positive control; K-, negative control. Each result is the mean ± standard error of at least three independent experiments.

To further characterize the cytotoxic profile of the polymers, SEM images were also acquired. In these images (Figure 2.16), it was possible to observe the proliferation and the adhesion of Caco-2 cells to the MIP (Figure 2.16A) and NIP (Figure 2.16B) particles. These results confirm that the polymers are biocompatible and that they can be used for drug delivery applications.

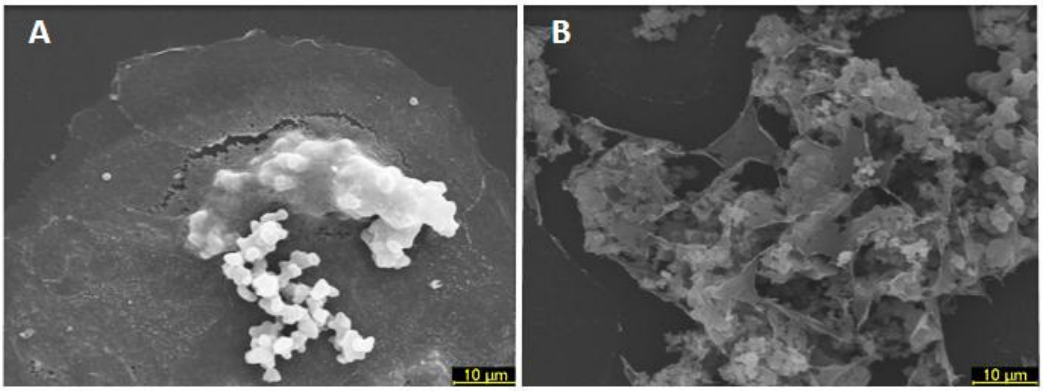

Figure 2.16 - Images of scanning electron microscopy. (A) MIP nanoparticles in contact with Caco-2 cells (1500x, 20Kv); (B) NIP nanoparticles in contact with Caco-2 cells (1500x, 20Kv).

2.2.2.3 Drug delivery experiments

In this work copolymers with molecular recognition ability to the template molecule, ibuprofen, were developed using supercritical carbon dioxide as polymerization and impregnation medium. Both copolymers, MIP and its corresponding NIP, were impregnated in batch mode in $scCO_2$. The impregnation experiment was performed in such conditions that the amount of ibuprofen loaded in the polymers was not limited by the amount of ibuprofen present in the supercritical environment. MIP was loaded with a much higher amount of ibuprofen than NIP, 33.1 wt% compared to only 10.2 wt% (Table 2.4), which reflects the higher affinity of the imprinted polymer towards the template drug than the non-imprinted polymer. This means that the presence of ibuprofen during polymerization greatly influences the drug partition between the supercritical fluid and the polymeric phases, having a real impact in the impregnation efficiency. Impregnation in supercritical medium can lead to high amounts of drug uptake by the polymers, as it was reported in literature, for example, in the impregnation of PVP with ketoprofen [36]. The significant difference between MIP and NIP is enhanced by the fact that the polymers are loaded with the drug in the same solvent that they were synthesized. In the imprinting process, rebinding of the drug in the same solvent of the polymerization is known to improve the imprinting factor [19]. This occurs because during polymerization the binding sites that are created adjust to the solvation of the polymer by the porogen, so the binding sites integrity is optimal when the rebinding solvent is the same that is used in the polymer synthesis [37].

Previously impregnated NIP and MIP were evaluated as sustained drug release systems in two different experimental conditions. In case I the matrices were allowed to release the impregnated drug for 70 hours, at 37 ºC and pH 7.4. In case II the copolymers were exposed to two different pHs in a total of 8 hours. In the first 3 hours the matrices were immersed in a solution of pH 2.2 and then moved to a solution of pH 7.4, both at 37 ºC. By performing the drug release experiments at those

conditions we wanted to evaluate the drug release kinetics from the polymeric networks in a situation that simulated an oral drug administration.

Figure 2.17 presents the cumulative amount of ibuprofen release profiles from both MIP and NIP at pH 7.4 for 70 hours. As it is shown the imprinted polymer, which was loaded with a higher amount of ibuprofen in the impregnation step, also released much more ibuprofen than the corresponding blank polymer. The release of ibuprofen after 24 hours was 181 mg/g polymer for MIP against only 65 mg/g polymer for NIP. After this time, the non-imprinted polymer almost reached the plateau of ibuprofen release whilst the imprinted polymer was still releasing the impregnated drug.

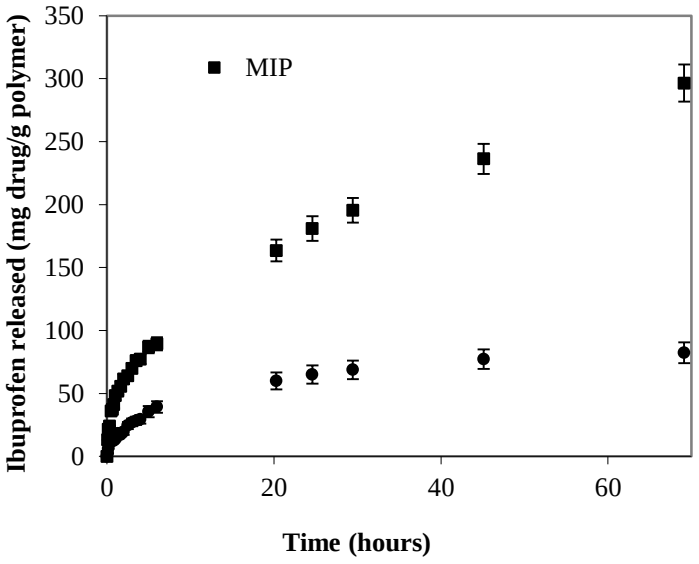

Figure 2.17 - Ibuprofen release profiles in phosphate buffer pH 7.4 from imprinted (filled squares) and non-imprinted (filled dots) DMAEMA-EGDMA copolymers. Each result is the mean ± standard error of the mean of at least three independent experiments.

Figure 2.18 shows the experimental release profiles of ibuprofen from impregnated samples of MIP and NIP as a function of time upon the matrices were put at pH 7.4 for 8 hours or pH 2.2 for 3 hours followed by a period of 5 hours at pH 7.4. At low pH the polymers just released a low amount of ibuprofen. These results are in accordance with the release profiles of ibuprofen from cationic matrices that can be found in the literature [38]. The lower solubility of ibuprofen at acidic pH may contribute to sustain the release process directly and indirectly by promoting hydrophobic interactions with the polymer. When the pH was changed to 7.4 the amount of ibuprofen released increased significantly, due to its higher solubility at neutral pH. As it is possible to observe, different release kinetics are obtained as the polymers are immersed in solutions with different pH. In drug delivery systems there are several parameters that can control burst release, such as the solubility of the drug in the release medium, the drug diffusion coefficient through the materials and the initial drug distributions within

the polymeric carrier [39]. As ibuprofen solubility at acidic pH is very small, the drug release is hindered with respect to the release at neutral pH.

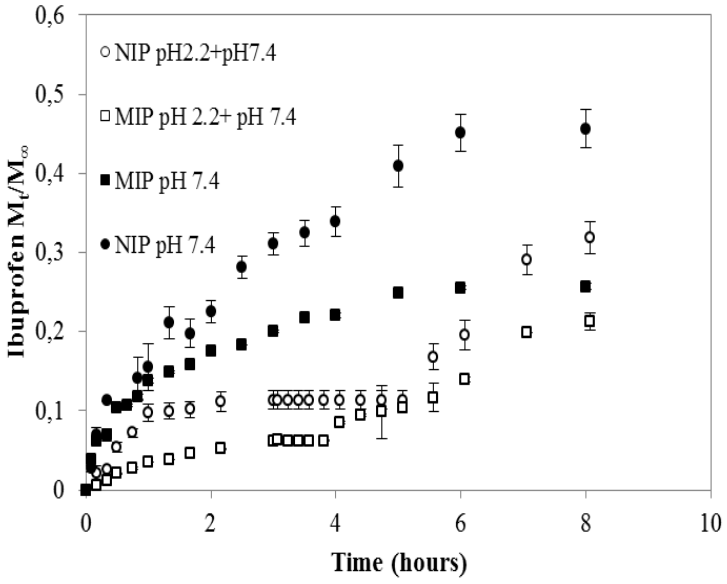

Figure 2.18 - In vitro release profiles of ibuprofen from MIP and NIP at 37ºC and different pH for 8 hours. Each result is the mean ± standard error of at least three independent experiments.

Mathematical modeling of drug delivery from polymeric systems during the first hour at pH 7.4 and pH 2.2 was accomplished through the semi-empirical Korsmeyer–Peppas Model (Equation 2.2) that was used to determine the release constants. Figure 2.19 presents the fit of experimental data to the empirical model and Table 2.5 summarizes the diffusional coefficient and the release exponent from the polymeric delivery systems as calculated by the theoretical equation.

Both systems NIP and MIP present the same release exponent, independently of the pH of the release solution, meaning the mechanism of drug transport through the particles is very similar. At neutral pH, release occurs by an anomalous transport ($0.43 < n < 0.85$, considering spherical particles) [40] explained by the superposition of both diffusion and swelling, whereas in an acidic solution the release follows a case-II transport ($n > 0.85$).

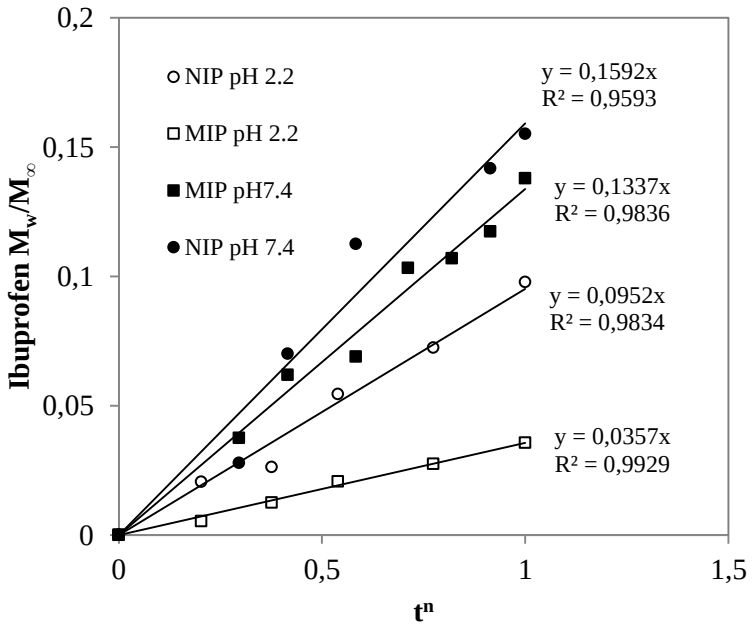

Figure 2.19 - Ibuprofen diffusion coefficients from NIP and MIP at 37ºC, pH 2.2 and pH 7.4 in the first hour of drug release.

Table 2.5 - Summary of diffusion coefficients and release exponents at different pH.

	Diffusion coefficient, k (h^{-1})		**Release exponent, n**	
	pH 2.2	**pH 7.4**	**pH 2.2**	**pH 7.4**
MIP	0.0357	0.1337	0.89	0.49
NIP	0.0952	0.1592	0.89	0.49

Diffusion coefficients of ibuprofen from the matrices to the release medium depend on the drug solubility and the affinity of the polymer to the drug. At pH 2.2 the solubility of ibuprofen is very low, which lowers the diffusion coefficients of the drug through the systems. When the release is performed at neutral pH, whereas ibuprofen has much higher solubility, the diffusion coefficients increase. At both pHs the diffusion coefficients are lower for MIP than for NIP, reflecting a more sustained drug delivery from the affinity polymers. This effect is more pronounced at acidic pH when hydrophobic interactions between ibuprofen and polymeric networks are enhanced due to ibuprofen low solubility. This suggests that not only hydrogen bonds are involved in the stabilization of imprinted polymer-drug complex but also hydrophobic interactions play a significant role.

2.2.3 Conclusion

In this work we have studied the possibility of using molecular imprinting strategy to impart drug specificity within low cross-linked matrices, synthesized and processed in $scCO_2$. It has been proved that it is possible to decrease considerably the crosslinking of polymeric matrices and still be able to imprint them and develop copolymers with molecular recognition to a drug molecule. Furthermore the imprinting during polymerization was able to produce copolymers with higher affinity to the template drug which was reflected in the higher drug uptake during impregnation in $scCO_2$ and consequently a higher drug release amount in the *in vitro* drug release experiments compared to the NIP copolymer. Cytotoxicity assays demonstrated that the synthesized matrices are biocompatible, with the imprinted polymer showing better results with concern to cell adhesion and proliferation. These promising results show that the right balance between rigidity and flexibility of the polymeric matrix can be achieved by lowering the crosslinking degree, and that a successful imprinted copolymer could be developed using a clean technology, such as supercritical fluid technology, leading to highly pure materials with affinity towards a specific drug. We believe that the present methodology is a promising way to develop polymeric systems for drug delivery applications, with additional degrees of control over the drug release profiles, in the near future.

2.3 References

[1] Chen, L., Xu, S., Jinhua, L., Recent advances in molecular imprinting technology: current status, challenges and highlighted applications, Chem. Soc. Rev. 2011, 40, 2922-2942.

[2] Hua, Z., Chen, Z., Zhao, M., Thermosensitive and salt-sensitive molecularly imprinted hydrogel for bovine serum albumin, Langmuir 2008, 24, 5773-5780.

[3] Li, S., Huang, X., Zheng, M., Li, W., Molecularly impronte polymers: modulating molecular recognition by a thermal phase transition in the binding framework, Anal. Bioanal. Chem. 2008, 392, 177-185.

[4] Temtem, M., Casimiro, T., Mano, J.F., Aguiar-Ricardo, A., Green synthesis of a temperature sensitive hydrogel, Green Chem. 2007, 9, 75-79.

[5] Nicholls, I.A., Adbo, K., Andersson, H.S., Andersson, P.O., Ankarloo, J., Hedin-Dahlstrom, J., Jokela, P., Karlsson, J.G., Olofsson, L, Rosegren, J., Shoravi, S., Svenson, J., Wikman, S., Can we reationally design molecularly imprinted polymers?, Anal. Chim. Acta 2001, 435, 9-18.

[6] Yilmaz, E., Mosbach, K., Haupt, K., Influence of functional and cross-linking monomers and the amount of template on the performance of molecularly imprinted polymers in binding assays, Anal. Commun. 1999, 36, 167-170.

[7] Soares da Silva, M., Nobrega, F. L. Aguiar-Ricardo, A., Cabrita, E.J., Casimiro, T., Development of molecularly imprinted co-polymeric devices for controlled delivery of flufenamic acid using supercritical fluid technology, DOI: 10.1016/j.supflu.2011.05.010.

[8] Casimiro, T., Banet-Osuna, A. M., Nunes da Ponte, M., Aguiar-Ricardo, A., Synthesis of highly cross-linked poly(diethylene glycol dimethacrylate) microparticles in supercritical carbon dioxide, Eur. Polym. J. 2005, 41, 1947-1953.

[9] Ellwanger,A., Berggren, C., Bayoudh, S., Crecenzi, C., Karlsson, L., Owens, P. K., Ensing, K., Cormack, P., Sherrington, D., Sellergren, B., Evaluation of methods aimed at complete removal of template from molecularly imprinted polymers, Analyst 2001, 126, 784-792.

[10] Barroso, T., Temtem, M., Casimiro, T., Aguiar-Ricardo, A., Development of pH-responsive poly(methylmethacrylate-co-methacrylic acid) membranes using $scCO_2$ technology. Application to protein permeation, J. Supercrit. Fluids 2009, 51, 57-66.

[11] Laitinen, A., Jauhiainen, O., Aaltonen, O., Solubility of Fluorinated Pharmaceuticals in Dense Carbon Dioxide, Org. Proc. Res. & Development 2000, 4, 353-356.

[12] Ivanova, G., Vão, E.R., Temtem, M., Aguiar-Ricardo, A., Casimiro, T., Cabrita, E.J., High-Pressure NMR Characterization of Triacetyl-beta-Cyclodextrin in Supercritical Carbon Dioxide, Magn. Res. Chem. 2009, 47, 133-141.

[13] Temtem, M., Casimiro, T., Gil Santos, A., Macedo, A. L., Cabrita, E. J., Aguiar-Ricardo, A., Molecular Interactions and CO_2-Philicity in Supercritical CO_2. A High-Pressure NMR and Molecular Modeling Study of a Perfluorinated Polymer in $scCO_2$, J. Phys. Chem. B 2007, 111, 1318-1326.

[14] Rufino, E.S., Monteiro, E.E.C., Infrared study on methyl methacrylate–methacrylic acid copolymers and their sodium salts, Polymer 2003, 44, 7189–7198.

[15]Alvarez-Lorenzo, C., Concheiro, A., Molecularly imprinted polymers for drug delivery, J. Chromatogr. B 2004, 804, 231-245.

[16] Yu, C., Mosbach, K., Molecular imprinting utilizing an amide functional group for hydrogen bonding leading to highly efficient polymers, J. Mol. Recogn. 1998, 11, 69-74.

[17] Soares da Silva, M., Vão, E.R., Temtem, M., Mafra, L., Caldeira, J., Aguiar-Ricardo, A., Casimiro, T., Clean synthesis of molecular recognition polymeric materials with chiral sensing capability using supercritical fluid technology. Application as HPLC stationary phases, Biosens. Bioelectron. 2010, 25, 1742-1747.

[18] Duarte, A.R.C., Casimiro, T., Aguiar-Ricardo, A., Simplício, A.L., Duarte, C.M.M., Supercritical fluid polymerisation and impregnation of molecularly imprinted polymers for drug delivery, J. Supercrit. Fluids 2006, 39, 102-106.

[19] Byrne, M.E., Kinam Park, K., Peppas, N.A., Molecular imprinting within hydrogels, Adv. Drug Deliv. Rev. 2002, 54, 149–161.

[20] Byrne, M.E., Salian, V., Molecular imprinting within hydrogels II: Progress and analysis of the field, Int. J. Pharm. 2008, 364, 188-212.

[21] Venkatesh, S., Sizemore, S.P., Byrne, M.E., Biomimetic hydrogels for enhanced loading and extended release of ocular therapeutics. Biomaterials 2007, 28, 717-724.

[22] Ali, M., Horikawa, S., Venkatesh, S., Saha, J., Hong, J.W., Byrne, M.E., Zero-order therapeutic release from imprinted hydrogel contact lenses within in vitro physiological ocular tear flow, J. Control. Release 2007, 124, 154-162.

[23] Suedee, R., Jantarat, C., Lindner, W., Viernstein, H., Songkro, S., Srichana, T., Development of a pH-responsive drug delivery system for enantioselective-controlled delivery of racemic drugs, J. Control. Release 2010, 142, 122–131.

[24] Dai, F., Sun, P., Liu, Y., Liu, W., Redox-cleavable star cationic PDMAEMA by arm-first approach of ATRP as a nonviral vector for gene delivery, Biomaterials 2010, 31, 559–569.

[25] Ou, S.H., Wu, M.C., Chou, T.C., Liu, C.C., Polyacrylamide gels with electrostatic functional groups for the molecular imprinting of lysozyme, Anal. Chim. Acta 2004, 504, 163-166.

[26] Kugimiya, A., Takeuchi, T., Molecular recognition by indoleacetic acid-imprinted polymers- effects of 2-hydroxyethyl methacrylate content, Anal. Bioanal. Chem. 2002, 372, 305-307.

[27] Cirillo, G., Parisi, O.I., Curcio, M., Puoci, F., Iemma, F., Spizzirri, U.G., Picci, N., Molecularly imprinted polymers as drug delivery systems for the sustained release of glycyrrhizic acid, J. Pharm. Pharmacol. 2010, 62, 577-582.

[28] Soares da Silva, M., Viveiros, R., Morgado, P.I., Aguiar-Ricardo, A., Correia, I.J., Casimiro, T., Development of 2-(dimethylamino)ethyl methacrylate- based molecular recognition devices for controlled drug delivery using supercritical fluid technology, 10.1016/j.ijpharm.2011.06.004.

[29] Maia, J., Ribeiro, M.P., Ventura, C. Carvalho, R.A., Correia, I.J., Gil, M.H., Ocular injectable formulation assessment for oxidized dextran-based hydrogels, Acta Biomater. 2009, 5, 1948-55.

[30] Baoum, A., Dhillon, N., Buch, S., Berkland, C., Cationic surface modification of PLG nanoparticles offers sustained gene delivery to pulmonary epithelial cells. J. Pharm. Sci. 2010, 99, 2413-2422.

[31] Ribeiro, M., Espiga, A., Silva, D., Baptista, P., Henriques, J., Ferreira, C., Silva, J., Borges, J., Pires, E., Chaves, P., Development of a new chitosan hydrogel for wound dressing. Wound Repair Regen. 2009, 17, 817-824.

[32] Rosellini, E., Barbani, N., Giusti, P., Ciardelli, G., and Cristallini, C., Molecularly imprinted nanoparticles with recognition properties towards a laminin H–Tyr–Ile–Gly–Ser–Arg–OH sequence for tissue engineering applications. Biomed. Mater. 2010, 5, 6, 065007.

[33] Baggiani, C., Anfossi, L., Baravalle, P., Anfossi, L., Tozzi, C., Comparison of pyrimethanil-imprinted beads and bulk polymer as stationary phase by non-linear chromatography, Anal. Chim. Acta 2005, 542, 125–134.

[34] Yanfeng, C. Min, Y., Swelling kinetics and stimuli-responsiveness of poly(DMAEMA) hydrogels prepared by UV-irradiation, Radiat. Phys. Chem. 2001, 61, 65–68.

[35] Ding, Y., Bian, X., Yao, W., Li, R., Ding, D., Hu, Y., Jiang, X., Hu, Y., Surface-potential-regulated transmembrane and cytotoxicity of chitosan/gold hybrid nanospheres, ACS Appl. Mater. Interfaces 2010, 2, 1456–1465.

[36] Manna, L., Banchero, M., Sola, D., Ferri, A., Ronchetti, S., Sicardi, S., Impregnation of PVP microparticles with ketoprofen in the presence of supercritical CO_2, J. Supercrit. Fluids 2007, 42, 378–384.

[37] Spivak, D., Gilmore, M. A., Shea, K.J., Evaluation of binding and origins of specificity of 9-ethyladenine imprinted polymers, J. Am. Chem. Soc. 1997, 119, 4388-4393.

[38] Rodríguez, R., Alvarez-Lorenzo, C., Concheiro, A., Interactions of ibuprofen with cationic polysaccharides in aqueous dispersions and hydrogels. Rheological and diffusional implications. Eur. J. Pharm. Sci. 2003, 20, 429–438.

[39] Bibby, D.C., Davies, N.M., Tucker, I.G., Mechanisms by which cyclodextrins modify drug release from polymeric drug delivery systems, Int. J. Pharm. 2000, 197, 1–11.

[40] Siepmann, J., Peppas, N.A., Modeling of drug release from delivery systems based on hydroxypropyl methylcellulose (HPMC), Adv. Drug Deliv. Rev. 2001, 48, 139–157.

CHAPTER 3

Molecular recognition hosts for chiral separations by HPLC

3. Molecular recognition hosts for chiral separations by HPLC

Chirality has an important role in biological processes, with the enantiomers of the same bioactive compound having different effects on biological systems. As the search for new drugs with improved pharmacological properties is growing, so is the importance of effectively differentiating and separating their enantiomers. Chiral separations are one of the most challenging areas of analytical chemistry and many efforts have been done to develop efficient chromatographic methods able to resolve the racemates of biological active molecules.

One of the aims of this thesis was to address the possibility of developing a high affinity material using supercritical fluid technology, able to distinguish very similar molecules such as enantiomeric species, which could have a real impact in chromatography.

Herein two types of chiral stationary phases were developed to resolve the racemic mixture of Boc-tryptophan. In a first approach, MIP-based chiral stationary phases were prepared. In a second approach, a dual recognition polymeric host was synthesized combining both MIPs and cyclodextrins. Both polymeric matrices were packed into blank HPLC columns and their ability to separate the enantiomers of Boc-Tryptophan evaluated. This chapter describes the work concerning the development of chiral stationary phases via molecular imprinting using supercritical fluid technology.

3.1 Green preparation of chiral stationary phases- MIPs

The rational design of a high affinity imprinted polymeric network depends on the optimization of several operational variables. The polymerization conditions, temperature, solvent polarity, pressure, monomer concentration and interactions solvent-monomers-template are known to have practical effects on selectivity, which are associated to the stability of the self-assembly complexes during polymerization, which in turn influences the recognition process.

The general mechanism of imprinting states the importance of the functional monomers as being essential in the establishment of stable bonds with the template. However, the first synthesis of a molecular recognition polymeric material using supercritical fluid technology was carried out using the crosslinker agent as the only monomer involved in the imprinting process. Micron-sized spherical particles of poly(diethylene glycol dimethacrylate), PDEGDMA MIP , were prepared in $scCO_2$ using salicylic acid and acetylsalicylic acids as model templates, for potential applications in controlled drug release devices [1]. Previously the optimization of the synthesis of this highly crosslinked material in $scCO_2$ had already been performed [2].

This work started with the homopolymerization of EGDMA in the presence of the template molecule, Boc-L-Tryptophan, in order to prepare the imprinted polymer. Tryptophan is an essential amino acid which is a precursor for a wide array of metabolites, such as serotonin, N-formylkynurenine and melatonin [3]. Tryptophan and metabolites are known for their bioactive effects and studies in the literature suggest that their depletion can lower the mood, bring some memory impairment and increase aggression levels [4]. Although D-tryptophan can be found in some naturally occurring peptides, L-Tryptophan is the most bioactive stereoisomer. For that reason, the L-stereoisomer was chosen as the template molecule. Figure 3.1illustrates the molecular structure of both enantiomers.

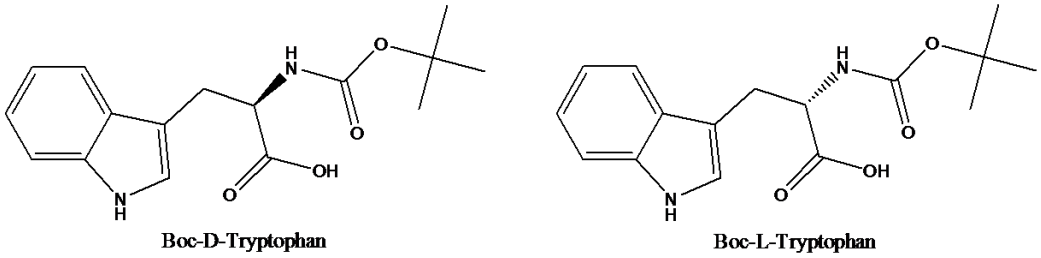

Figure 3.1 - Molecular structure of Boc-D and Boc-L-Trp.

The structural similarity of the molecules demands a chiral polymeric phase with high selectivity towards the template. Moreover, in this work, it was decided to use an aqueous eluent in the chromatographic method, because we wanted to develop a clean and sustainable alternative process. Thus the imprinting system had to be chosen in such a way that the monomer would have to be able to establish hydrogen bonds with the template in an apolar medium, such as $scCO_2$ and afterwards, in the rebinding process, the polymer would have to selectively bind the Boc-L in a polar aqueous phase. Hence, a functional monomer was introduced in the system to increase the molecular affinity of the imprinted matrix. As literature evidences the ability of amides to establish hydrogen bonds in polar solvents [5], N-isopropyl acrylamide (NIPAAm) was chosen as functional monomer.

Process optimization for obtaining a chiral stationary phase and an analytical method able to efficiently resolve the racemic mixture, involved innumerable attempts. Several combinations of monomers were used to prepare alternative copolymers to P(NIPAAm-EGDMA), such as P(MAA-EGDMA), P(2-Vpy-EGDMA) and P(2-Vpy-MAA-EGDMA). Also several combinations of solvents, in isocratic and gradient mode, were used to obtain an aqueous eluent that, in combination with the right copolymer could deliver a resolved racemic mixture. The influence of the morphology of the polymeric particles in the enantioselectivity was also investigated by means of adding Krytox to the

reactional mixture, in order to synthesize spherical particles of imprinted PEGDMA. This study will be presented in this section.

The copolymers were then slurry packed into blank HPLC columns and a new chromatographic method was developed and optimized to deliver the best conditions for the separation of the racemic mixture. Moreover, the molecular recognition capability of the developed materials was investigated concerning the influence of functional monomer addition, sample load and temperature.

This part of the thesis was published in Biosensors and Bioelectronics [6].[1]

3.1.1 Experimental

3.1.1.1 Materials

Ethylene glycol dimethacrylate (EGDMA, 98% purity) as cross-linker, N-isopropylacrylamide (NIPAAm, 97% purity), methacrylic acid (MAA, 99% purity) and 2-Vinylpyridine (2-Vpy, 97% purity) as functional monomers, Boc-L-tryptophan (Boc-L-trp, 99% purity) as template molecule, Boc-D-tryptophan (Boc-D-trp, 98% purity) and azobis(isobutyronitrile) (AIBN, 98% purity) were purchased from Sigma-Aldrich. Krytox 157 FSL, the stabilizer agent, was supplied from DuPont. Phosphate buffer solution (PBS) was purchased from Sigma-Aldrich. HPLC grade acetonitrile (MeCN), acetic acid and n-hexane from Scharlau were used. Carbon dioxide was obtained from Air Liquide with purity better than 99.998%. All chemicals were used without further purification.

3.1.1.2 MIP and NIP synthesis in $scCO_2$

The experimental procedure of polymerization reactions in $scCO_2$ was described in Chapter 2. In this work, the total weight of monomers was kept constant and equal to 3.43 g. In a typical procedure to produce MIPs with recognition to Boc-L-tryptophan, crosslinker (3.43g when it was the only monomer used or 3.08 g when used in combination with a functional monomer), monomer (12 wt% with respect to the amount of cross-linker, if included), initiator (2 wt %) and template (1 wt%) were loaded into the high-pressure cell. When used, the Krytox amount introduced corresponded to 4 wt% of the monomer. For the production of NIPs the same procedure was followed except no template was added. Several copolymers were synthesized and tested as potential chiral stationary phases. The imprinted polymers will be herein referred as MIPs, whilst the non-imprinted polymers will be referred as NIPs.

[1] Reproduced with the authorization of the editor and subjected to the copyrights imposed.

3.1.1.3 HPLC analysis

The synthesized polymers were slurry packed into a blank column (Supelco; 150 mm x 4.6 mm) using a Millipore aqueous mixture of acetonitrile. Chromatographic analyses were carried out using a Merck L-7100 HPLC pump equipped with an L-7400 UV detector, D-7000 computer interface and a XT Maraton autosampler. UV detection was made at 275 nm. Prior to the experiments column was thoroughly washed with acetonitrile with 1% v/v of acetic acid until a stable baseline was achieved. Experiments were carried out at 25ºC and 65ºC using a column oven (XT Maraton). Numerous eluent compositions, flow rates and isocratic/gradient mixtures of water and organic solvents were tested for different stationary phases. Table 3.1 resumes some variables that were tested.

Table 3.1 – Experimental variables studied during the analytical method optimization.

Polymeric system	**Analytical variables**		
	Flow rate	**Solvents**	**Sample Load**
PEGDMA PEGDMA_Krytox P(MAA-EGDMA) Poly(2-Vpy-EGDMA) Poly(2-Vpy-MAA-EGDMA) Poly(NIPAAm-EGDMA)	The flow rates studied ranged from 0.1 - 1 mL/min	As eluents I studied different mixtures of water (0-100%), acetonitrile (0-100%), acetic acid (0-3.5%) and hexane (0-6%)	Concentrations of the injected mixtures ranged from 0.25 – 8 mM

The majority of the experimental conditions herein reported did not yield chromatographic enantiomeric differentiation. The copolymers of P(MAA-EGDMA), P(2Vpy-EGDMA) and P(2-Vpy-MAA-EGDMA) were not able to differentiate the enantiomers injected whatever the analytical conditions tested. Only the imprinted polymers of P(EGDMA) and P(NIPAAm-EGDMA) showed molecular selectivity for Boc-L-Trp. For these polymeric packings the mobile phase used was hydro-organic with 8% acetonitrile by volume at a flow rate of 0.5 mL min^{-1}. 0.25-4 mM samples were injected for analysis using a loop volume of 5 µL. Acetone was used as void marker, to determine the column dead time. Poly(NIPAAm-EGDMA) was packed in a longer column (Supelco; 250mm x 4.6mm) in order to increase the enantiomeric resolution. This column was also tested in a Knauer equipment, with IR detection Smartline 2300 and pump Smartline 1000.

3.1.1.4 Polymer characterization

SEM and Nitrogen porosimetry

Polymers were morphologically characterized using scanning electron microscopy (SEM) in a Hitachi S-2400 instrument, with an accelerating voltage set to 15 kV. Samples were mounted on aluminium stubs using carbon tape and were gold coated.

Specific surface area and pore diameter of the polymeric particles were determined by adsorption of N_2 according to the BET method. An accelerated surface area and porosimetry system (ASAP 2010 Micromeritics) was used under nitrogen flow.

Solid State NMR

^{13}C CPMAS NMR spectra were recorded on a Bruker AVANCE 400 (DSX) WB spectrometer (9.4 T), using a double-resonance 4 mm VTN probe, with a Larmor frequency of 100.62 MHz. The samples were packed into a 4mm diameter ZrO2 cylindrical rotor and spun at MAS rates of 7 and 10 kHz. The 13C CPMAS spectrum was recorded using a RAMP-CP shape (100% to 50% amplitude); rf field strengths between 50 and 70 kHz for Hartman-Hahn condition calibration for 13C and 1H channels; number of scans = 2-4K; recycle delay of 5s; contact time = 1.5 ms; ^{1}H decoupling was employed using the Small Phase INcremental ALternation (SPINAL64) multiple pulse scheme with 64 steps (Fung et al., 2000), during the ^{13}C acquisition. A pulse length of 4.5 μs (ca. 165° degree pulses) was used for the basic unit of the SPINAL64 scheme, while the ^{1}H radio-frequency field strength ($\omega_1/2\pi$) employed was 105 kHz. Chemical shifts were quoted in parts per million (ppm) from solid glycine.

3.1.2 Results and Discussion

3.1.2.1 Characterization of the synthesized polymers

The molecular imprinted and non-imprinted polymers were obtained as dry, free-flowing powders in high yields (~99%, determined gravimetrically) and all the polymeric particles were useful to be slurry packed which can be considered a major advantage over traditional MIPs that have to be ground and sieved, leading to product loss of about 50% [7]. The pressure-temperature conditions of the reaction assure an initial homogeneous system, as it can be seen through the sapphire windows.

As already mentioned in the experimental part, copolymers of methacrylic acid and 2-vinylpyridine did not show selective affinity to the template molecule. For that reason, those copolymers were not fully characterized. Instead, a detailed characterization of PEGDMA and P(NIPAAm-EGDMA) MIPs and NIPs was carried out and will be discussed in the next pages.

SEM images revealed that the imprinted and non-imprinted polymers show similar morphology, aggregates of smooth surfaced discrete submicron particles. Figure 3.2 shows a SEM image of PEGDMA NIP and MIP. It seems that by introducing a small amount of template during the polymerization step, the morphology of the polymers is not greatly affected. Also, the introduction of a functional monomer in the reactional system does not change significantly the morphology of the polymers in such a way that it can be detected by SEM, as images revealed no visible differences between homopolymers and copolymers.

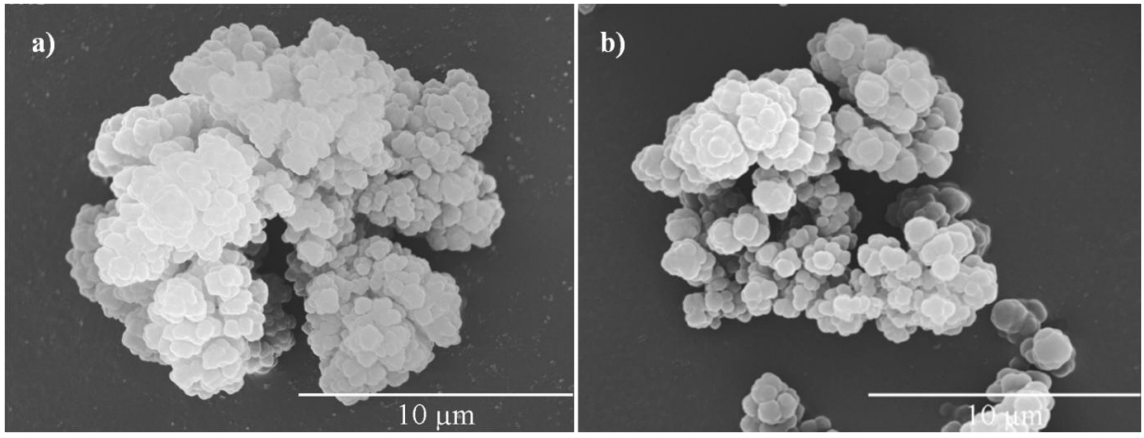

Figure 3.2 - SEM images of PEGDMA a) MIP and b) NIP.

The physical characteristics of both MIPs and NIPs concerning surface area, average pore diameter and specific pore volume, were obtained by multipoint BET method (type II). The surface areas obtained were very similar with those obtained for PNIPAAm synthesized in $scCO_2$, [8]. PEGDMA NIP and MIP show a slight increase on the surface area compared to P(NIPAAm-EGDMA) NIP and MIP (10.3 and 10.1 respectively, compared to 8.4 and 8.5) which could be explained by the fact that the primary particles in this case are smaller, thus, providing a material with higher porosity comprising micron-sized agglomerates of nano-primary particles, as it can be observed on SEM images. This morphology is consistent with other reported precipitation polymerizations in $scCO_2$ without using stabilizers [9,2]. The small differences observed, on the pore volume and diameter for the MIPs and NIPs could be explained by the interference of the template molecule in the nucleation process and/or the presence of template residues within the final polymer.

Table 3.2 - Physical characteristics (surface area, average pore diameter and specific pore volume) of both MIPs and NIPs, obtained by multipoint BET method (type II).

Polymer	Surface Area (m^2/g)	Pore Volume (cm^3/g)	Pore Diameter (nm)
MIP1	10.30	0.0122	4.7
NIP1	10.14	0.0133	5.2
MIP2	8.41	0.0102	4.8
NIP2	8.53	0.0120	5.6

Figure 3.3 depicts the ^{13}C CPMAS NMR spectra of imprinted and non-imprinted polymers. The strong similarities in the ^{13}C chemical shifts and relative intensities between P(NIPAAm-EGDMA) NIP and MIP copolymers, and PEGDMA NIP and MIP polymers, suggest that imprinted and non-imprinted materials are chemically equivalent. Being aware of the insensitive character of NMR to detect very diluted species, the NMR data indicates that the Boc-L-Trp template is not visible on the ^{13}C spectra after washing-out the drug template from imprinted PEGDMA and P(NIPAAm-EGDMA). This observation suggests a successful polymer cleaning upon washing (if not completely removed, at least only a very low template concentration remains).

Structural differences between the copolymers of P(NIPAAm-EGDMA) and the polymers of PEGDMA may be observed by the presence of a faint resonance at *ca.* 42 ppm on P(NIPAAm-EGDMA) due to the additional contribution of the αCH_2 groups on NIPAAm's ligands, which have slightly more shielded chemical shifts. Moreover, the additional peak intensity at *ca.* 22 ppm, observed on P(NIPAAm-EGDMA) (Figure 3.3b and d), with respect to same chemical shift region on the PEGDMA (compare Figure 3.3a and c), is originated from NIPAAm's terminal methylic carbons, which are only present on the copolymers. A detailed peak assignment of the relevant ^{13}C resonances is also shown in Figure 3.3. The presence of weak resonances appearing at *ca.* 125, 137 ppm ($\alpha\beta$ unsaturated carbons from NIPAAm and EGDMA) and *ca.* 167 ppm (carbonyl groups from NIPAAm and EGDMA) shows that a relatively small amount of unreacted double bonds exists on the polymers, which is in accordance with other works found in literature [10].

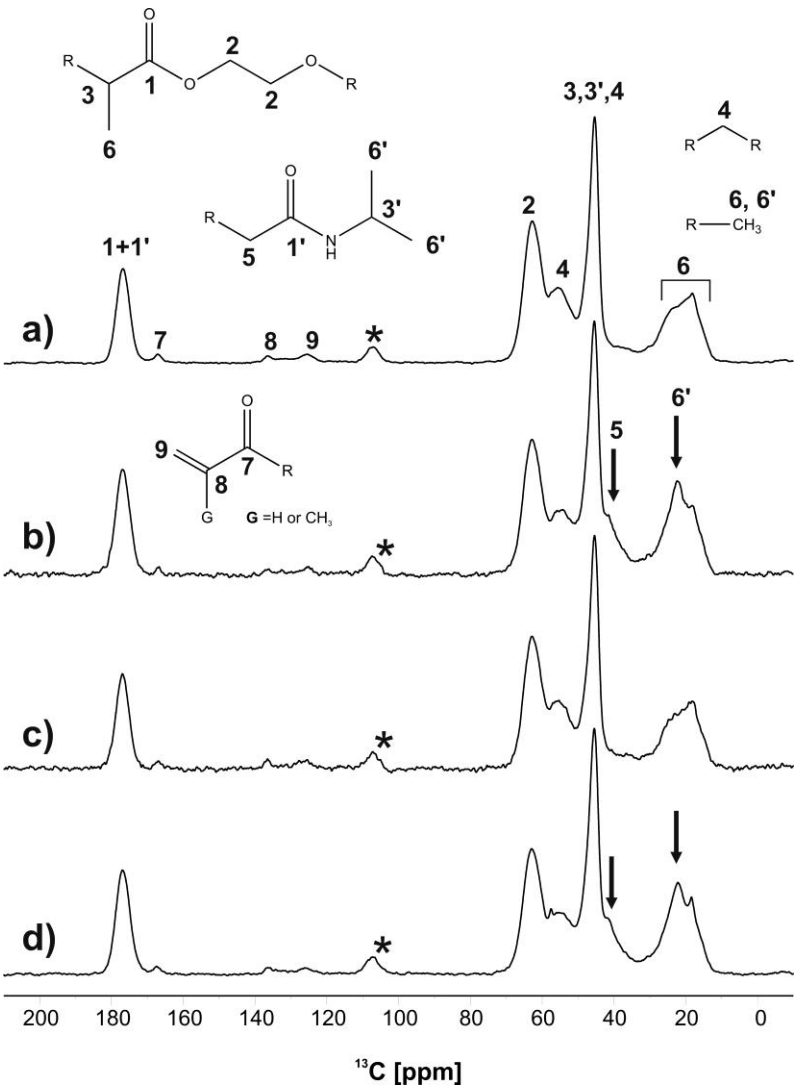

Figure 3.3 - ^{13}C CPMAS NMR spectra and peak assignment. Imprinted matrices, a) PEGDMA; b) P(NIPAAm-EGDMA) and non-imprinted matrices c) PEGDMA and d) P(NIPAAm-EGDMA). Asterisks depict spinning sidebands.

3.1.2.2 Retention factor and Enantioselectivity

The molecular recognition and affinity of the polymers for the template enantiomer was gauged by their ability to selectively retain this molecule. Retention or capacity factors, *k`*, of the prepared MIPs were evaluated according to Equation 3.1.

$$k' = \frac{t_r - t_0}{t_0} \qquad \text{(Equation 3.1)}$$

where t_r is the retention time of the amino acid enantiomer and t_0 is the retention time of the void marker on the column, acetone. The enantioseparation factor, α, was calculated using the following equation:

$$\alpha = \frac{k'_L}{k'_D} \qquad \text{(Equation 3.2)}$$

Resolution of the racemic mixture was calculated from Equation 3.3, where w_D and w_L are the baseline widths at 4.4% of peak height.

$$R = 2 \times \frac{t_{L-} t_D}{W_D + W_L} \qquad \text{(Equation 3.3)}$$

In order to evaluate the cross-linker capability of creating specific bonds with the imprinted molecule, the imprinted PEGDMA synthesized was tested as chromatographic stationary phase. The HPLC Knauer equipment used in the work is shown in Figure 3.4.

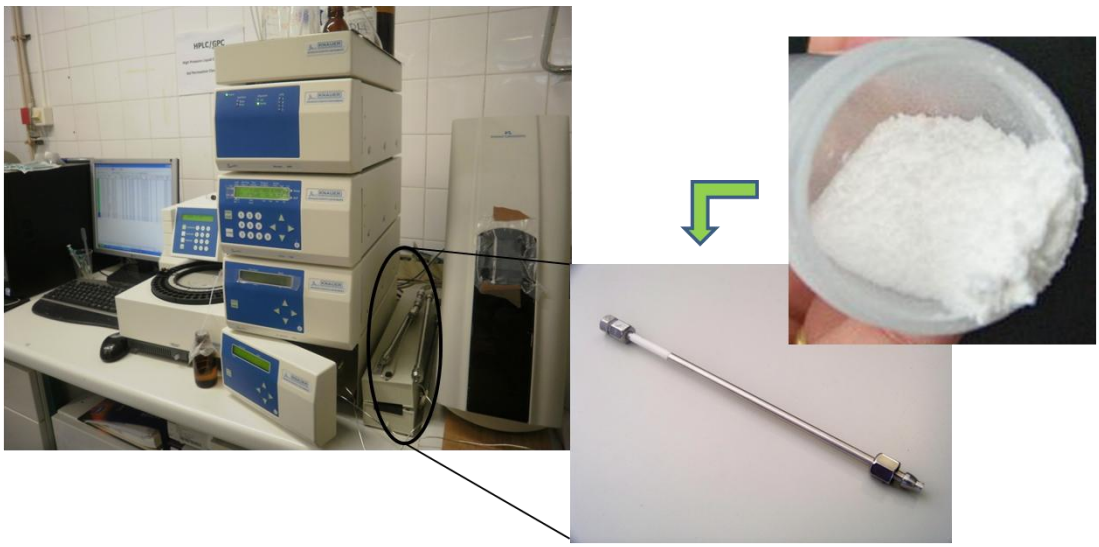

Figure 3.4 - Illustration of the Knauer HPLC equipment used, blank HPLC columns and typical synthesized polymer.

PEGDMA imprinted stationary phase was injected with 1 mM amino acid solutions of Boc-L-Trp and Boc-D-Trp. Figure 3.5 shows the chromatograms obtained using this stationary phase.

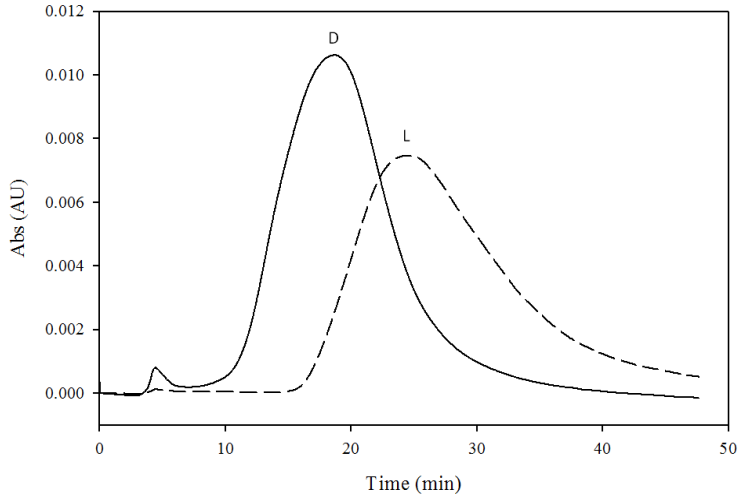

Figure 3.5 - Chromatograms obtained with the separated injections of Boc-D-Trp and Boc-L-Trp using PEGDMA MIP as stationary phase, at 25ºC.

The HPLC peaks obtained are broad and show some asymmetry, which could be explained by the heterogeneity of the binding sites within the matrix. It is reported in literature that this heterogeneity is the major contributor to broad and asymmetric peaks in chromatography [11]. Imprinted polymer of PEGDMA shows some molecular recognition for Boc-D-Trp, although it is evident that higher retention factors are obtained for the template molecule ($t_D \approx$ 19 min compared to $t_L \approx$ 25 min). This means that the imprinted stationary phase has non-specific sites (recognizes both enantiomers) but shows higher specificity for Boc-L-Trp (better recognition of the template enantiomer).

Analytical method optimization engaged several attempts to achieve the best recognition conditions for a given polymer. In this context, gradient elution was tested in PEGDMA MIP stationary phase. Figure 3.6 shows the chromatograms obtained when using the gradient elution as illustrated. By using a gradient with an increasing percentage of acetonitrile, a small difference in the retention times of D and L stereoisomers was achieved ($t_D \approx$ 19.6 min and $t_L \approx$ 21.4 min). Although the difference was not very high, as the peaks became less broad due to the presence of more acetonitrile in the mobile phase, a racemic mixture was injected to investigate if PEGDMA MIP was enantiomeric selective. The chromatogram obtained showed that this polymer was not able to resolve the racemic mixture.

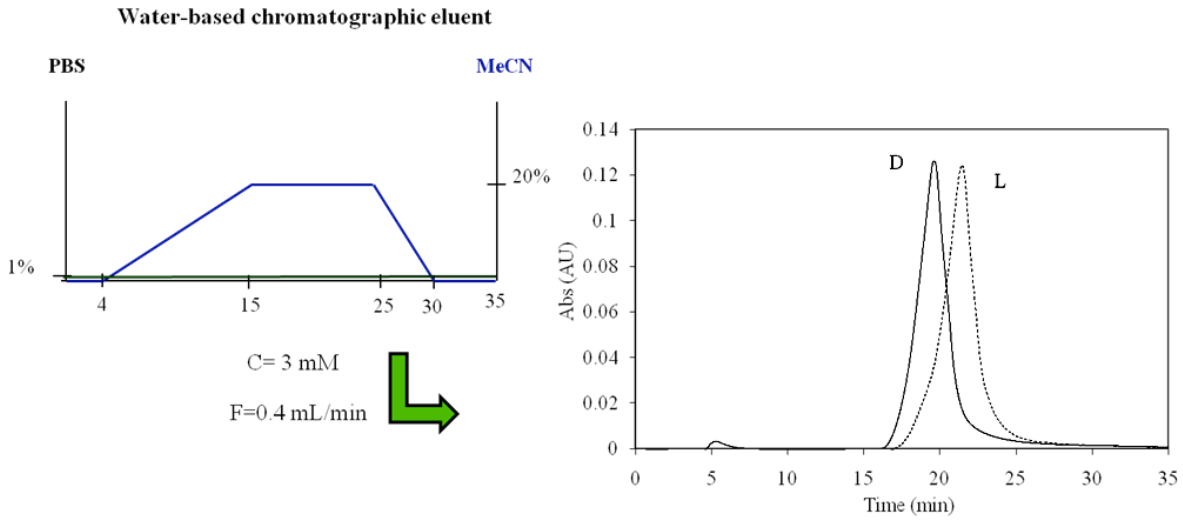

Figure 3.6 - Gradient elution and chromatograms obtained using those conditions.

The influence of the morphology of the polymeric particles on molecular recognition was also studied. Spherical particles of imprinted PEGDMA were synthesized by adding 4 wt% of Krytox to the reaction mixture of imprinting. Figure 3.7 shows the SEM image of this polymer and the chromatograms obtained when injecting D and L stereoisomers, separately. Analytical conditions were the same that were used in the gradient elution on PEGDMA MIP stationary phase. This turn possible to compare both polymers with respect to their molecular recognition ability. As it can be seen in Figure 3.7, the addition of a small amount of Krytox in the synthesis, yielded a polymer with less specific recognition ability than the neat PEGDMA MIP, without Krytox. We suggest that this effect may be due to a possible destabilization of the complexes that otherwise would establish between the crosslinker agent and the template molecule. This possible destabilizing effect of surfactants on molecular imprinting systems is already reported in the literature [12]. However, other analysis would have to be carried out to understand if the issue was really related with a non-viable thermodynamic imprinting system, or instead a physical characteristic disadvantage related with a different morphology.

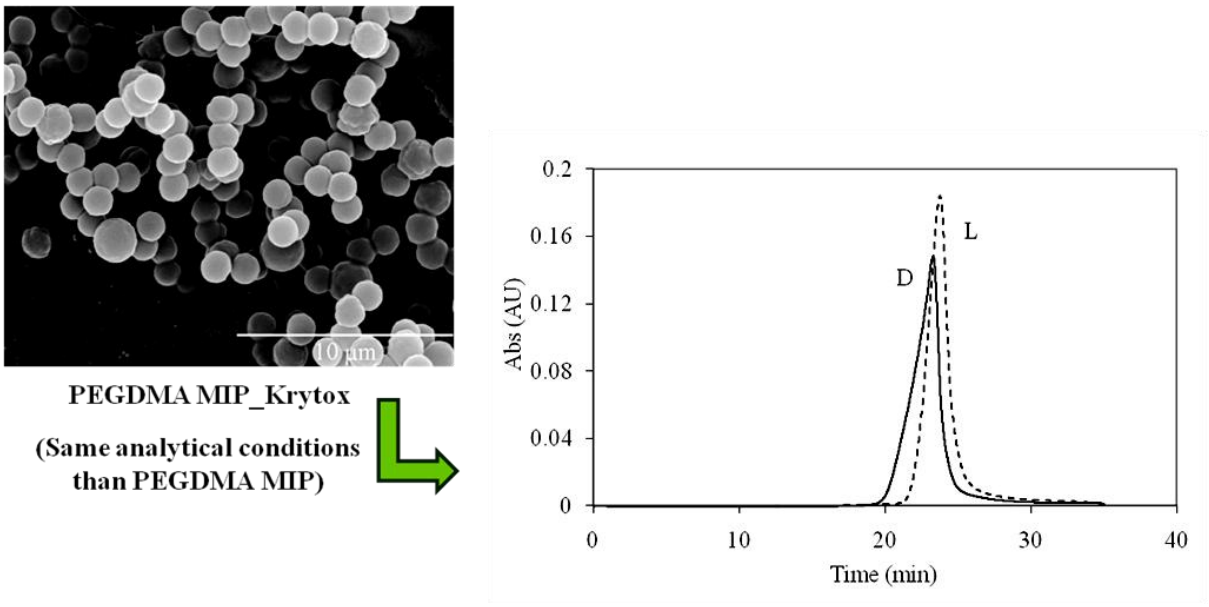

Figure 3.7 - SEM image of PEGDMA_Krytox MIP and chromatograms obtained for D and L stereoisomers using this stationary phase with a gradient elution. Sample load concentration was set as 3 mM and flow rate at 0.4 mL.min^{-1}. For more information about the gradient, please consult Figure **3.6**.

In order to increase the selectivity of the matrix towards Boc-L-Trp, it was decided to introduce a functional monomer in the imprinting system. This monomer would establish more stable complexes with the template molecule, yielding therefore copolymers with higher selectivity to Boc-L-Trp. As functional monomers were tested NIPAAm, MAA, 2-Vpy and a monomeric mixture of MAA and 2-Vpy, in equimolar ratios. The copolymers were then tested with respect to their ability to differentiate the stereoisomers by testing several analytical conditions. The results obtained show that not always the introduction of a functional monomer yields a copolymer with high affinity towards the template. P(MAA-EGDMA), P(2-Vpy-EGDMA) and P(MAA-2-Vpy-EGDMA) did not show any specific molecular recognition. Retention factors were always equal for both enantiomers, independently of the analytical conditions tested. This means that the binding sites in the copolymers, if present, are not highly specific. Further studies would have to be carried out to clearly understand the reason why the matrices containing additional functional groups were not able to differentiate the enantiomers, at least, at the same extent of PEGDMA MIP. We hypothesize that this poor recognition ability in aqueous medium can be related with the solvent memory effect that imprinted polymers present [13]. During polymerization, in a certain solvent, the complexes between template and monomers become spatially fixed due to the presence of the crosslinker, and the growing polymer chains adapt to a certain solvation. When the polymer chains are solvated by other solvents, the solvation is different and therefore there is a distortion of the created binding sites that can greatly affect the affinity of the polymer. As enantiomers possess very similar structures, a slight distortion can be sufficient to the polymer lose its enantiomeric differentiation. In this work we synthesized the polymers in supercritical CO_2 and performed the rebinding studies in aqueous medium. With PEGDMA polymer this effect is

not very significant because, as the polymer is totally crosslinked, the chains do not have enough mobility to swell to a considerable extent. If the complexes between template and monomer, during imprinting process, are not present in enough number and strength, the resulting binding sites in the polymer will not be able to rebind the template when the solvent is changed. We think that this can explain the unexpected results that were obtained with the majority of the copolymers. However, to confirm this hypothesis HP NMR experiments would be very useful, as it will give an insight on the existence of intermolecular interactions (hydrogen bonds) between template and monomers in supercritical environment. If those interactions were present, we could assure that specific binding sites had been created and were just not with the right conformation in aqueous medium. For that reason, we could also test the imprinted copolymers using supercritical fluid chromatography. By keeping the same solvent of the synthesis, better recognition would be achieved.

The ability of the functional groups of the polymers to establish hydrogen bonds with the template is also a function of the solvent. The ability of amides to establish hydrogen bonds in both polar and apolar solvent is reported [5]. Thus, we chose to add NIPAAm to the reactional imprinting mixture and evaluate the performance of the imprinted copolymer as chiral stationary phase.

Figure 3.8 shows the chromatograms of 0.25 mM amino acid solutions of Boc-L-Trp and Boc-D-Trp injected separately on P(NIPAAm-EGDMA) MIP and NIP columns. The ability of a MIP stationary phase to retain the template molecule compared to the retention at the corresponding non-imprinted column is a commonly accepted indicator for the affinity of the produced MIP [14]. As it can be seen the injected amino acid derivatives do not show any retention on the non-imprinted stationary phase of P(NIPAAm-EGDMA). In opposition the imprinted copolymer show affinity for both molecules, although presenting a much higher retention factor for the Boc-L-Trp, the template molecule present during polymerization, than for its enantiomer. Also the peak is broader meaning that there are more interactions of this molecule with the stationary phase, retarding its elution time.

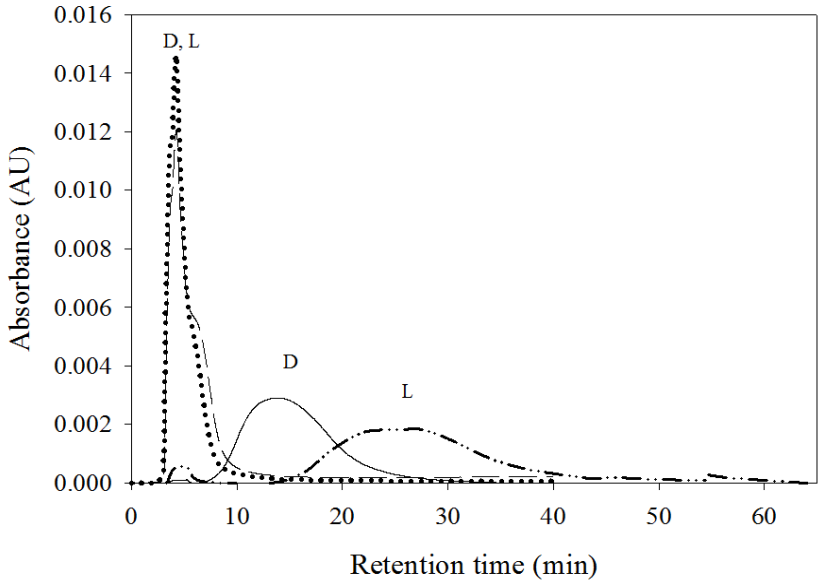

Figure 3.8 - Chromatograms of P(NIPAAm-EGDMA) MIP and NIP injected with solutions of 0.25 mM each tryptophan enantiomer at 25ºC. Boc-L-trp (dotted line) and Boc-D-trp (solid line).

Chromatographic experiments were performed at two different column temperatures 25ºC and 65ºC. Figure 3.9 shows the capacity factors of Boc-L-Trp and Boc-D-Trp for both imprinted polymers, PEGDMA and P(NIPAAm-EGDMA), for the range of sample loads studied, as calculated by Equation 3.1.

As it can be seen higher capacity factors can be obtained at 25ºC than at 65ºC, for both matrices and both enantiomers and for all the range of compositions. We suggest that this could be due to the increasing solvent power of the mobile phase with temperature, destabilizing the hydrogen bonds between the eluted species and the stationary phase material and leading to lower retention times at 65ºC. This temperature dependency of the capacity factor is also typically observed in literature [15].

Also the difference between $k`_L$ and $k`_D$ is more pronounced for P(NIPAAm-EGDMA) than for PEGDMA as it can be seen comparing Figure 3.9c and d, with Figure 3.9a and b, meaning that the copolymer with the amide group is more selective for the template enantiomer. P(NIPAAm-EGDMA) MIP has less affinity to Boc-D-Trp than PEGDMA MIP, while it shows higher retention times for Boc-L-trp. This can be explained by the introduction of NIPAAm as functional monomer. The introduction of an amide functional group increases the available hydrogen bonds with the template, which establishes stronger interaction with the stationary phase in both organic and aqueous solvents. This is in accordance with literature [5,16]. For example, Boc-L-Trp showed a higher retention factor on P(NIPAAm-EGDMA) MIP at 25ºC and sample load of 0.5 mM ($k`$=5.03), while the corresponding MIP without amide functional monomer showed a much lower capacity factor ($k`$=3.06) at the same conditions.

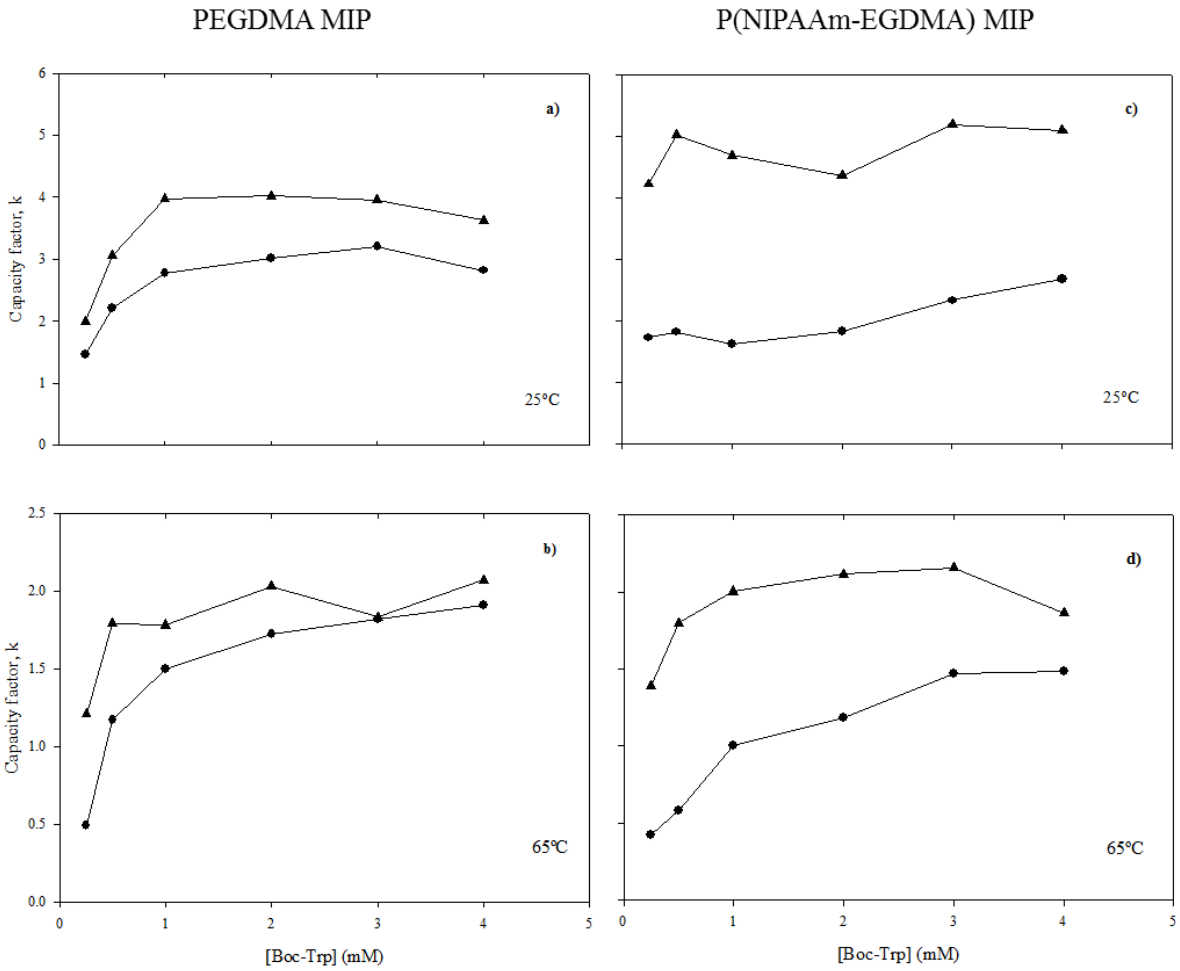

Figure 3.9 - Effect of sample load and temperature on the capacity factors of Boc-L- trp (▲) and Boc-D-trp (●). PEGDMA MIP: (a) 25ºC; (b) 65ºC and P(NIPAAm-EGDMA) MIP: (c) 25ºC; (d) 65ºC.

For imprinted PEGDMA at 25 ºC, $k`_L$ and $k`_D$ increase for loads up to 1mM, remaining constant for higher sample loads. For imprinted P(NIPAAm-EGDMA) at the same temperature, both capacity factors are almost constant, only a slight increasing trend is observed up to 4 mM. At 65 ºC the capacity factors of imprinted polymer and copolymer for both enantiomers have a notorious increase for injection loadings up to 1mM, followed by a less pronounced increase. Around 3 mM the retention factors tend to approach meaning that the stationary phase loses selectivity due to the saturation of the column.

The capacity factor cannot be directly related to enantiomeric separation since besides the specific interactions between the template and MIP, there is also the binding site competition by the enantiomeric species when injecting the racemic solution. The racemic mixture of Boc-Trp was injected on the 150x4.6 mm columns loaded with both imprinted PEGDMA and P(NIPAAm-EGDMA), but no resolution of the peaks was obtained despite the different capacity factors obtained for each enantiomer. This can be explained by the competition for the specific and non-specific sites

within the matrix. By increasing the length of the column we were expecting to increase the enantiomeric resolution. Gilar *et al* [17] described an increase of the column efficiency with the increase of the column length. Figure 3.10 shows the enantioseparation chromatograms for P(NIPAAm-EGDMA) by injecting the racemate at 65 ºC and 25 ºC respectively, using a longer column (250mm×4.6 mm). As it can be seen there was a significant improvement in the resolution of the enantiomers by using a longer column, since both species can be clearly distinguished.

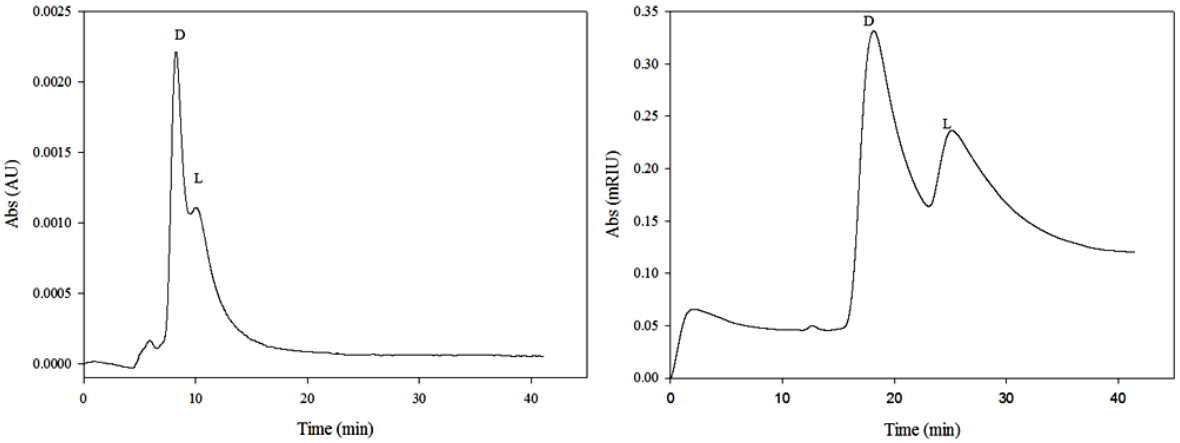

Figure 3.10 - Enantioseparation on P(NIPAAm-EGDMA) of a 1 mM trypthophan racemic mixture at a) 65ºC and b) 25ºC.

Table 3.3 presents the retention, enantioselectivity and resolution for Boc-Trp enantiomers on P(NIPAAm-EGDMA) at different temperatures. As it can be seen promising enantiomeric separation factors and resolutions were obtained for both temperatures. By decreasing the column temperature the stationary phase increased its affinity for the template enantiomer, with an evident increase of the capacity factor.

Table 3.3 - Retention, enantioselectivity and resolution factors of Boc-Trp enantiomers on P(NIPAAm-EGDMA) at different temperatures.

Temperature	$k`_L$	$k`_D$	α	**R**
25 ºC	0.98	0.43	2.27	0.55
65 ºC	0.71	0.40	1.76	0.41

These results would be quite suitable for instance, for moving-bed chromatography, where full separation of pure enantiomers is obtained even when the resolution of the two peaks is not excellent [18].

Typically MIPs show better selectivity/rebinding results when analysed in the same solvent used in their preparation. It has been reported that changing solvents can affect the integrity of the binding sites weakening the molecular recognition of the template [16]. Since the polymers were synthesized in $scCO_2$, future work should involve the test of these materials in supercritical fluid chromatography.

Furthermore it was proven that a small amount of the template molecule is enough for preparing imprinted matrices, as only 1 wt % of Boc-L-Trp was added to the imprinting mixture. This is a very important issue, especially when developing imprinted materials at preparative scale for the recognition of high-value molecules.

3.1.3 Conclusion

In this work it was possible to prepare polymeric materials with chiral recognition capability by molecular imprinting in $scCO_2$. This technology showed to be a promising "greener" alternative to conventional techniques in the preparation of chromatographic columns for enantioseparation. We proved that the synthesised polymers demonstrate high affinity to the template molecule introduced in the polymerization step, being able to recognize and differentiate molecules as similar as enantiomeric species by HPLC. We foresee that a wide range of areas such as sensors, separation, catalysis etc, could benefit from the clean development of these high affinity materials, especially when purity and morphology of the molecular sensing materials is a key issue.

3.2 Development of dual recognition hosts- MIPs and Cyclodextrins

Cyclodextrins are particularly interesting molecules because of their host cavity that can complex with molecules and ions with an appropriate size, geometry and affinity to establish chemical bonds with the cavity. The macrocyclic ring of β-cyclodextrin is composed of seven glucose units, with each glucose having three hydroxyl groups. Two secondary hydroxyls are on the C-2 and C-3 positions and one primary is on the C-6 position. Hydroxyls can be easily substituted by other groups, yielding different molecules. These cyclodextrin derivatives have different physicochemical properties and complexation behaviours than native molecules. Although native cyclodextrins are able to resolve some enantiomeric species, this ability can be enhanced by means of synthesizing derivatized compounds [19,20,21].

Over the last years there has been a growing interest in the use of cyclodextrins to prepare imprinted matrices, especially in the development of chiral stationary phases. The imprinting concept is the same except that, taking advantage of the host cavity of cyclodextrins, no other functional monomer is usually used [22,23]. As crosslinker agents, toluene 2,4-diisocyanate (TDI) and 4,4′- Diphenylmethane diisocyanate (DDI) are the most common, but others such as *N*,*N*-methylenebisacrylamide and EGDMA can be used when the cyclodextrin derivative possesses an acrylated moiety. To the best of my knowledge there are very few works concerning the combination of "typical" imprinting monomers and cyclodextrins [24,25,26].

The goal of this work was to prepare a dual recognition host, joining together the properties of imprinted polymers and cyclodextrins, to prepare a chiral matrix using supercritical fluid technology. Ever since the first report concerning the preparation of inclusion complexes within cyclodextrins in $scCO_2$ in the late 90's [27] that other authors have been exploring this route as an alternative medium for the processing of cyclodextrins [28, 29, 30, 31, 32]. Supercritical carbon dioxide appears as an alternative medium for the preparation of inclusion complexes. As it is a gas under ambient conditions, a simple depressurization of the system yields highly pure complexes with no residues of solvent, therefore avoiding time-consuming steps of product drying. Also, the stability of the complexes is not disadvantageously affected as it was attested in other work that is in preparation. In that study we had carried out, in liquid and supercritical CO_2, the inclusion of omeprazole in several cyclodextrins at different temperatures and pressures and then evaluated the drug release profiles. As it was confirmed by HPLC, no degradation of the drug was observed in materials processed in liquid and supercritical CO_2.

In the aim of an on-going collaboration with Dr. Maria Manuel Marques (Requimte, FCT/UNL), several acryloyl- β-cyclodextrin were synthesized and copolymerized with NIPAAm, MAA and EGDMA, in $scCO_2$, in order to prepare hydrogels for sustained drug delivery of metronidazole. The matrices were impregnated in supercritical CO_2 and the drug release profiles were evaluated at

different pH. Results show that the hydrogels containing the cyclodextrin derivatives had a more sustained delivery of the drug than their corresponding control polymers. This suggests a higher interaction of the drug with the matrix due to the presence of the cyclodextrin.

Herein novel copolymers of 2-monoacryloyl-β-cyclodextrin with NIPAAm and EGDMA, in the presence of Boc-L-Trp, were synthesized in supercritical CO_2 to prepare an imprinted polymeric network able to resolve the racemic mixture of Trp. Figure 3.11 shows the molecular structure of the derivatized cyclodextrin monomer used in this work.

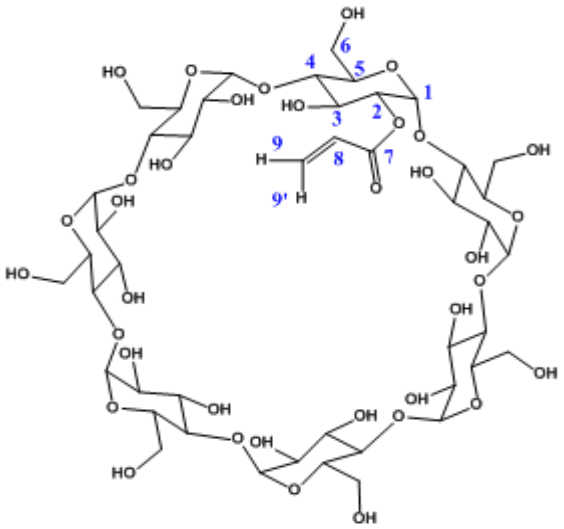

Figure 3.11 - Molecular structure of the β-cyclodextrin derivative used in this work.

The imprinted copolymers were then slurry packed into blank HPLC columns and evaluated as potential chiral stationary phases in a similar procedure to the one developed and described in the last section. Nevertheless, the optimal analytical conditions for the MIP-CD enantio-differentiation of Boc-Trp were different from the neat MIP stationary phase. This suggests that the introduction of the acryloyl-β-CD in the reactional mixture for polymer synthesis yields a final polymeric network significantly different from the single MIP product.

3.2.1 Experimental

3.2.1.1 Materials

β-Cyclodextrin (β-CD, 97% purity), acryloyl chloride (97% purity) and pyridine (99% purity) were purchased from Sigma-Aldrich. Tetrahydrofuran (THF p.a.) was purchased from Riedel-de-Haën. Ethylene glycol dimethacrylate (EGDMA, 98% purity) as cross-linker, N-isopropylacrylamide (NIPAAm, 97% purity) as functional monomer, Boc-L-Tryptophan (Boc-L-Trp, 99% purity) as template molecule, Boc-D-Tryptophan (Boc-D-Trp, 98% purity) and azobis(isobutyronitrile) (AIBN,

98% purity) were purchased from Sigma-Aldrich. HPLC grade acetonitrile from Scharlau was used. Glycine (Gly, 99% purity) was purchased from Sigma and Hydrochloric acid (HCl, 37%) was purchased from Fluka. Carbon dioxide was obtained from Air Liquide with purity better than 99.998%. All chemicals were used without further purification.

3.2.1.2 Synthesis of a monoacryloyl-β-Cyclodextrin

The cyclodextrin derivative monomer was synthesized by adding dropwise an ice chilled solution of acryloyl chloride (0.315 mL, 3.88 mmol) in THF, to a 0 ºC solution of β-CD (2 g, 1.76 mmol) in freshly distilled pyridine. The solution was slowly warmed to room temperature then stirred for 16 h. Evaporation of solvent under reduced pressure afforded a white solid, after recrystallization from ethanol.

3.2.1.3 Characterization of Acryloyl-β-Cyclodextrin monomer

1H NMR and MALDI-TOF

Nuclear Magnetic Resonance spectroscopy (NMR) analyses of the monomer were recorded in Bruker CXP 300, 400 MHz and 100 MHz, for ^{1}H NMR and ^{13}C NMR respectively. In the description of the spectra data are presented in the following order: deuterated solvent, chemical shift (δ, in ppm), multiplicity of the signal (s – singlet, d- duplet, dd- duplet dupleto, m- multiplet), coupling constant (J in Hertz), identification of carbon and number of protons. The assignment of the peaks was as follows: ^{1}H-NMR (δ_{ppm}, D_2O): 6.33 (d, J=16 Hz, H_8, 1H); 6.16-6.09 (m, H_9, 1H); 5.93 (d, J=4 Hz, H_9, 1H); 4.85 (s, H_1, 7H); 3.69-3.61 (m, $H_{3,6}$, 21); 3.58 (d, J= 8 Hz, H_5, 7H); 3.37-3.32 (m, $H_{4,2}$, 14H); ^{13}C-NMR (δ_{ppm}, D_2O): 165.9 (C_7), 132.4 (C_9), 128.7 (C_9), 102.4 (C_1), 82.1 (C_4), 73.6 (C_3), 72.9 (C_2), 72.5 (C_5), 60.4 (C_6).

Matrix-assisted laser desorption/ionization – time of flight mass (MALDI-TOF) analysis was carried out in Mass Spectrometry Unit, University of Santiago of Compostela using DHB + Na as matrix. In the description of the spectra, data is presented by showing the load mass ratio (m/z) assignment of a molecular fragment. EM [M+23] m/z 1134.43 ($C_{42}H_{70}O_{35}$), 1242.39 ($C_{45}H_{72}O_{36}$), 1296.40 ($C_{48}H_{74}O_{37}$).

3.2.1.4 Polymerizations in $scCO_2$

The influence of the addition of the monoacryloyl-β-CD to the imprinting system was studied by means of synthesizing four different copolymers. The neat MIP, composed of NIPAAm and EGDMA, the MIP CD, composed of NIPAAm, EGDMA and monoacryloyl-β-CD and the corresponding non-imprinted copolymers, NIP and NIP CD. The copolymers were synthesized using the experimental procedure already described in section 2.1. Briefly, in a typical procedure to prepare the MIP CD,

EGDMA (3.08 g), NIPAAm (0.37 g, corresponding to 12 wt% of the amount of crosslinker), monoacryloyl-β-CD (3.9 wt% with respect to the amount of EGDMA plus NIPAAm), initiator (2 wt % with respect to the amount of EGDMA and NIPAAm) and template (1 wt%, also with respect to the amount of EGDMA and NIPAAm introduced) were loaded into the high-pressure cell. P(NIPAAm-EGDMA) MIP with no cyclodextrin added is a replica of the copolymer that was described in the last section. For the production of NIPs the same procedure was followed except no template was added.

3.2.1.5 Materials characterization

SEM

Acryloyl-β-Cyclodextrin monomer and all the synthesized copolymer, with or without cyclodextrin, were morphologically characterized using scanning electron microscopy (SEM) in a Hitachi S-2400 instrument, with an accelerating voltage set to 15 kV. Samples were mounted on aluminium stubs using carbon tape and were gold coated.

HPLC analysis

The copolymer of P(ACrylCD-NIPAAm-EGDMA) was slurry packed into a 25 cm length blank HPLC column and tested in a Knauer equipment, with UV detection Smartline 2500 and pump Smartline 1000. The samples were injected for analysis using a loop volume of 5 µL. Acetone was used as void marker, to determine the column dead time.

Method development was carried out with the univariate approach, in which the variables that may affect the separation were studied one by one, while the others remain constant. Analytical method optimization involved the study of different acetonitrile percentages in the mobile phase as well as different flows, pH and temperature. The analytical conditions tested in this work and the corresponding chromatographic results are shown in Table 3.4 of Results and Discussion.

3.2.2 Results and Discussion

Characterization of Cyclodextrin-based monomer and copolymers

All the synthesized copolymers were obtained as dry, free-flowing powders in high yields (~90%, determined gravimetrically) and ready-to-pack into the blank HPLC column.

The morphology of the monomer and copolymers was investigated by SEM. Figure 3.12 shows the SEM images of mono-acryloyl-β-cyclodextrin, imprinted copolymer without CD and both imprinted and non-imprinted copolymers with CD. As it can be seen, the synthesized cyclodextrin derivative appears as irregularly shaped crystals. All the copolymers show similar morphology, with aggregates

of smooth surfaced discrete particles sizing less than 1 µm. The addition of the CD derivatized monomer and the template molecule to the imprinting system does not seem to affect the morphology of the copolymer, in such a way that it can be detected by SEM images. This is in agreement with the imprinting systems studied in $scCO_2$ [6] and with the acryloyl-cyclodextrin-based hydrogels developed for drug delivery purposes in an on-going work (from project PTDC/QUI/66086/2006). Further physical characterization studies concerning the surface area and pore volume could provide additional information about the influence of adding different molecules, in the synthesis, on the final product.

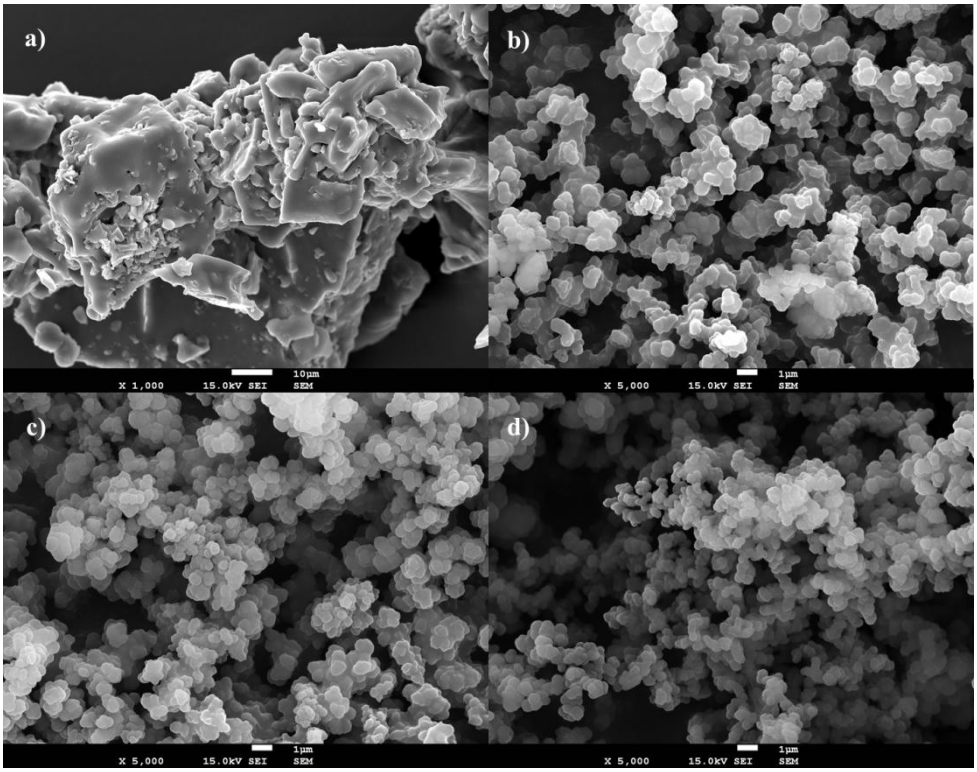

Figure 3.12 - SEM images of the synthesized materials. a) Mono-acryloyl-β-CD monomer, b) MIP, c) NIP CD and d) MIP CD.

Evaluation of the retention factor and enantioselectivity

Typical packings for HPLC columns are silica-based materials with particle size around 3-5 µm. Smaller particles usually improve chromatographic performance, by reducing the plate height values, as they generally provide higher surface areas. With a reduced mass transfer resistance those particles yield good separations even when higher linear velocities are used. The main drawback associated with the benefit of smaller particle sizes is the increased pressure drop. As the pressure drop is proportional to the particle diameter, using the same flow rate, the pressure drop can be up to 27 times higher when particles of 1.7 µm are used instead of 5 µm silica particles [33]. The particles used herein are polymeric and thus less stiff than silica, leading to lower pressure drops. Extremely high

pressure drops were never a problem, as in HPLC experiments, the higher pressure drop obtained was 86 bar for the P(NIPAAm-EGDMA) imprinted stationary phase using a flow rate of 1 mL/min with a mobile phase of 92:8 (v/v) of water and acetonitrile.

This work was an extension of the previously studied P(NIPAAm-EGDMA) system, therefore the first analytical conditions used to test the enantiomeric differentiation in the MIP CD stationary phase were the previously optimized for the MIP system. However, these conditions proved not to be the optimal when the acryloyl-cyclodextrin monomer was part of the polymeric matrix, as the amino acid enantiomers were not retained in column when using those conditions. This lead to several attempts for optimizing the HPLC conditions. Table 3.4 shows some experimental variables studied and the corresponding capacity factors for both enantiomers, injected separately in the MIP CD column.

Table 3.4 – Analytical conditions tested during method optimization.

	Mobile phase composition		**Buffer pH**	**Flow rate (mL/min)**	**Temperature (ºC)**	**Retention factors**	
	Buffer (%)	**MeCN (%)**				**k'_L**	**k'_D**
Entry 1	75	25	3.0	1	25	1.02	0.88
Entry 2	80	20	3.0	1	25	2.14	1.71
Entry 3	85	15	3.0	1	25	2.80	1.82
Entry 4	80	20	3.0	0.5	25	5.91	1.90
Entry 5	85	15	3.0	0.5	25	14.80	4.71
Entry 6	85	15	3.0	0.5	60	2.02	2.02
Entry 7	90	10	7.4	0.5	25	0.20	0.20

Despite the several attempts to resolve the racemic mixture, no enantioseparation was achieved when the enantiomers were injected together. This could be related with the position of the acryloyl group in the cyclodextrin, in the C_2. The non-specific functionalization of the cyclodextrin led to the insertion of the group inside the cavity. By the time these cyclodextrin-copolymers were synthesized, no information about the position of the acryloyl-group in the CD was available. Nevertheless, some trends in the retention factors of the stereoisomers were found while carrying the optimization of the analytical method.

Table 3.4 shows the influence of several experimental parameters on the recognition of the amino acids. As it can be seen, the mobile phase composition has an enormous impact on the retention of the analytes in the column. This can be observed by comparing entries 1-3, that were performed with

different ratios between the HCl-Gly pH 3.0 buffer solution and the organic solvent acetonitrile. As the amount of acetonitrile present in the eluent decreases, the retention times of the analytes increase and higher capacity factors are obtained. This can be attributed to a higher number of hydrophobic interactions between the analytes and the stationary phase as the amount of aqueous solvent increases.

By comparing entries 4 and 5 it is possible to observe that the same effect was attained when the flow rate decreased from 1 mL/min (entries 1-3) to 0.5 mL/min (entries 4-5). The flow rate determines the time that the analyte has to interact with the stationary phase. A very high flow rate can adversely affect the quality of the chromatogram by not giving sufficient time for the analyte to establish interactions with the column packing. On the other hand a lower flow rate can, depending on the other analytical conditions, provide too extensive retention times and very broad chromatograms. When the flow rate was changed from 1 mL/min to 0.5 mL/min, at 85:15 (v/v) mobile phase compositions, the capacity factors for the stereoisomer Boc-L-Trp increased dramatically from 2.8 to 14.8 (entry 5), this latter corresponding to a retention time of 104 min. Given the long time for the analyte to leave the column, these conditions were not viable. However, when the percentage of acetonitrile was increased from 15 to 20 (v/v)% (entry 4) acceptable capacity factors were achieved.

When the temperature was changed from 25 ºC (entry 5) to 60 ºC (entry 6) a significant decrease was observed in the capacity factors, with the stationary phase showing no molecular recognition for the template molecule. This reduction in the retention factors was already stated in the neat MIP (without cyclodextrin) [6] and is reported in the literature [15].

The influence of the mobile phase pH on the capacity factors of Boc-Trp was further investigated by using PBS 7.4 (entry 7). By changing the pH of the solution, a sharp decrease in the capacity factors was observed when compared with the analysis using pH 3.0 (entry 5) and a lower percentage of buffer solution. Following the trend of the influence of the mobile phase composition at low pH, one could expect that by increasing the percentage of buffer solution, higher retention times would be achieved. However, the pH seems to have higher effect and the stereoisomers were almost eluted with the injection peaks, at pH 7.4, yielding the lowest capacity factors obtained in the study. This pH influence on the retention properties of Boc-Trp was already stated by other authors [15, 34].

Figure 3.13 shows the chromatograms obtained for the separated injections of Boc-D-Trp and Boc-L-Trp using the analytical conditions described in entry 4 of Table 3.4. As it can be seen, although the retention times of both enantiomers are very different when injected separately, the racemic mixture could not be resolved. The loss of selectivity of this MIP CD towards the template molecule, when compared with the neat MIP, can be explained by the position of the acryloyl group in the cyclodextrin monomer introduced in the system. Since the reactive double bond is inside the cavity and the cyclodextrin reacts with the acrylated monomers by means of that double bond, the cavity is less available to form inclusion complexes with the template molecule. For that reason, the introduction of

cyclodextrin does not improve the enantiomeric separation. Instead, the acryloyl-cyclodextrin copolymer showed a poorer HPLC performance than the pure MIP. This can be explained by some kind of competition between the acryloyl-cyclodextrin and the template for the NIPAAm molecules, in the polymerization. If the amide monomer has higher affinity to the cyclodextrin cavity than to the template Boc-L-Trp, it will mainly interact with the cyclodextrin and will not be available to establish hydrogen bonds with the template. As a lower number of template-monomer complexes are present during the polymerization, the resultant imprinted polymer has a lower number of affinity binding sites, which adversely affects the molecular recognition ability.

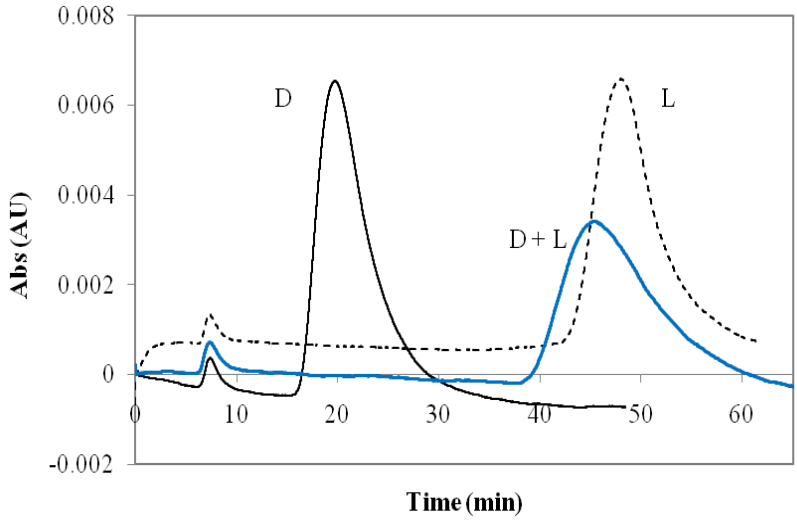

Figure 3.13 - Chromatograms obtained for the separated injections of 1 mM Boc-D-Trp, Boc-L-Trp and racemic mixture in the MIP CD stationary phase, using a mobile phase compositions described in entry 4 of Table 3.4.

Also, the nature of the complexes will be different when the cyclodextrin monomer is added to the reaction mixture. If cyclodextrin-NIPAAm/cyclodextrin-EGDMA inclusion complexes are established in supercritical environment, less monomer will complex with the template and therefore the ratio (available) monomer:template will not be the same as when cyclodextrin is not present. Different ratios between template and monomer can yield different complex states, as one template molecule can attach to more than one monomer molecule. Higher orders of template-monomer complexes lead to binding sites with higher selectivity. In this case the acryloyl-β-cyclodextrin-NIPAAm-EGDMA-Boc-Trp complexes should be of lower order of stability and therefore would lead to the formation of site populations of lower selectivity [35].

In order to have an insight on the interactions that are occurring in the pre-polymerization mixture, HP NMR experiments could be carried out. The analysis could give important information concerning the ability of the template to interact with the monomeric species present in the system and, in addition,

the capability of the derivatized cyclodextrin to include the monomers in $scCO_2$. Moreover, given the "solvent-memory" effect, the selectivity of the imprinted copolymer should be tested in supercritical fluid chromatography.

3.2.3 Conclusion

This work reports the first approach to the synthesis of a dual molecular recognition polymeric host with enantiomeric affinity, synthesized and processed using supercritical fluid technology. The incorporation of 2-mono-acryloyl-β-cyclodextrin in the already developed imprinting system proved to be disadvantageous to the selective recognition of Boc-L-Trp. This could be explained by the position of the acryloyl group, inside the cyclodextrin cavity. Other cyclodextrin derivatives should be tested, particularly one with the cavity available. With a different copolymeric stationary phase and using the information taken from this work concerning the best analytical conditions to separate the enantiomers (pH, mobile phase composition and temperature), significant improvements in the racemic resolution could be achieved.

3.3 References

[1] Duarte, A.R.C., Casimiro, T., Aguiar-Ricardo, A., Simplício, A.L., Duarte, C.M.M., Supercritical fluid polymerisation and impregnation of molecularly imprinted polymers for drug delivery, J. Supercrit. Fluids 2006, 39, 102-106.

[2] Casimiro, T., Banet-Osuna, A.M., Nunes da Ponte, M., Aguiar-Ricardo, A., Synthesis of highly cross-linked poly(diethylene glycol dimethacrylate) microparticles in supercritical carbon dioxide, Eur. Polym. J. 2005, 41, 1947-1953.

[3] Herderich, M., Gutsche, B., Tryptophan-derived bioactive compound in food, Food Rev. Int. 1997, 13, 103-135.

[4] Bell, C., Abrams, J., Nutt, D., Tryptophan depletion and its implications for psychiatry, Brit. J. Psychiat. 2001, 178, 399-405.

[5] Yu, C., Mosbach, K., Molecular imprinting utilizing an amide functional group for hydrogen bonding leading to highly efficient polymers, J. Org. Chem. 1997, 62, 4057-4064.

[6] Soares da Silva, M., Vão, E.R., Temtem, M., Mafra, L., Caldeira, J., Aguiar-Ricardo, A., Casimiro, T., Clean synthesis of molecular recognition polymeric materials with chiral sensing capability using supercritical fluid technology. Application as HPLC stationary phases, Biosens. Bioelectron. 2010, 25, 1742-1747.

[7] Baggiani, C., Anfossi, L., Baravalle, P., Anfossi, L., Tozzi, C., Comparison of pyrimethanil-imprinted beads and bulk polymer as stationary phase by non-linear chromatography, Anal. Chim. Acta 2005, 542, 125–134

[8] Temtem, M., Casimiro, T., Mano, J.F., Aguiar-Ricardo, A., Green synthesis of a temperature sensitive hydrogel, Green Chem. 2007, 9, 75-79.

[9] Cooper, A.I., Hems, W.P., Holmes, A.B., Synthesis of highly cross-linked polymers in supercritical carbon dioxide by heterogeneous polymerization. Macromolecules 1999, 32, 2156-2166.

[10] Skogsberg, U., Meyer, C., Rehbein, J., Fischer, G., Schauff, S., Welsch, N., Albert, K., Hall, A. J., Sellergren, B., A solid-state and suspended-state magic angle spinning nuclear magnetic resonance spectroscopic investigation of a 9-ethyladenine molecularly imprinted polymer. Polymer 2007, 48, 229-238.

[11] Sellergren, B., Shea, K.J., Origin of peak asymmetry and the effect of temperature on solute retention in enantiomer separations on imprinted chiral stationary phases, J. Chromatogr. A 1995, 690, 29.

[12] Chen, L., Xu, S., Li, J., Recent avances in molecular imprinting technology: current status, challenges and highlighted applications, Chem. Soc. Rev. 2011, 40, 2922-2942.

[13] Wang, J., Guo, R., Chen, J., Zhang, Q., Liang, X., Phenylurea herbicides-selective polymer prepared by molecular imprinting using N-(4-isopropylphenyl)-N‘-butyleneurea as dummy template, Anal. Chim. Acta 2005, 540, 307-315.

[14] O`Mahony, J., Molinelli, A., Nolan, K., Smyth, M.R., Mizaikoff, B., Anatomy of a successful imprint: analysing the recognition mechanisms of a molecularly imprinted polymer for quercetin. Biosens. Bioelectron. 2006, 21, 1383-1392.

[15] Haginaka, J., Kagawa, C., Chiral resolution of derivatized amino acids using uniformly sized molecularly imprinted polymers in hydro-organic mobiles phases. Anal. Bioanal. Chem. 2004, 378, 1907-1912.

[16] Yu, C. Mosbach, K., Insights into the origins of binding and the recognition properties of molecularly imprinted polymers prepared using an amide as the hydrogen-bonding functional group. J. Mol. Recognit. 1998, 11, 69-74.

[17] Gilar, M., Daly, A. E., Kele, M., Neue, U.D., Gebler, J.C., Implications of column peak capacity on the separation of complex peptide mixtures in single- and two-dimensional high-performance liquid chromatography. J. Chromatogr. A 2004, 1061, 183-192.

[18] Juza, M., Mazzotti, M., Morbidelli, M., Simulated moving-bed chromatography and its application to chirotechnology. Trends Biotechnol. 2000, 18, 108-118.

[19] Zhong, Q., He, L., Beesley, T.E., Trahanovsky, W.S., Sun, P., Wang, C., Armstrong, D.W., Development of dinitrophenylated cyclodextrin derivatives for enhanced enentiomeric separations by high-performance liquid chromatography, J. Chromatogr. A 2006, 1115, 19-45.

[20] Ai, F., Li, L., Siu-Choon Ng, S.-C., Tan, T.T.Y., Sub-1-micron mesoporous silica particles functionalized with cyclodextrin derivative for rapid enantioseparations on ultra-high pressure liquid chromatography, J. Chromatogr. A 2010, 1217, 7502–7506.

[21] Li, Y. Song, C., Zhang, L., Zhang, W., Fu, H.,Fabrication and evaluation of chiral monolithic column modified by β-cyclodextrin derivatives, Talanta 2010, 80, 1378–1384.

[22] Xu, Z., Li Xu, L., Kuang, D., Zhang, F.,Wang, J., Exploiting β-cyclodextrin as functional monomer in molecular imprinting for achieving recognition in aqueous media, Mater. Sci. Eng. C 2008, 28, 1516–1521.

[23] Asanuma, H., Hishiya, T., Komiyama, M., Tailor-Made Receptors by Molecular Imprinting, Adv. Mater. 2000, 12, 1019-1030.

[24] Sergey A. Piletsky, Häkan S. Andersson and Ian A. Nicholls, The rational use of hydrophobic effect-based recognition in molecularly imprinted polymers, . J. Mol. Recognit. 1998, 11, 94–97.

[25] Xu, Z., Kuang, D., Liu, L., Deng, Q., Selective adsorption of norfloxacin in aqueous media by an imprinted polymer based on hydrophobic and electrostatic interactions, J. Pharmaceut. and Biomed. 2007, 45, 54–61.

[26] Qin, L., He, X.-W., Wen-You Li, W.-Y., Zhang, Y.-K., Molecularly imprinted polymer prepared with bonded β-cyclodextrin and acrylamide on functionalized silica gel for selective recognition of tryptophan in aqueous media, J. Chromatogr. A 2008, 1187, 94–102.

[27] Van Hees, T., Piel, G., Evrard, B., Otte, X., Thunus, L., Delattre, L:, Application of supercritical carbon dioxide for the preparation of a piroxicam-β-cyclodextrin inclusion compound, Pharmaceut. Res. 1999, 16, 1864-1870.

[28] Scondo, A., Dumarcay-Charbonnier, F., Marsura, A., Barth, D., Supercritical CO2 phosphine imide reaction on peracetylated β-cyclodextrins, J. Supercrit. Fluids 2009, 48, 41-47.

[29] Al-Marzouqi, A.H., Elwy, H.M., Shehadi, I., Adem, A., Physicochemical properties of antifungal drug-cyclodextrin complexes prepared by supercritical carbon dioxide and by conventional techniques, Journal of Pharmaceutical and Biomedical Analysis 2009, 49, 227-233.

[30] Sauceau, M., Rodier, E., Fages, J., Preparation of inclusion complex of piroxicam with cyclodextrin by using supercritical carbon dioxide, J. Supercrit. Fluids 2008, 47, 326-332.

[31] Nunes, A.V.M., Almeida, A.P.C., Marques, S.R., Sampaio de Sousa, A.R., Casimiro, T., Duarte, C.M.M., Processing triacetyl-β-cyclodextrin in the liquid phase using supercritical CO_2, J. Supercrit. Fluids 2010, 54, 357-361.

[32] Ivanova, G.I., Vão, E.R., Temtem, M., Aguiar-Ricardo, A., Casimiro, T., Cabrita, E.J., High-pressure NMR characterization of triacetyl-β-cyclodextrin in supercritical carbon dioxide, Magn. Reson. Chem. 2009, 47, 133-141.

[33] Nguyen, D. T.-T., Guillarme, D., Rudaz, S., Veuthey, J.-L., Fast analysis in liquid chromatography using small particle size and high pressure, J. Sep. Sci. 2006, 29, 1836-1848.

[34] Perrin, C., Vargas, M.G., Heyden, V., Maftouh, M., Massart, D.L., Fast development of separation methods for the chiral analysis of amino acid derivatives using capillary electrophoresis and experimental designs, J. Chromatogr. A 2000, 883, 249-265.

[35] Andersson, H.S., Karlsson, J.G., Piletsky, S.A., Koch-Schidt, A.-C., Mosbach, K., Nicholls, I.A., Study of the nature of recognition in molecularly imprinted polymers, II [1] Influence of monomer-template ratio and sample load on retention and selectivity, J. Chromatogr. A 1999, 848, 39-49.

CHAPTER 4

Imprinted structures for extraction of environmental pollutants. Case study: Bisphenol A

4. Imprinted structures for extraction of environmental pollutants. Case study: Bisphenol A

Over the last years, there has been a growing interest in the design and development of advanced polymeric materials to selectively remove common pollutants from environmental waters. This part of the thesis aims to show a new methodology for the production of imprinted materials with specific application in the adsorption of BPA, an estrogenic compound.

Section 4.1 of this thesis describes the immobilization of imprinted particles into membranes, prepared using a supercritical CO_2-assisted phase inversion method. The immobilization of molecularly imprinted particles in porous structures, such as membranes, offers the possibility of designing affinity materials with extended applications over the polymeric beads powders. Furthermore, by immobilizing MIPs into membranes, processes such as filtration and sensing can have their efficiency enhanced by molecular imprinting technique.

Section 4.2 reports the synthesis of a molecularly imprinted polymer in $scCO_2$ using, for the first time, the semi-covalent approach. The selectivity of the polymer was studied in aqueous solutions and the adsorption capacity for BPA was compared with the adsorption of progesterone and ethinylestradiol.

4.1 $ScCO_2$-assisted preparation of hybrid imprinted membranes

Ever since the first work concerning the preparation of membranes by $scCO_2$-assisted phase inversion method was reported [1] others have recognized its potential [2,3,4]. The preparation of membranes using this methodology encounters numerous advantages due to the tuneable properties of supercritical carbon dioxide.

In the vicinity of the critical point, a small variation in pressure leads to a sharp increase in density and therefore in the solvent strength [5]. Given the non-solvent role of CO_2 in the phase inversion process, a variation in its density alters the phase diagram of the ternary system polymer/solvent/non-solvent and enables to control the membrane characteristics through the non-solvent effect. [6,7,8] The production of membranes using a $scCO_2$-assisted method introduces new experimental parameters (temperature, pressure, depressurization rate) over the traditional process variables (polymer concentration, solvent), allowing a higher control of the morphology and porosity. This can be a powerful tool in the design of porous structures for effective processes in filtration [9] and sensing [10].

New trends in membrane technology encounter the development of affinity membranes with inherent high-throughputs. The design of affinity membranes with molecular recognition character is inspired in natural mechanisms. Molecularly imprinted membranes emerge as potential affinity materials due to their low cost, ease of preparation and good molecular recognition performance. The concept of creating affinity sites in a molecularly imprinted membrane lays in the molecular imprinting mechanism.

In literature we could found several works concerning the development of molecularly imprinted membranes [11,12,13,14]. However, much has to be done to rationally design valuable molecularly imprinted membranes. To the best of our knowledge, the incorporation of pre-synthesized MIPs in a casting solution for membrane preparation has been reported only few times up to date [15]. In analogy to the already marketed SPE membranes, this approach could open further possibilities for the design of molecular recognition structures [16]. The development of hybrid membranes using supercritical fluid technology could yield affinity membranes with controlled porosity and permeability combined to the green aspects of this clean technology, both in terms of purity and process sustainability.

This work describes the successful immobilization of highly crosslinked polymeric particles with affinity to BPA (Figure 4.1) into a PMMA-based porous structure, by blending the synthesized imprinted polymer within a PMMA casting solution, followed by $scCO_2$-assisted phase inversion. Membranes were characterized in terms of morphology, mechanical performance and transport properties. The ability of the polymers and hybrid membranes to adsorb bisphenol A was tested in aqueous solutions.

It is known that small daily doses of exposure to BPA increase the risk of breast and prostate cancer [17] and diabetes [18]. It has also been reported the elution of BPA from polycarbonate plastics and epoxy resins used in haemodialysis systems, which poses in risk the health of patients undergoing dialysis [19]. The proposed devices could have a real application in this area by combining a completely pure and solvent-free material with enhanced affinity to adsorb this molecule.

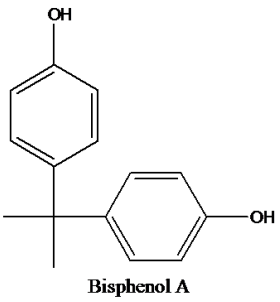

Figure 4.1 - Molecular structure of BPA.

This work was published in Chemical Engineering Science [20].[1]

4.1.1 Experimental

4.1.1.1 Materials

Bisphenol A (BPA, 99 % purity) as template, methacrylic acid (MAA, 99 % purity) as functional monomer and ethylene glycol dimethacrylate (EGDMA, 98 % purity) as cross-linker were purchased from Sigma-Aldrich, Azobis(isobutyronitrile) (AIBN, 98 % purity) from Fluka was used as initiator. Poly(methyl methacrylate) (PMMA) (molecular weight 996,000) was obtained from Sigma-Aldrich. Dimethylformamide (DMF, 99.8 % purity) was purchased from Riedel-de Haën and ethanol (PA), from Panreac. Methanol isocratic HPLC grade (99.7 % purity) from Scharlau was used. Carbon dioxide was obtained from Air Liquide with purity better than 99.998 %. All chemicals were used without further purification.

4.1.1.2 MIP and NIP synthesis in $scCO_2$

Polymerization reactions in $scCO_2$ were carried out using the protocol described in section 2.1. In a typical imprinting system, the synthesis of the non-covalent MIP was carried out by mixing 0.49 mmoles of the template molecule BPA, 2.54 mmoles of the functional monomer MAA, 12.88 mmoles of the cross-linker agent EGDMA (molar ratios 1:5:25) and 1 wt % of the radical initiator AIBN in a high-pressure cell. For the synthesis of the control polymer, NIP, the same procedure was followed except no template was added. Carbon dioxide was added up to 21 MPa and polymerization reactions proceeded for 24 hours under stirring. At the end of the reaction, the polymer was slowly washed with fresh high-pressure CO_2 for 1 hour.

4.1.1.3 $scCO_2$-assisted template desorption

Template desorption from the imprinted matrices at the end of the polymerization is a crucial step in molecular imprinting process because the formerly created binding sites have to be emptied to become available for future rebinding. $ScCO_2$-assisted BPA desorption was performed by loading a 33 mL stainless steel high-pressure cell with 1.5 g of the pre-synthesized polymer, 10 mL of methanol and CO_2 until 21 MPa was reached. The cell was immersed in a thermostated water bath at 40 ºC and 24 hours. The polymer was then slowly washed for 3 hours with fresh high-pressure CO_2 in order to remove all the template and co-solvent. The residual amount of BPA entrapped in the highly cross-linked matrix was assessed by crushing 20 mg of polymer, stirring it with 3 mL of methanol for 3

[1] Reproduced with the authorization of the editor and subjected to the copyrights imposed.

days and quantifying the template amount that was released by UV spectroscopy. BPA calibration curves were performed in a Perkin-Elmer λ 25 spectrophotometer at 275 nm.

4.1.1.4 scCO$_2$-assisted production of hybrid molecularly imprinted membrane

The production of molecularly imprinted supported membranes by scCO$_2$-assisted phase-inversion was carried out in a high-pressure apparatus already described elsewhere [21,22] in a high-pressure cell specially developed for membrane production. Figure 4.2 illustrates the experimental apparatus used. Briefly, to produce the membranes, the casting solution with 30 wt % of polymer blend consisting in 70:30 of PMMA and MIP or NIP, in 5 mL of DMF was loaded into a teflon cap and placed inside the high-pressure cell. The cell has a porous structure that supports a bed of Raschig rings, in order to disperse CO_2 in the top of the casting solution. Membrane production was performed at 45 ºC by immersing the cell in a thermostated water bath, heated by means of a controller (Hart Scientific, Model 2200) that maintained the temperature within ± 0.01 ºC. CO_2 was added, using a Gilson 305 piston pump, until an operational pressure of 20 MPa was reached. Pressure was set at 20 MPa by means of a back pressure regulator (Jasco BP-2080 plus) which separates the CO_2 from the DMF present in the casting solution. All the experiments were performed with a CO_2 flow of 9.8 g.min^{-1} for 3 hours. The pressure inside the system is monitored with a pressure transducer (Setra Systems Inc, Model 204) with a precision of ± 0.100 kPa. At the end, the system was slowly depressurized during 20 min and a thin homogeneous membrane was obtained. The pure PMMA membrane was prepared using the same procedure except that no pre-synthesized polymer was added to the casting solution. Figure 4.3 shows the high-pressure cell used for membrane preparation and a typical membrane.

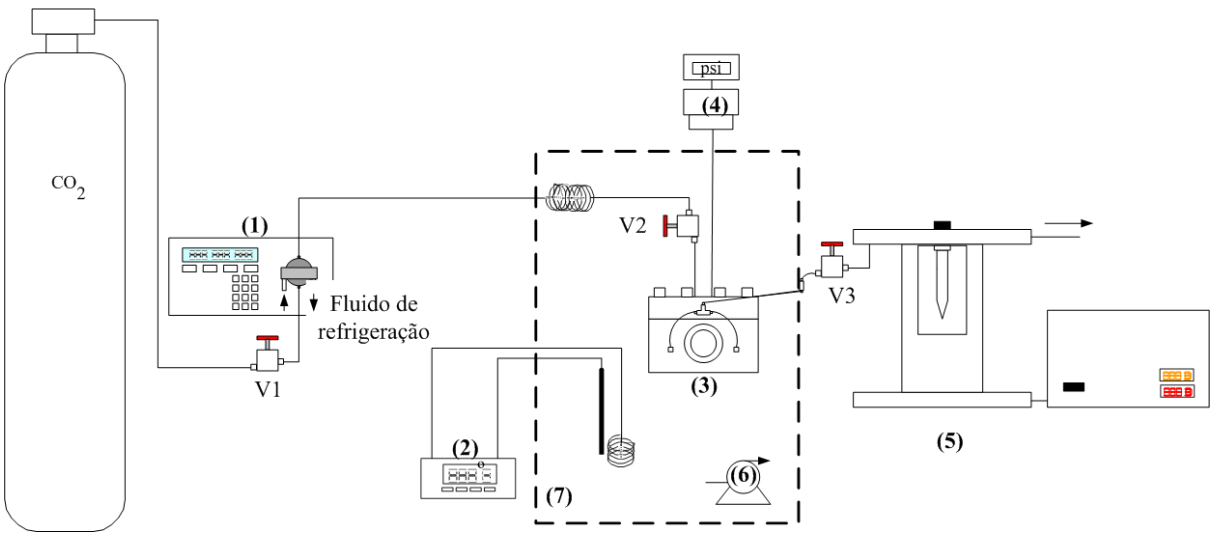

Figure 4.2 - Layout of the high-pressure apparatus for the membrane formation [23]. 1 - Gilson 305 piston pump, 2 - temperature controller, 3 - high-pressure cell, 4 - pressure transducer, 5 - back pressure regulator, 6 – water recirculation pump, 7 – water bath. V1 to V3 – high-pressure valves.

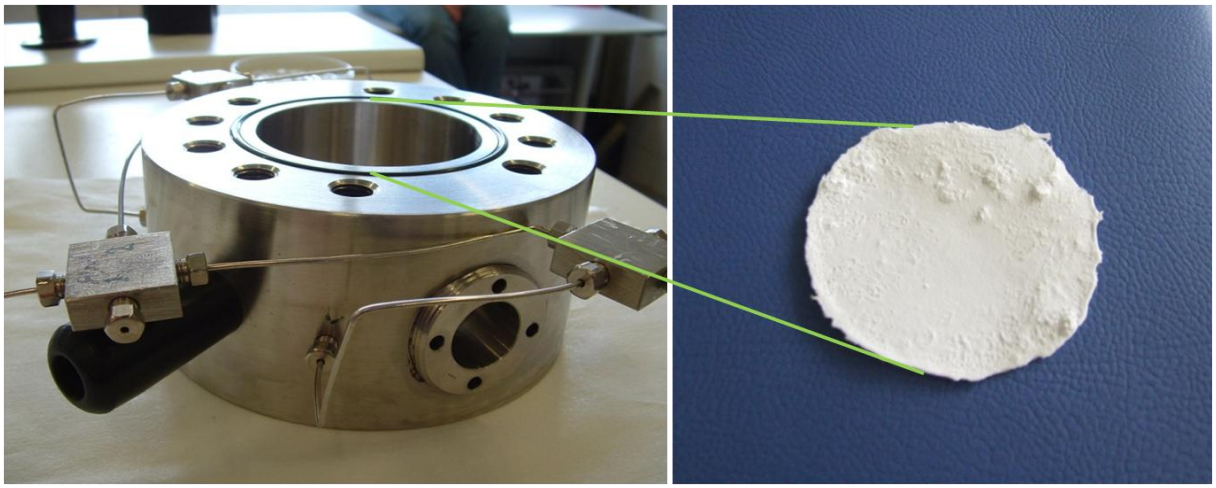

Figure 4.3 - High pressure-cell used for $scCO_2$-assisted membrane preparation and typical membrane obtained.

4.1.1.5 Morphological, chemical and physical characterization of imprinted materials

Imprinted materials were characterized in terms of morphology using scanning electron microscopy (SEM) in a Hitachi S-2400 instrument, with an accelerating voltage set to 15 kV. For cross-section analysis the membrane samples were frozen and fractured in liquid nitrogen. Samples were mounted on aluminium stubs using carbon tape and were gold coated. Specific surface area and pore diameter of polymer powders were determined by N_2 adsorption according to the BET method. An accelerated surface area and porosimetry system (ASAP 2010 Micromeritics) was used under nitrogen flow. Fourier transform infrared spectroscopy (FTIR) analysis measurements were performed using a Bruker Tensor 27 (16 scans and 1 cm^{-1} resolution). Pellets containing finely grounded powder of a small amount of each copolymer mixed with dried KBr (1:5 mass ratio) were made before recording.

The hydrophobicity of the membranes was evaluated through the measurement of the contact angles with Millipore water droplets in a KSV Goniometer model CAM 100 at room temperature. The permeability of the membranes to pure water was determined by calculating the water flux through the membranes using a 10 mL filtration unit (Amicon Corp., model 8010) with an effective area of 4.1 cm^2. All the experiments were carried out varying the applied hydrostatic pressure from 0 to 0.50 MPa.

The tensile properties of the membranes were tested by dynamic mechanical analysis (DMA) with a tensile testing machine (MINIMAT firm-ware v.3.1) at room temperature. The samples were cut into 5 mm × 15 mm strips. The length between the clamps was set at 5 mm and the speed of testing was set to 0.1 $mm.min^{-1}$. A full scale load of 20 N and maximum extension of 35 mm were used. Measurements were performed with dried membranes. The Young´s modulus was calculated from the slope of the linear portion of the stress-strain curve. All samples were tested in dry state at room temperature. Load extension graphs were obtained during testing and converted to stress-strain curves

through Equations 4.1 and 4.2, with σ being the stress ($N.mm^{-2}$), F the applied force (N), A the cross sectional area (mm^2), ε the strain, ΔL the change in length (mm) and L the length between clamps (mm).

$$\sigma = \frac{F}{A} \quad \text{(Equation 4.1)}$$

$$\varepsilon = \frac{\Delta L}{L} \quad \text{(Equation 4.2)}$$

4.1.1.6 Template static adsorption experiments

Batch binding experiments were carried out to evaluate the static adsorption capacity of the synthesized polymers and membranes by adding 20 mg of polymeric material MIP, its corresponding blank polymer, NIP, PMMA membrane and its corresponding blends of PMMA-MIP and PMMA-NIP in 50 mL volume of aqueous solution of BPA, stirred at 50 rpm, with concentrations ranging from 50 to 300 μM. Equilibrium was achieved after 24 hours, as confirmed by the quantification of free BPA in solutions. The amount of substrate adsorbed by the matrices was assessed through Equation 4.3 where [S] corresponds to the amount of BPA bound, C_0 represents the initial molar concentrations of BPA, C_t corresponds to the concentrations at predetermined time intervals, V represents the volume of the solution and W corresponds to the weight of the polymeric sample.

$$[S] = \frac{(C_0 - C_t).V}{W} \quad \text{(Equation 4.3)}$$

4.1.1.7 Template filtration experiments

To assess the performance of the imprinted membrane to adsorb the template molecule in dynamic conditions, the membrane was put in the permeability apparatus and hydrostatic pressure was adjusted to assure a constant filtration flow rate of 0.33 $mL.min^{-1}$. Previous to the adsorption experiments, the membrane was equilibrated with 30 mL (3 x 10 mL) of distilled water. The filtration unit was then loaded with 30 mL of an aqueous solution containing 300 μM of BPA and the amount of template adsorbed in the imprinted membrane was quantified. The membrane was easily restored by washing it with 10 mL of methanol at the same flow rate and no loss of binding capacity was observed. As control, the non-imprinted hybrid membrane was also studied with respect to its ability to bind the

template in non-equilibrium conditions. All samples collected were quantified by UV spectroscopy. The amount of BPA bound to the membranes was determined using Equation 4.3.

4.1.2 Results and discussion

4.1.2.1 Morphological, chemical and physical characterization

Imprinted and non-imprinted polymers were obtained as dry, free-flowing powders in high yields (~99 %, determined gravimetrically). These yields are in accordance with other reported precipitation polymerizations in $scCO_2$ [24]. The synthesis and processing of MIPs in $scCO_2$ offers numerous advantages over traditional methods. Besides the high stabilization of the template-monomer complex and the inexistence of traces of solvent, the imprinted polymers synthesized in $scCO_2$ do not need to be ground and sieved prior to use, therefore avoiding posterior time-consuming steps and partial destruction of the recognition sites. The immobilization of highly crosslinked particles in an acrylate-based membrane cast was successfully achieved, what can be explained by the similar structures of P(MAA-EGDMA) and PMMA, as the incorporation of the same polymeric particles in a polysulfone-based membrane, in a first approach, led to distinct segregation of the two polymers and therefore turn that system impossible to study. Successful hybridization was assessed by gravimetric analysis, with the membrane dry, before and after water elution in the filtration cell and visually by SEM.

The morphology of the polymeric materials used in this work was assessed through scanning electron microscopy. Figure 4.4 presents the SEM images of imprinted polymer, and neat and hybrid PMMA porous structures. SEM image of the synthesized polymers show aggregates of smooth surfaced discrete nanoparticles, with imprinted and blank polymer presenting similar morphology. Using $scCO_2$-assisted phase inversion method to prepare membranes, homogeneous structures are obtained, as it can be confirmed by SEM images. The pure PMMA membrane (Figure 4.4 a and b) produced herein possesses a homogeneous morphology with low porosity on the top layer of the membrane and regular pores across the structure. By SEM images it is possible to assess the hybridization of the matrices and the influence of incorporating crosslinked particles in the morphology of the membranes. Hybrid membranes present spherical and regular pores in the top and across the membrane and a homogeneous distribution of pre-synthesized polymeric particles over the membrane scaffold. The introduction of the highly crosslinked particles in the PMMA membrane cast does not seem to have a significant effect on the pore size, but significantly changes the top surface of the structure, with hybrid membranes possessing higher roughness and a higher amount of pores.

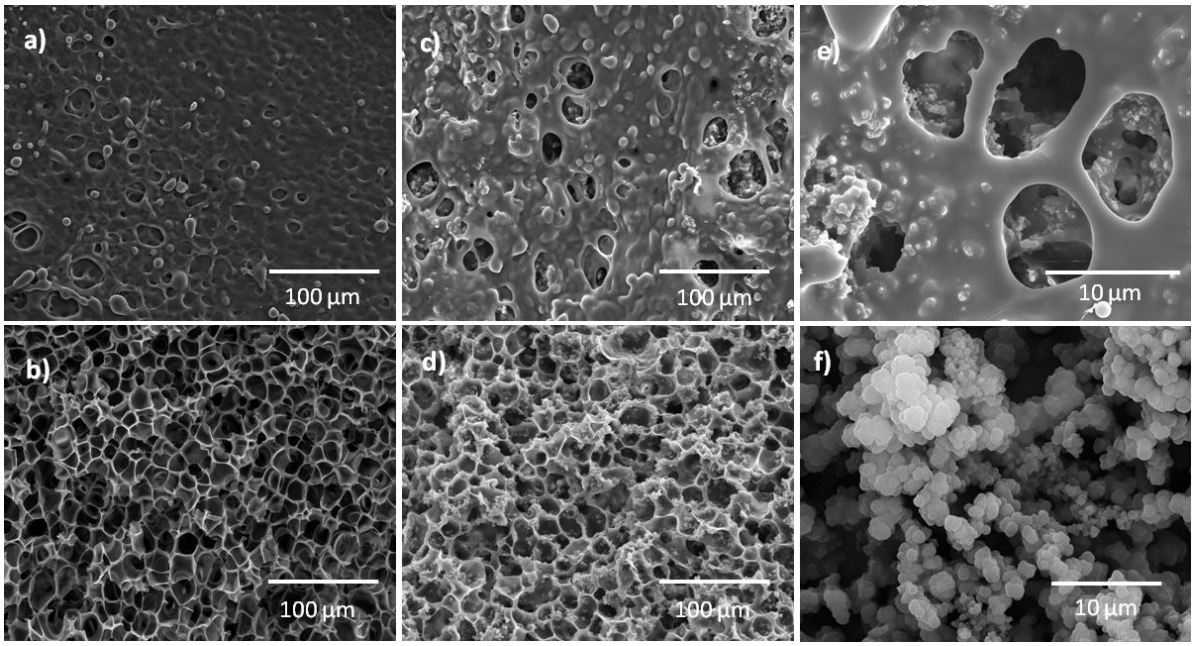

Figure 4.4 - SEM images of the developed structures. a) top surface and b) cross section of PMMA membrane, c) top surface and d) cross section of PMMA MIP hybrid membrane, e) detail of the top surface of PMMA MIP, f) MIP.

FTIR analysis was performed to both synthesized polymers and membranes and the characteristic bands of methacrylic acid and methacrylate were identified at the respective wavenumber. The carbonyl stretching absorption by free carbonyl groups for methacrylate units is described at 1730 cm^{-1} whilst the carbonyl stretching bands of methacrylic acid range from 1742 to 1699 cm^{-1}, according if the groups are free or hydrogen bonded, respectively. In this work NIP and MIP are copolymers of MAA and EGDMA, in the molar ratio of 1:5 and the stretching absorption of carbonyl appears at 1728 cm^{-1}. In agreement with the same composition, NIP and template-desorpted MIP present similar spectra. The incorporation of NIP and MIP in the matrix of PMMA membranes was not possible to assess by the analysis of FTIR spectra as the carbonyl stretching of PMMA and hybrid PMMA membranes appear both at 1734 cm^{-1}.

Nitrogen adsorption experiments were performed to both MIP and NIP and the physical characteristics concerning surface area, pore volume and pore diameter were calculated and presented in Table 4.1.

Table 4.1 - Physical characteristics of NIP and MIP polymers obtained by multipoint BET method (type II).

Polymer	BET surface area ($m^2.g^{-1}$)	Pore volume ($cm^3.g^{-1}$)	Average pore diameter (nm)
NIP	49.8	0.072	5.8
MIP	39.8	0.070	7.0

The introduction of the template molecule in the imprinting process somehow influences the nucleation process during polymerization with MIP presenting lower surface area than NIP and higher average pore diameter. This is in accordance with other imprinting polymerizations reported in the literature using methacrylic acid as functional monomer and ethylene glycol dimethacrylate as crosslinker [25].

Table 4.2 shows the contact angles measured for each membrane. Contact angle measurements are dependent on both the hydrophilicity of the surface as well as the roughness and porosity. Hybrid membranes are shown to have higher contact angles, which is probably related with an increase in the roughness of the surfaces due to the incorporation of the highly crosslinked polymeric particles in the matrices.

Table 4.2 - Physical and mechanical properties of PMMA and hybrid PMMA membranes.

Membrane	Water Flux ($L.m^{-2}.h^{-1}.MPa^{-1}$)	Contact angle (°)	Young's Modulus (MPa)
PMMA	0*	46	0.539
PMMA NIP	465	91	0.419
PMMA MIP	143	94	0.437

*With a maximum applied pressure of 0.5 MPa

The pure water flux, which is defined as the ratio between the volumetric flow rate and the membrane area and the pressure difference, is a crucial parameter in processes that involve membranes. In this work we have studied the water flux through the produced membranes by ranging the hydrostatic pressure from 0 to 0.5 MPa. At these conditions the pure PMMA membrane was not permeable, even when the maximum pressure was applied. There are several parameters, which can influence the permeability of the membranes, such as hydrophilicity, porosity, pore size and interconnectivity of the pores. The experimental conditions used in the preparation of the membranes can be adjusted to tune the properties of the porous structure. In this work we have tried to prepare a PMMA membrane with measurable water flux by increasing the depressurization rate, however no viable structure was obtained, as the membrane foamed turning unfeasible to put it on the filtration unit. Other experimental variables could be changed, such as the solvent used and the polymer concentration, however that was not the scope of this work. As it is shown in Table 4.2, the addition of the synthesized polymers in the casting solution for membrane preparation significantly increases the permeability of the structures. Some years ago, Merkel *et al.* [26] discovered that the introduction of nonporous, fumed silica particles to high-free-volume glassy polymers significantly influenced the rearrangement of the polymer chains and could favourably increase the membrane flux. Our results show that the incorporation of imprinted polymers in the membrane scaffold could be considered an

additional parameter to control the pore morphology, which can lead to increased top surface porosity and therefore reduce or eliminate the diffusional resistance.

Processes engaging membranes often require controlled mechanical loadings. Thus, the information about mechanical strength and elasticity of the membranes is an important indication on the limits of the experimental conditions that the membranes can support. In this work, DMA was used to study the mechanical properties of PMMA and hybrid PMMA membranes. Membranes exhibited low stress break (3-4 MPa) and elongation (±7.5 % strain) in agreement with the low ductility of PMMA [27]. By blending 30 wt% of NIP and MIP particles with PMMA, a slight decrease in the stress break was observed. In literature we could found some evidences that the stress break of silica composite membranes is dependent of the silica content and that for high percentages of silica, the stress break decreases, due to the agglomeration of the particles [28]. The Young's modulus is given by the slope of stress-strain curves and translates the stiffness of the membrane. Table 4.2 shows the Young's modulus measured for the membranes prepared in this work. The incorporation of the highly crosslinked copolymers NIP and MIP into the hybrid membranes, led to a slight decrease in the Young's modulus of the structures that can be related with small differences in the porosity and pore morphology of the membranes [29].

4.1.2.2 Template binding affinity characterization

Imprinted polymers and membranes were evaluated with respect to their ability to rebind the template molecule in aqueous solutions in static and dynamic conditions.

Batch binding experiments were performed to assess qualitatively and quantitatively the template binding affinity of the materials developed. Figure 4.5 shows the experimental adsorption isotherms of template bound on both imprinted and non-imprinted materials as a function of the initial concentration of BPA.

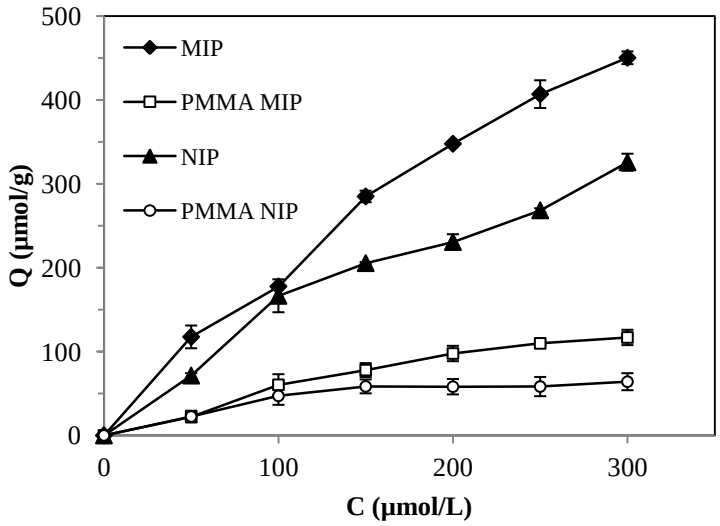

Figure 4.5 - Equilibrium binding curve of BPA to the synthesized polymers and membranes.

Higher adsorption of BPA was achieved by the imprinted polymer reflecting an increased binding affinity to the template molecule. Polymeric powders, NIP and MIP, have higher adsorption capacity for BPA than the corresponding membranes. Adsorption of a template molecule in an imprinted membrane is dependent not only on the chemical affinity introduced by the recognition sites but also on the type of polymer, structural characteristics of the molecule, solution chemistry and membrane morphology and operating conditions. The low binding affinity of PMMA structures for BPA molecule was already reported by Ye *et al.* (2003) [30]. Nevertheless, the introduction of imprinted particles in the porous structure clearly increases the affinity of the membranes towards the corresponding non-imprinted hybrid membrane, as PMMA MIP is able to adsorb more BPA from the aqueous solutions than PMMA NIP.

The adsorption equilibrium data of BPA on MIP and PMMA MIP were fitted using a linearized form of the Langmuir equation, as described in Equation 4.4.

$$\frac{1}{Q_{eq}} = \frac{1}{Q_{max}} + \frac{1}{bQ_{max}C_{eq}} \qquad \text{(Equation 4.4)}$$

Where, Q_{eq} (µmol.g^{-1}) is the equilibrium adsorbed amount of BPA, Q_{max} (µmol.g^{-1}) is the maximum apparent binding capacity, C_{eq} (µM) is the equilibrium concentration and b (M^{-1}) is the adsorption equilibrium constant. The high correlation coefficient (0.997) obtained when fitting the MIP adsorption data with this model, suggests that adsorption takes place at specific homogeneous sites within the MIP surface. When blending the imprinted copolymer with PMMA, heterogeneity in the

structure is introduced, so the correlation coefficient is lower (0.953), nevertheless a specific trend was observed due to the incorporation of MIP. Figure 4.6 shows the adsorption data of BPA by MIP and hybrid PMMA MIP membrane fitted to the linearized Langmuir equation.

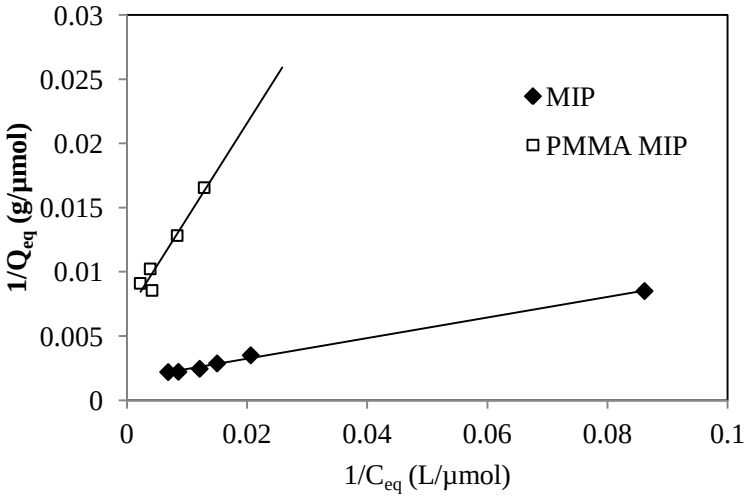

Figure 4.6 - Binding data for MIP and PMMA MIP fitted to a linearized Langmuir equation.

In agreement with higher experimental adsorbed amounts, the apparent saturation capacity, Q_{max}, of MIP is higher than the saturation capacity of PMMA MIP, 625 µmol.g^{-1} and 147 µmol.g^{-1} respectively. Also the binding equilibrium constant is higher for MIP, 19950 M^{-1} versus 9190 M^{-1}. These binding properties of the imprinted materials are consistent with their affinity to the template molecule as the imprinted membrane was prepared with only 30 wt % of imprinted polymer. By tuning the amount of imprinted polymer added to the membrane cast, it should be possible to obtain hybrid membranes with different binding affinity to the template molecule.

4.1.2.3 Filtration of BPA from aqueous solutions

The incorporation of imprinted polymers in porous structures such as in membranes can extend the applications of these molecular recognition systems, as membranes can sense and entrap the analyte at high throughputs. The main challenge is to optimize the recognition and the membrane transport properties at the same time. Regarding dynamic binding, the amounts of BPA that hybrid membranes were able to remove from an aqueous solution with 300 µM of BPA at a flow rate of 0.33 mL.min^{-1}, are presented in Figure 4.7.

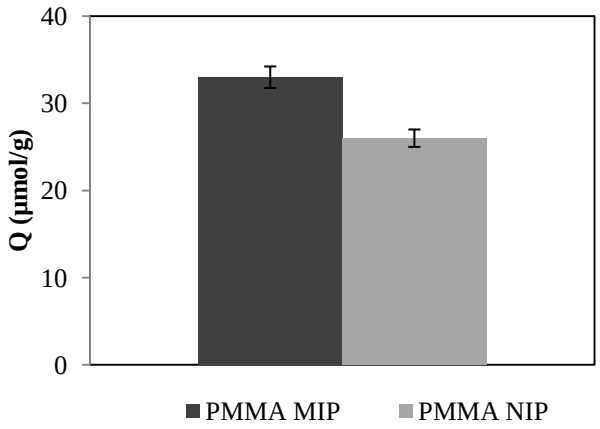

Figure 4.7 - BPA filtration data of hybrid PMMA membranes.

With low time of contact between membrane and template, the structures should have high recognition kinetic, so that an increased affinity adsorption could be observed. As shown, the hybrid imprinted membrane was able to adsorb a higher amount of BPA than its corresponding non-imprinted membrane. With a partial amount of imprinted particles in its structure and regarding dynamic conditions, we believe this is a promising result. Furthermore, at the end of the filtration experiments it was possible to regenerate the membrane without loss of the binding capacity.

4.1.3 Conclusion

This work demonstrates that the immobilization of imprinted polymers in a porous membrane structure, by incorporation of the functional polymers into a casting solution for membrane production is a viable method to produce affinity membranes. Moreover, the feasibility of $scCO_2$-assisted phase inversion method to prepare hybrid imprinted membranes was also attested. The main challenge when preparing imprinted membranes is to optimize both molecular recognition and membrane transport properties. The results show these goals were achieved since the incorporation of highly crosslinked polymeric particles with molecular affinity in a porous structure considerably enhanced the affinity of imprinted membrane to the template while also increased the permeability of the PMMA membrane.

4.2 Semi-covalently imprinted polymers

This part of the thesis describes the synthesis of an imprinted polymer using a semi-covalent imprinting route. By means of this approach instead of using two different molecules such as template and monomer, a single molecule is used. The template possesses a polymerizable counterpart that reacts with the crosslinker agent yielding the affinity polymer. At the end of the polymerization the template is removed from the matrix by cleavage and the binding sites become available to future rebinding through hydrogen bonds. Semi-covalent approach combines both the strict control of functional group location and uniform distribution, characteristic of covalent imprinting, and the reduced kinetic restriction during rebinding, characteristic of non-covalent imprinting. Due to the coupled advantages, semi-covalently imprinted polymers usually show efficient rebinding. Figure 4.8 shows the molecular structure of the polymerizable template used in this work, bisphenol A dimethacrylate.

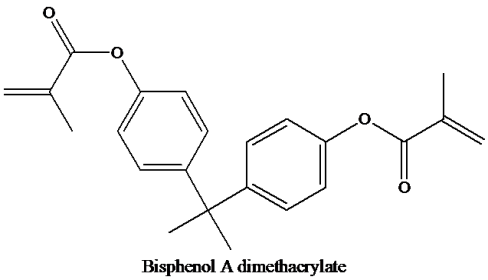

Figure 4.8 - Molecular structure of BPADM.

Bisphenol A is an endocrine disruptor that binds to natural receptors and can mimic the body's own hormones. For that reason, the semi-covalent MIP was tested with respect to its selectivity for BPA, progesterone (a natural steroid hormone) and α-ethinylestradiol (a xenoestrogen used in oral contraceptive formulations), through binding tests in aqueous solutions. Figure 4.9 shows the molecular structures of BPA, PRO and EE.

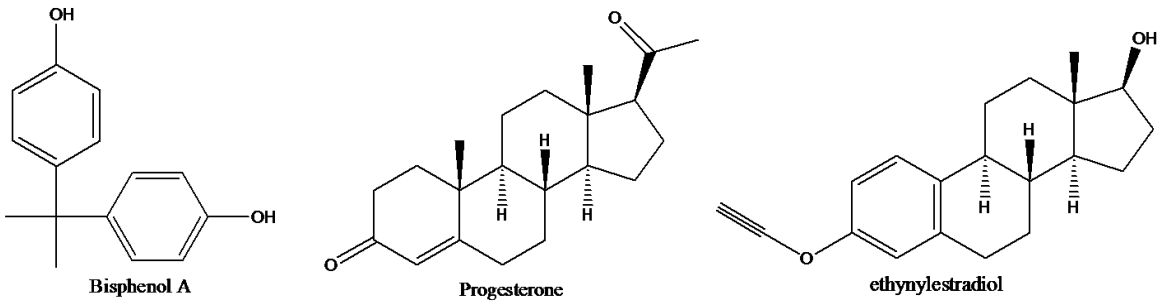

Figure 4.9 - Molecular structure of BPA, progesterone (PRO) and α-ethinylestradiol (EE).

This work also reports the influence that the addition of a co-solvent, acetonitrile, in the reactional system has on the physical characteristics of the polymeric particles. The addition of co-solvents, such as ethanol and acetic acid, in precipitation polymerizations in $scCO_2$, has already been reported [31]. Herein, this effect will be discussed with respect to the ability of the polymer to adsorb BPA.

A scientific research paper concerning the development of the semi-covalently imprinted polymer described in this section is currently being written.

4.2.1 Experimental

4.2.1.1 Materials

Bisphenol A (BPA, 99 % purity) as the analyte of interest, Bisphenol dimethacrylate (BPADM, 99 % purity) as template-monomer, methacrylic acid (MAA, 99 % purity) as functional monomer and ethylene glycol dimethacrylate (EGDMA, 98 % purity) as crosslinker were purchased from Sigma-Aldrich. Azobis(isobutyronitrile) (AIBN, 98 % purity) from Fluka was used as initiator. Tetratbutylammonium hydroxide (*n*-Bu_4NOH) 1.0 M solution in MeOH, as the cleavage agent and poly(methyl methacrylate) and (PMMA) (molecular weight 996,000) were obtained from Sigma-Aldrich. Progesterone (PRO, 99% purity) and α-Ethinylestradiol (EE, 98% purity) were purchased from Sigma-Aldrich. Dimethylformamide (DMF, 99.8 % purity) was purchased from Riedel-de Haën and ethanol (PA), from Panreac. Methanol isocratic HPLC grade (99.7 % purity) from Scharlau was used. Carbon dioxide was obtained from Air Liquide with purity better than 99.998 %. All chemicals were used without further purification.

4.2.1.2 Semi-covalent MIP and NIP synthesis in $scCO_2$

Polymerization reactions in $scCO_2$ were carried out using the experimental apparatus described in section 2.1. In a typical reaction using acetonitrile as co-solvent, 3 mL of the organic modifier (10 wt% with respect to CO_2) were added to the high-pressure cell. For the synthesis of the NIP, 2.54 mmol of the functional monomer MAA, 12.88 mmoles of the crosslinker agent EGDMA and 1 wt % of the radical initiator AIBN were loaded into the reactor. To synthesize the semi-covalent MIP, 1.26 mmol of BPADM, 12.58 moles of EGDMA and 1 wt % of the radical initiator AIBN were loaded into the high-pressure cell. Carbon dioxide was added up to 21 MPa and polymerization reactions proceeded for 24 hours under stirring. At the end of the reaction, the polymer was slowly washed with fresh high-pressure CO_2 for 1 hour.

4.2.1.3 $scCO_2$-assisted hydrolysis and BPA removal

The removal of BPA from the BPA-imprinted polymer was performed in $scCO_2$. In a typical experiment P(BPADM-*co*-EGDMA) (0.925 g), tetrabutylammonium hydroxide (*n*-Bu_4NOH) 1.0 M

in methanol (1.6 mL, 1.6 mmol), and a magnetic stir bar were introduced into a high-pressure cell. The cell was immersed in a thermostated water bath at 65 ºC and pressurized with CO_2 until a final pressure of 20 MPa. Figure 4.10 illustrates the cleavage mechanism. After 24 h of reaction the polymer was washed with fresh CO_2 (20 MPa) for 1h. Methanol (20 mL) was added to the polymer and the suspension was filtered under vacuum. The polymer was then slurry packed in a high-pressure stainless steel extractor (ID 7mm, 15 cm length). This extractor was connected to a 33 mL high-pressure cell that was loaded with 5 mL of MeOH. Carbon dioxide was added up to 21 MPa and a continuous stream of CO_2 and methanol was used to remove BPA from the copolymer.

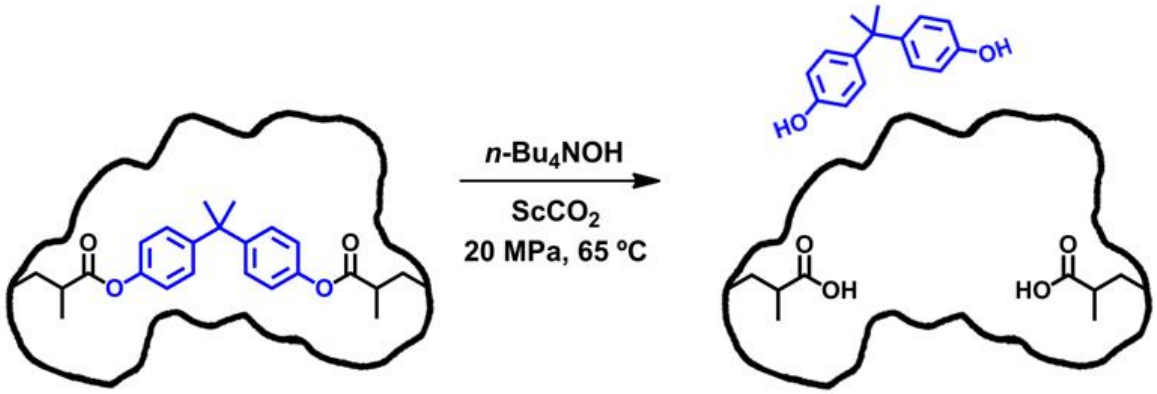

Figure 4.10 – Scheme of the BPA cleavage mechanism used in this work.

4.2.1.4 Morphological and physical characterization of imprinted materials

The synthesized polymers were characterized in terms of morphology using scanning electron microscopy (SEM). Specific surface area and pore diameter of polymer powders were determined by N_2 adsorption according to the BET method. The analyses were carried out following the procedure described in section 4.1.

4.2.1.5 Binding experiments

Batch binding experiments were carried out to evaluate the ability of the synthesized polymers to adsorb BPA, PRO or EE, from aqueous solutions. The polymers (20 mg) were added to 50 mL of aqueous solutions of BPA (5-50 μM) and stirred at 50 rpm for 24 hours. For the binding tests of PRO and EE, given their low water solubility, 0.2 (v/v) % of acetonitrile was added to the aqueous solution and concentrations in the range of 5-16 μM were tested. However, to compare the results with the ones obtained for BPA, lower amounts of polymer were used. By keeping the same ratios between analyte in solution and weight of polymer that were tested for BPA, independently of the concentrations used, the results can be compared.

The amount of substrate adsorbed by the matrices was assessed through Equation 4.3, described in detail in section 4.1. The samples collected were quantified by UV spectroscopy at 275, 248 and 278 nm for BPA, PRO and EE, respectively. All the experiments were carried out in duplicates.

Scatchard analysis is frequently performed to estimate the association constant, K_a, and the apparent maximum binding capacity, B_{max}, of imprinted polymers for the template molecule. For that reason, the data of equilibrium adsorption experiments were processed with the Scatchard equation [32].

$$\frac{B}{C_e} = -B \cdot K_a + \cdot B_{max} K_a \qquad \text{(Equation 4.5)}$$

where C_e represents the free concentration of substrate in equilibrium and B corresponds to the amount of BPA bound to the polymer.

4.2.2 Results and Discussion

4.2.2.1 Morphological and physical characterization

Imprinted and non-imprinted polymers were obtained as dry, free-flowing powders in high yields (80-90%, determined gravimetrically), in accordance with the yields obtained for other polymerizations carried out in the scope of this thesis.

The morphology of the polymers was assessed by scanning electron microscopy. Figure 4.11 shows the SEM images of both MIP and NIP synthesized using a solvent mixture of $scCO_2$ and acetonitrile. The polymers present as aggregates of smooth surface discrete nanoparticles. The addition of a co-solvent seems to contribute to a higher heterogeneity of the particles size, when compared with the polymer synthesized in neat $scCO_2$ (see Figure 4.4, in section 4.1). Also, the addition of 10 wt% of acetonitrile leads to the coalescence of the particles, with special emphasis in the NIP.

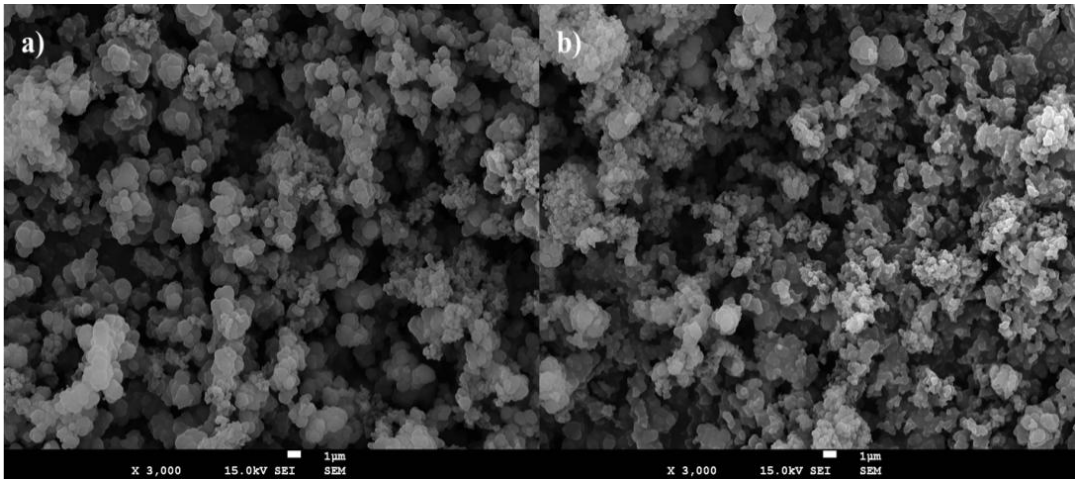

Figure 4.11 - SEM images of the polymers synthesized in the presence of acetonitrile. a) MIP, b) NIP.

The porogen used for the imprinting polymerization is of considerable importance. The morphological properties of the polymers, such as porosity and surface area are determined by the type of solvent. In literature one can find evidences that polymers synthesized in acetonitrile have higher surfaces areas than those synthesized in chloroform or toluene [33]. As the polymers were designed to function as affinity sorbents, acetonitrile was added to the reactional mixture to increase the surface areas of the particles. Table 4.3 shows the physical properties, namely surface area and porosity of the copolymers synthesized.

Table 4.3 - Physical characteristics of NIP and MIP polymers obtained by multipoint BET method (type II).

Polymer	BET surface area ($m^2.g^{-1}$)	Pore volume ($cm^3.g^{-1}$)	Average pore diameter (nm)
NIP	58.2	0.072	5.0
MIP	49.5	0.057	4.6

The results show that semi-covalent MIP has a slightly lower surface area than NIP. This had already been observed in non-covalent MIP with recognition to BPA. It seems that the presence of BPA somehow influences the nucleation and particles growth and precipitation. By comparing these results with those of copolymers synthesized without acetonitrile (Table 4.3), it is possible to conclude that, as expected, the introduction of acetonitrile increases the surface area of the particles. This effect is explained by the solubility parameters of the polymers in the solvents. As porosity arises from phase separation of solvent and polymer, when a good solvent is used the phase separation of the polymer gel phase is delayed and a large number of small microparticles with high surface area are formed [34,35]. Although it does not seem that binding is dependent on a particular porosity and pore size in MIPs, this result will be discussed later with respect with the ability of NIP to adsorb BPA.

4.2.2.2 Template binding affinity characterization

Semi-covalently imprinted polymer and its corresponding control were evaluated with respect to their ability to bind the template molecule, BPA, in aqueous solutions in equilibrium conditions.

In this work, the synthesis of the copolymers was carried out using $scCO_2$ as solvent and acetonitrile as co-solvent. Ye *et al* [36] had performed the synthesis of imprinted polymers in supercritical CO_2 using acetonitrile as co-solvent. In their study, the introduction of 2.5 wt% of acetonitrile (with respect to CO_2) in the synthesis yielded an imprinted polymer with poorer recognition ability than the polymer synthesized without organic solvent modifier. In this work it is not possible to compare the affinity of MIPs synthesized with and without acetonitrile, to adsorb BPA, because the matrices were designed using different imprinting approaches (non-covalent and semi-covalent). It is, however, noteworthy the influence that the addition of acetonitrile in the synthesis has on the BPA adsorption ability by the NIP. Figure 4.12 illustrates the equilibrium binding amounts of BPA by the control polymers at 50 µM as a function of the addition of acetonitrile.

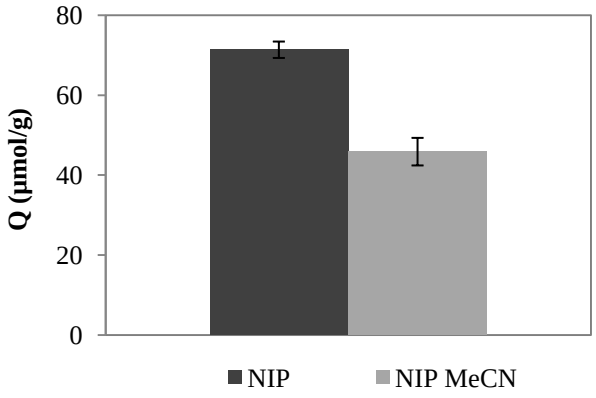

Figure 4.12 - BPA adsorbed by the NIPs synthesized with and without acetonitrile.

As the only difference between the control polymers is the presence or absence of acetonitrile in the polymerization, it is possible to conclude that the introduction of organic solvent is the responsible for the decreased adsorption ability. The reason for this can encounter on a different rearrangement of the polymeric chains, with the functional groups of methacrylic acid being differently disposed and/or different morphological properties. In fact, the results obtained by nitrogen porosimetry show that although the polymers synthesized in the presence of acetonitrile possess higher surface areas, they have smaller pore sizes, which can eventually convey some mass transfer resistance.

The binding affinity of BPA by NIP and semi-covalent MIP in aqueous solutions was tested in the range of 5-50 µM. Prior to binding experiments, the template was removed from the imprinted polymer by hydrolysis. Common procedures for BPA cleavage from imprinted polymers use conventional acid and basic conditions [37,38]. Herein, we report the use of *n*-Bu_4NOH-$scCO_2$ system

as an alternative hydrolysis of highly crosslinked BPA-imprinted polymers. The successful hydrolysis of polypeptide esters by tetraalkylammonium hydroxide strong bases reported in the literature [39], led us to use *n*-Bu_4NOH in the hydrolysis of P(BPADM-*co*-EGDMA).

Figure 4.13 shows the binding isotherms for NIP and MIP. As it can be seen, the equilibrium binding of BPA increases with the initial concentration of the analyte, suggesting that no saturation was reached for the imprinted polymer at these concentrations. Also, by looking at both curves it is obvious the higher adsorption ability by the MIP. This is, usually, indicative of the presence of affinity binding sites created by the molecular imprinting process.

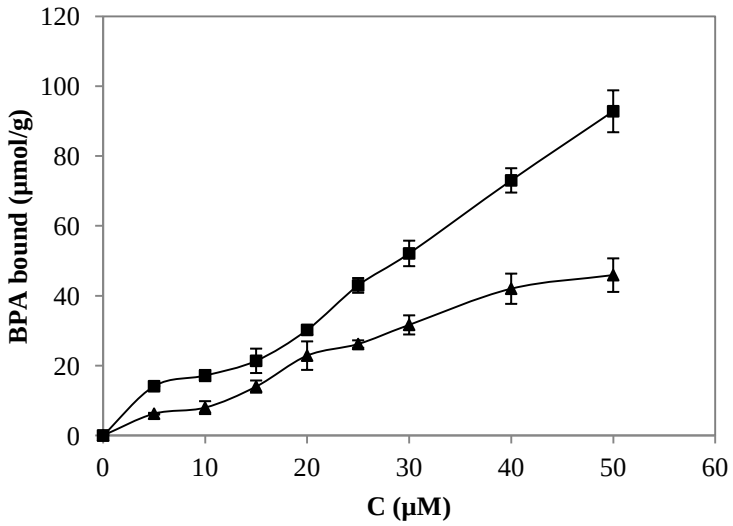

Figure 4.13 - Binding isotherms for BPA adsorption by NIP (filled triangles) and MIP (filled squares).

Scatchard analysis was carried out to evaluate the binding properties of the semi-covalently imprinted polymer. Figure 4.14 illustrates the scatchard plots for BPA adsorption in MIP and NIP. As it can be seen, two straight lines could be withdrawn for the MIP. This result is symptomatic of different binding sites affinity, very common in imprinted polymers [40]. Although the copolymer was prepared by the semi-covalent approach, with the template and the monomer covalently bound, the available binding sites in aqueous solutions do not possess the same overall affinity to BPA, as two different affinity constants were obtained. This may be explained by an incomplete cleavage of the template from all the binding sites and a different solvation of the chains in aqueous medium, that can influence the binding sites geometry and, therefore, the free access of the analyte to internal cavities. The Scatchard plot for the control polymer fits to only one affinity constant, reflecting the absence of high specific binding sites.

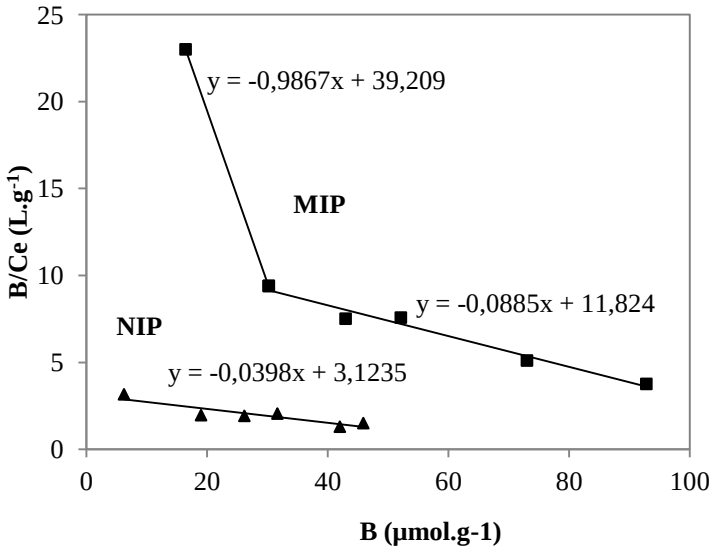

Figure 4.14 - Scatchard plot for BPA in MIP and NIP sorbents within the range of 5–50 µM.

The association constants and maximum binding capacities for BPA adsorption by both NIP and MIP were calculated from Scatchard plots. Table 4.4 lists the results obtained. From the straight area in the range of 16 - 30 µmol/g, an affinity constant for the high-affinity binding sites in MIP was estimated to be 9.9 × 10^5 M^{-1} and an apparent maximum binding capacity of 39.7 µmol.g^{-1} was attained. Ikegami *et al* [38] synthesized a BPA-imprinted polymer in chloroform and evaluated the rebinding ability of the polymeric matrix in the same solvent. The association constant of that polymer in the high-recognition range is in the same order of magnitude than ours (1.7 × 10^5 M^{-1}), although the MIP synthesized in this work shows an adsorption ability 3.7 times higher. The high adsorption capacity obtained in aqueous solutions may be attributed to the hydrophobic interactions between analyte and polymer. In the low affinity range, the association constants for MIP and NIP were, respectively, 0.88 × 10^5 M^{-1} and 0.40 × 10^5 M^{-1}, whilst the maximum binding capacities were calculated to be 133.6 µmol.g^{-1} and 74.5 µmol.g^{-1}. The results show that the imprinted polymer possesses an overall higher affinity and binding capacity of the template than the control polymer.

Table 4.4 - Binding constants for MIP and NIP as calculated by the Scatchard equation.

Polymer	**High-affinity binding sites**		**Low affinity binding sites**	
	$K_a \times 10^5$ (M^{-1})	B_{max} (µmol.g^{-1})	$K_a \times 10^5$ (M^{-1})	B_{max}(µmol.g^{-1})
MIP	9.9	39.7	0.88	133.6
NIP	-	-	0.40	74.5

4.2.2.3 Selectivity studies

The selectivity of MIP in aqueous solutions was assessed by evaluation of its capability to bind PRO and EE in comparison with BPA. The ability of imprinted polymers to selectively adsorb the template molecule in aqueous environment is one of the most challenging features of MIPs and much attention is being focused in this topic [41]. Zhongbo and Hu [42] synthesized a 17β-estradiol imprinted polymer in acetonitrile and found out that the material showed reduced selectivity in aqueous solutions, although in acetonitrile the recognition was almost 7 times superior.

Figure 4.15 illustrates the results obtained in this work for the selectivity experiments in aqueous solutions for both NIP and MIP, concerning the maximum adsorption capacities.

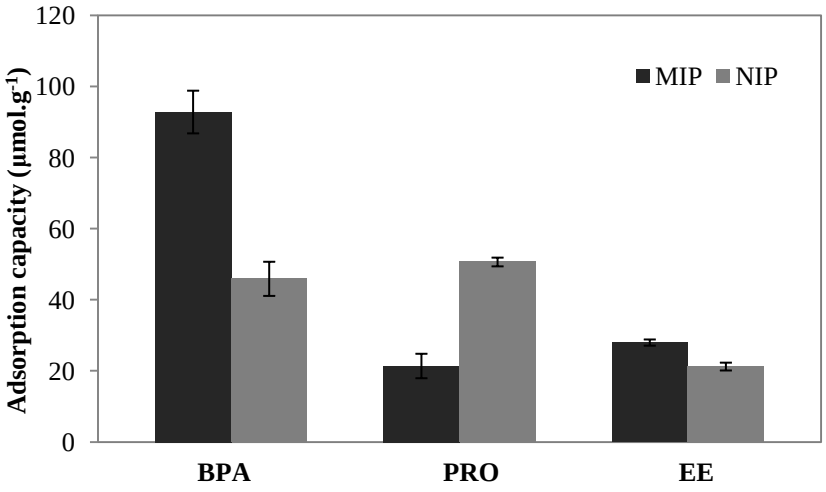

Figure 4.15 - Maximum adsorption capacities of BPA, PRO and EE obtained in the selectivity experiments.

The results show that NIP binds BPA and progesterone at the same extent, whereas the imprinted polymer binds progesterone at much lower degree. This occurs because within a MIP, the functional groups are organized as a system of affinity binding sites, with a structure dependent upon the complementarity introduced at the imprinting stage, by the template molecule, BPA. In the NIP the functional groups of MAA have a comparative random distribution, yielding different binding characteristics.

The imprinted polymer with molecular recognition to BPA, synthesized using supercritical CO_2 as the porogen, shows an adsorption capacity for the template that corresponds to 4.3 and 3.3 times the maximum adsorption of PRO and EE, respectively, showing that MIP has a water-compatible performance.

4.2.3 Conclusion

The work herein reported shows that supercritical fluid technology is a viable alternative to prepare molecularly imprinted polymers, using the semi-covalent approach. Further, the synthesized polymer with molecular recognition to BPA, an endocrine disruptor, showed a significant selectivity in aqueous solutions. The MIP adsorbs higher amounts of BPA than the NIP, whereas the adsorption capacity for PRO and EE remains low. The results demonstrate the feasibility of preparing MIPs capable of keeping their molecular recognition in aqueous media, using supercritical fluid technology. We envisage that these polymers could have a real application in sensor devices, waste water treatments and even biomedical applications due to the high purity of the materials obtained using this clean technology.

4.3 References

[1] Kho Y.W., Kalika D.S., Knutson B.L., Precipitation of Nylon 6 membranes using compressed carbon dioxide. Polymer 2001, 42, 6119-6127.

[2] Temtem M., Pompeu D., Barroso T., Fernandes J., Simões P.C., Casimiro T., Rego A.M.B., Aguiar-Ricardo A., Development and Characterization of a Thermoresponsive Polysulfone Membrane using an Environmental Friendly Technology. Green Chem. 2009; 11, 638-645.

[3] Reverchon E., Cardea S., Formation of cellulose acetate membranes using a supercritical fluid assisted process. J. Membrane Sci 2004, 240, 187-195.

[4] Reverchon E., Cardea S., Rappo E.S., Production of loaded PMMA structures using the supercritical CO_2 phase inversion process. J. Membrane Sci. 2006, 273, 97-105.

[5] DeSimone, J.M., Practical approaches to green solvents, Science 2002, 297, 799-803.

[6] Reverchon, E., Cardea, S., Formation of cellulose acetate membranes using a supercritical fluid assisted process, J. Membrane Sci. 2004, 240, 187-195.

[7] Matsuyama, H., Yano, H., Maki, T., Teramoto, M., Mishima, K., Matsuyama, K., Formation of porous flat membrane by phase separation with supercritical CO_2, J. Membrane Sci. 2001, 194, 157-163.

[8] Reverchon, E., Cardea, S., PVDF-HFP Membrane formation by supercritical CO_2 processing: elucidation of formation mechanisms, Ind. Eng. Chem. Res. 2006, 45, 8939-8945.

[9] Van der Marel, P., Zwijnenburg, A., Kemperman, A., Wessling, M., Temmink, H., Van der Meer, W., Influence of membrane properties on fouling in submerged membrane bioreactors. J. Membrane Sci. 2010, 348, 66-74.

[10] Wang, X., Ding, B., Sun, M., Yu, J., Sun G., Nanofibrous polyethyleneimine membranes as sensitive coatings for quartz crystal microbalance-based formaldehyde sensors, Sens. Actuators B-Chem. 2010, 144, 11-17.

[11] Sergeyeva, T.A., Piletsky, S.A., Piletska, E., Brovko, O.O., Karabanova, L.V., Sergeeva, L.M., El'skaya, A.V., Turner, A.P.F., In Situ Formation of Porous Molecularly Imprinted Polymer Membranes. Macromolecules 2003, 36, 7352-7357.

[12] Donato L., Tasselli, F., Drioli E., Molecularly Imprinted Membranes with Affinity Properties for Folic Acid. Separ. Technol. 2010, 45, 2273-2279.

[13] Hattori, K., Hiwatari, M., Iiyama, C., Yoshimi, Y., Kohori, F., Sakai, K., Piletsky, S.A., Gate effect of theophylline-imprinted polymers grafted to the cellulose by living radical polymerization, J. Membrane Sci. 2004, 233, 169-173.

[14] Kobayashi, T., Leong, S.S., Zhang, Q.J., Using polystyrene-co-maleic acid for molecularly imprinted membranes prepared in supercritical carbon dioxide, J. Appl. Polym. Sci. 2008, 108, 757-768.

[15] Takeda, K,, Abe, M,, Kobayashi, T., Molecular-imprinted nylon membranes for the permselective binding of phenylalanine as optical-resolution membrane adsorbents, J. Appl. Polym. Sci. 2005, 97, 620-626.

[16] Ulbricht, M., Membrane separations using molecularly imprinted polymers, J. Chromatogr. B 2004, 804, 113-125.

[17] Dairkee, S,H., Seok, J., Champion, S., Sayeed, A., Mindrinos, M., Xiao, W., Davis, R,W., Goodson, W,H., Bisphenol A induces a profile of tumor aggressiveness in high-risk cells from breast cancer patients, Cancer Res. 2008, 68, 2076-2080.

[18] Lang, I,A,, Galloway, T.S., Scarlett, A., Henley, W.E., Depledge, M., Wallace, R.B., Melzer, D., Association of Urinary Bisphenol A Concentration With Medical Disorders and Laboratory Abnormalities in Adults. J. Amer. Med. Assoc. 2008, 300, 1303-1310.

[19] Murakami, K., Ohashi, A., Hori, H., Accumulation of bisphenol A in hemodialysis patients, Blood Purif. 2003, 3, 290-294.

[20] Soares da Silva, M., Viveiros, R., Coelho, M., Aguiar-Ricardo, A.,Casimiro, T., Supercritical CO2-assisted preparation of a PMMA composite membrane for Bisphenol A recognition in aqueous environment, Chemical Engineering Science, *in press*, DOI:10.1016/j.ces.2011.09.015.

[21] Temtem, M., Casimiro, T., Aguiar-Ricardo, A., Solvent power and depressurization rate effects in the formation of polysulfone membranes with CO_2-assisted phase inversion method. J. Membrane Sci. 2006, 283, 244-252.

[22] Temtem, M., Casimiro, T., Mano, J.F., Aguiar-Ricardo, A., Preparation of membranes with polysulfone/polycaprolactone blends using a high pressure cell specially designed for a CO_2 -assisted phase inversion, J. Supercrit. Fluids 2008, 43, 542-548.

[23] Temtem, M., Development of biocompatible and "smart" porous structures using CO_2-assisted processes, PhD thesis, 2009.

[24] Cao, L., Chen, L., Influence of reaction parameters on synthesis of temperature-sensitive materials in supercritical carbon dioxide by precipitation polymerization, Polym. Bull. 2006, 57, 651-659.

[25] Shi, X., Wu, A., Qu, G., Li, R., Zhang, D., Development and characterisation of molecularly imprinted polymers based on methacrylic acid for selective recognition of drugs, Biomaterials 2007, 28, 3741-3749.

[26] Merkel, T.C., Freeman, B.D., Spontak, R.J., He, Z., Pinnau, I., Meakin, P., Hill, A.J., Ultrapermeable, reverse-selective nanocomposite membranes, Science 2002, 296, 519-522.

[27] Lin, D.-J., Chang, C.-L., Lee, C.-K., Cheng, L.P., Preparation and characterization of microporous PVDF/PMMA composite membranes by phase inversion in water/DMSO solutions, Eur. Polym. J. 2006, 42, 2407-2418.

[28] Zou, H., Wu, S., Shen, J., Polymer/Silica nanocomposites: preparation, characterization, properties and applications, Chem. Rev. 2008, 108, 3893-3957.

[29] Barroso, T., Temtem, M., Casimiro, T., Aguiar-Ricardo, A., Development of pH-responsive poly(methacrylate-co-methacrylic acid) membranes using $scCO_2$ technology. Application to protein permeation, J. Supercrit. Fluids 2009, 51, 56-66.

[30] Ye, S., Morita, S., Li, G., Noda, H., Tanaka, M., Uosaki, K., Osawa, M., Structural Changes in Poly(2-methoxyethyl acrylate) Thin Films Induced by Absorption of Bisphenol A. An Infrared and Sum Frequency Generation (SFG) Study, Macromolecules 2003, 36, 5694-5703.

[31] Xu, Q., Han, B., Yan, H., Effect of cosolvents on the precipitation polymerization of acrylic acid in supercritical carbon dioxide, Polymer 2001, 42, 1369-1373.

[32] Yan, H., Row, K.H., Yang, G., Water-compatible molecularly imprinted polymers for selective extraction of ciprofloxacin from human urine, Talanta 2008, 75, 227–232.

[33] Esfandyari-Manesh, M., Javanbakht, M.m Atyabi, F., badiei, A., Dinarvand, R., Effect of porogenic solvent on the morphology, recognition and release properties of carbamazepine-molecularly imprinted polymer nanospheres, J. Appl. Polym. Sci. 2011, 121, 1118–1126.

[34] Cameron, N.R., Barbetta, A., The infuence of porogen type on the porosity, surface area and morphology of poly(divinylbenzene) PolyHIPE foams, J. Mater. Chem. 2000, 10, 2466-2471.

[35] Spivak, D.A., Optimization, evaluation, and characterization of molecularly imprinted polymers, Adv. Drug Deliver. Rev. 2005, 57, 1779– 1794.

[36] Ye, L., Yoshimatsu, K., Kolodziej, D., Francisco, J.D.C., Dey, E.S., Preparation of molecularly imprinted polymers in supercritical carbon dioxide. J. Appl. Polym. Sci. 2006, 102, 2863-2867.

[37] Kobayashi, T., Takeda, K., Ohashi, A., Makoto, M., Sugiyama, S., Selective removal of bisphenol A from serum using molecularly imprinted polymer membranes, Ther. Apher. Dial. 2009, 13, 19–26.

[38] Ikegami, T., Mukawa, T., Nariai, H., Takeuchi, T., Bisphenol A-recognition polymers prepared by covalent molecular imprinting, Anal. Chim. Acta 2004, 504, 131-135.

[39] Abdel-Magid, A. F. , Cohen, J. H. , Maryanoff, C. A. , Shah, R. D., Villani, F. J., Zhang, F., Hydrolysis of polypeptide esters with tetrabutylammonium hydroxide, Tetrahedron Lett. 1998, 39, 3391–3394.

[40] Allender, C.J., Brain, K.R., Heard, C.M., Binding cross-reactivity of boc-phenylalanine enantiomers on molecularly imprinted polymers, Chirality 1997, 9, 233-237.

[41] Chen, L., Xu, S., Li, J., Recent advances in molecular imprinting technology: current status, challenges and highlighted applications, Chem. Soc. Rev. 2011, 40, 2922-2942

[42] Zhongbo, Z., Hu, J., Selective removal of estrogenic compounds by molecular imprinted polymer (MIP), Water Res. 2008, 42, 4101-4108.

CHAPTER 5

Conclusions and Prospects

5. Conclusions and Prospects

5.1 Concluding remarks

Over the last years, tailor-made synthetic receptors created by molecular imprinting technique have been the subject of an exponential attention due to their performance and applicability in a wide range of applications. Nevertheless, conventional polymerization methods use harmful organic solvents and typical bulk polymerization yields a hard block polymer which has to be ground and sieved leading to product loss up to 50%.

The work developed within this thesis is the first rational approach to the validation of supercritical CO_2 as a green and viable alternative medium for the synthesis and processing of molecular recognition polymers. By performing the synthesis in an apolar aprotic solvent such as $scCO_2$, the template-functional monomer complexes are more stable than in a protic solvent, because $scCO_2$ does not interfere in the complex formation. This can give rise to well-defined active sites in the polymer matrix, leading to materials with high affinity. MIPs with molecular recognition to different molecules were designed for concrete purposes in drug delivery, chromatography and extraction showing the broad range of applications that these materials can encounter.

The affinity to the target molecules, introduced by molecular imprinting, provides imprinted polymers the ability to load higher amounts of the analyte molecule, either in aqueous solutions or in supercritical environment, than non-imprinted polymers. In vitro drug delivery experiments revealed that the macromemory effect yields polymeric drug delivery systems that release the drug molecule in a more sustained way. Moreover, batch extraction of the target analyte in aqueous solutions revealed that the association constant between template and imprinted matrix is higher than for the control polymer, which reflects the higher affinity of MIP to the target molecule. The immobilization of imprinted particles in porous structures, such as membranes, showed to be a feasible option in the preparation of affinity membranes.

The most fascinating achievement obtained within this thesis was the chiral recognition ability of the synthesized MIPs, which shows that with the proper imprinting system, an enantiomeric differentiation can be achieved when loading the imprinted stationary phase with a racemic mixture. Furthermore, the affinity structures were able to maintain their selective recognition properties in aqueous environment. This was a real challenge because traditionally MIPs demonstrate better performance in hydrophobic organic solvents, although the need exists to develop MIPs with water-compatible performance.

The experimental work herein reported embodies a step forward for the elimination or drastic reduction of hazardous organic solvents from molecular imprinting technique practices. Further it

renews some of the application fields of polymeric materials synthesized in supercritical CO_2, such as affinity separations and sustained drug delivery.

5.2 Future Perspectives

In 2010 Biotage, a swedish analytical and medicinal chemistry services company, acquired MIP Technologies for about €1.8 million. With this agreement, Biotage envisaged a strategic expansion providing state-of-the-art solutions in the boundary of chemistry and materials science. Polyintell, a French company, brings innovative solutions for selective extraction, separation and detection of target molecules using MIPs. These successful cases show that the market exists for high performance products.

The features of MIPs synthesized in supercritical CO_2 could be further optimized to deliver highly efficient products. A thorough study of the prearrangement between template and monomer in supercritical medium would allow to choose the most appropriate monomer in each case. Spectroscopic evaluation through HP-NMR experiments or computer simulation should be considered.

Given the known "solvent-memory" effect, MIPs have a predictable better rebinding performance in the solvent used for the synthesis. Therefore, the evaluation of MIPs as stationary phases should be carried using supercritical fluid chromatography as this could greatly improve the chiral recognition ability and reduce the peak broadening.

The immobilization of MIPs into porous structures could be extended to produce affinity scaffolds and membranes with molecular recognition ability to two or more target molecules, by introducing different MIPs in the casting solution.

Although remarkable achievements have been attained there are still substantial challenges and opportunities. MIPs could be tested as sensing devices, artificial antibodies and catalysts and their selective recognition properties should be evaluated using real samples. Nevertheless, given the high cost associated with the development of these materials using supercritical fluid technology, only high-value target molecules and materials should be considered to turn the process economically viable.